Winter School Siramm Project 2021 http://www.siramm.unipr.it/

Local Approaches in Fatigue

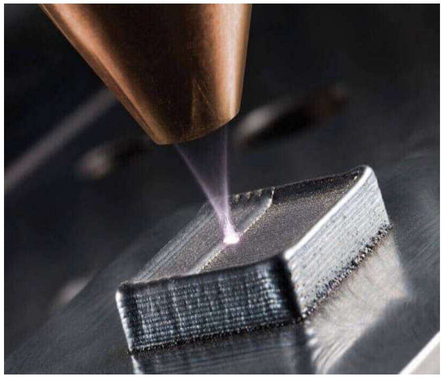

Filippo Berto

Department of Mechanical and Industrial Engineering
NTNU Trondheim Norway

NTNU

Filippo Berto
Chair of Fracture Mechanics, Fatigue Design, Structural Integrity

Institutt for maskinteknikk og produksjon
Fakultet for ingeniørvitenskap
filippo.berto@ntnu.no
+4748500574
Verkstedteknisk, Administration area, Gløshaugen, Richard Birkelands vei 2b, 7491 Trondheim

Position

- NTNU Top Research Program for highly qualified scientists
- International Chair
- Stephen Timoshenko fellow 2018 at Stanford University
- Award of Merit 2018 from ESIS

Current research topics

- Fatigue and fracture of traditional and advanced materials
- Structural integrity of additively manufactured materials
- Local approaches for fatigue design
- Multiaxial fatigue
- Notch Effect
- Energy based methods, Data-driven approaches

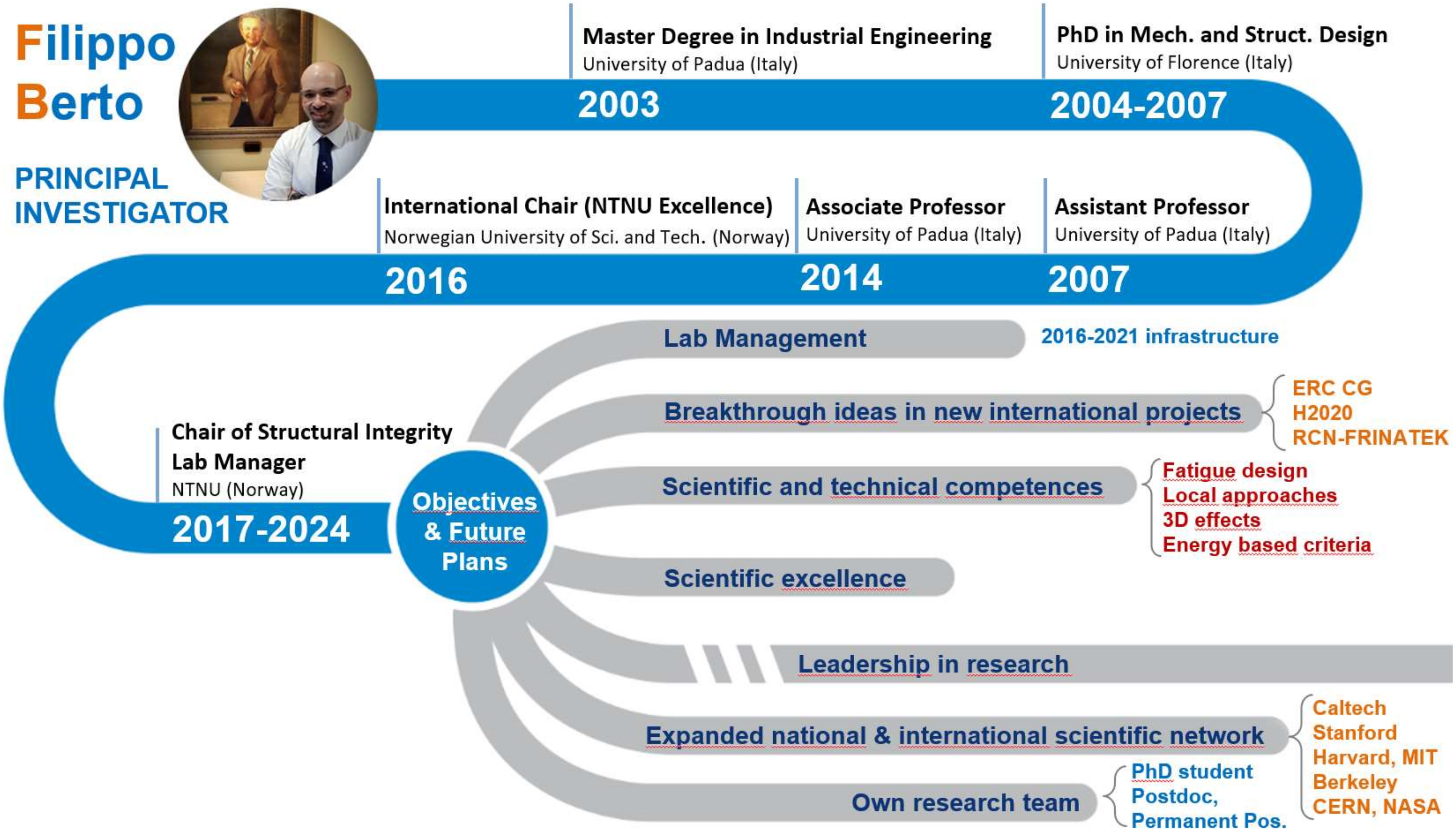
Filippo
Berto
PRINCIPAL
INVESTIGATOR
Master Degree in Industrial Engineering
University of Padua (Italy)
2003
PhD in Mech. and Struct. Design
University of Florence (Italy)
2004-2007
International Chair (NTNU Excellence)
Norwegian University of Sci. and Tech. (Norway)
2016
Associate Professor
University of Padua (Italy)
2014
Assistant Professor
University of Padua (Italy)
2007
Chair of Structural Integrity
Lab Manager
NTNU (Norway)
2017-2024
Objectives
& Future
Plans
Lab Management
2016-2021 infrastructure
Breakthrough ideas in new international projects
ERC CG
H2020
RCN-FRINATEK
Scientific and technical competences
Fatigue design
Local approaches
3D effects
Energy based criteria
Scientific excellence
Leadership in research
Expanded national & international scientific network
Caltech
Stanford
Harvard, MIT
Berkeley
CERN, NASA
Own research team
PhD student
Postdoc,
Permanent Pos.

Fatigue and Fracture Lab

Laboratory equipment
Universal testing machines:
•Zwick 250kN
•Multiaxial MTS 100kN and 2000 Nm
•MTS 50 kN
•Instron 100kN (Servohydr. with hydr. grips)
•Instron 50kN (Servohydr. with hydr. grips)
•Instron 40kN (Servohydr. with hydr. grips)
•MTS 5 kN

Crack propagation in cyclically loaded metallic components

Part 1: Introduction to fatigue

Norwegian University of Science and Technology

NTNU

Learning Philosophy- Competence Orientation[1]

Have a good understanding of failure mechanisms

“Failure is central to engineering. Every single calculation that an engineer makes is a failure calculation. Successful engineering is all about understanding how things break or fail.“

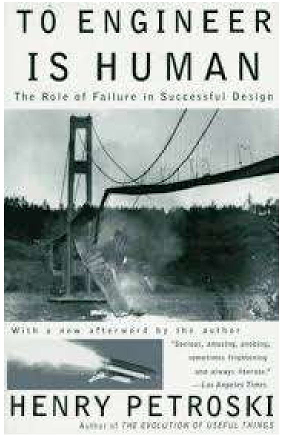

Henry Petroski
American engineer in failure analysis
Professor of civil engineering and history Duke University
Industrial design history of common everyday objects
Frequent lecturer and a columnist for the magazines American Scientist and Prism.

1) F. E. Weinert, in Defining and selecting key competencies, Hogrefe & Huber Publishers, Ashland, OH, US, 2001, pp. 45–65.

Fatigue- “Suddenly it happened”

Versailles rail accident 1842

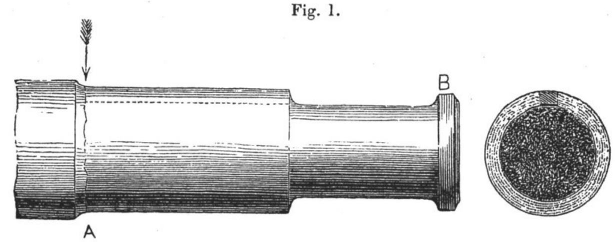

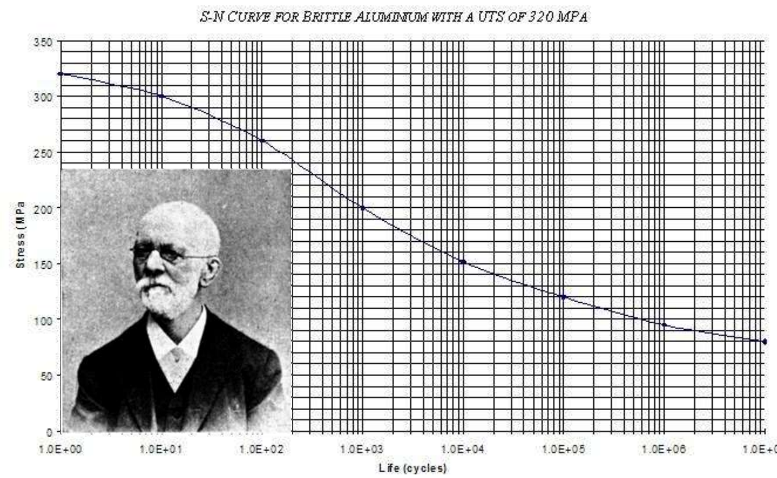

August Wohler, Railway engineer, 1819-1914

Fatigue- “Suddenly it happened”

First systematic investigation of S-N curves.

- Fatigue occurs suddenly, also in ductile materials
- Minimization of fatigue by lowering the stress at critical points of the component
- Fatigue occurs by crack growth from surface defects until product can not longer support the load

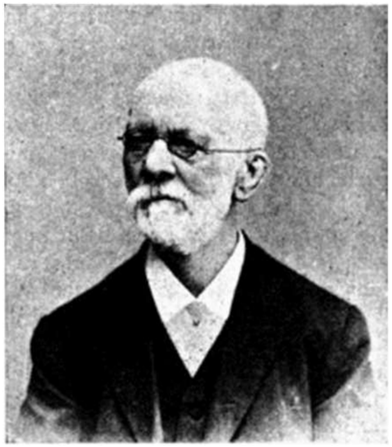

August Wohler
Railway engineer
1819-1914

Woehler Curves

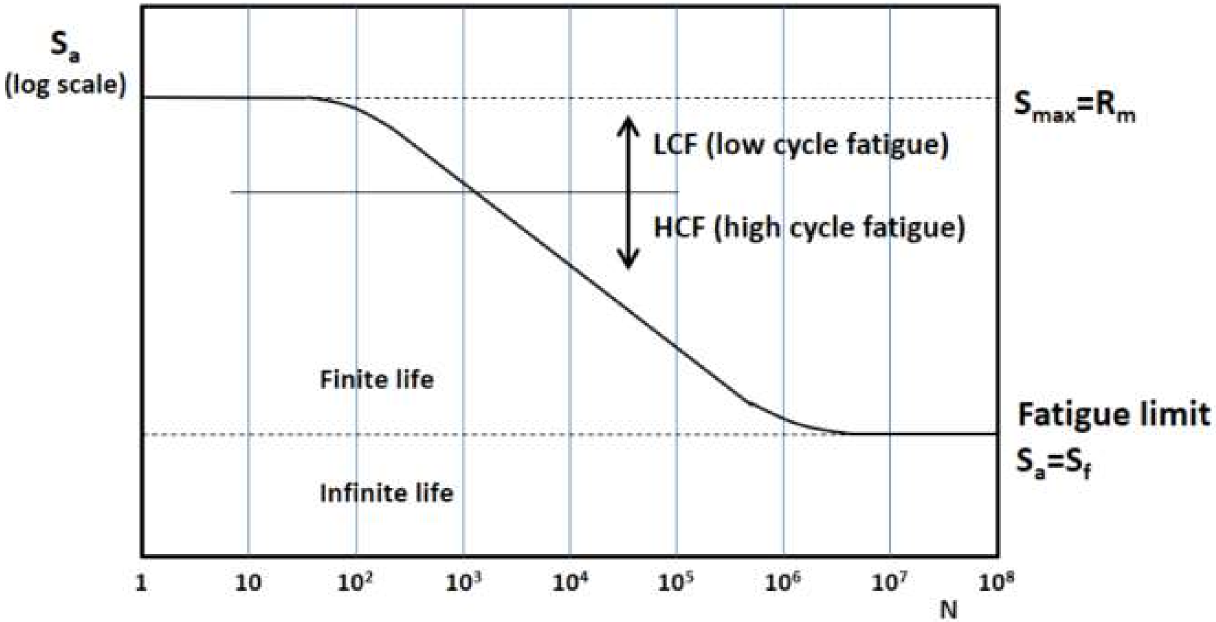

- Relation between cyclic stress amplitude and number of cycles to failure.
- S-N curves are derived from fatigue tests (constant amplitude)
- Kt=1 unnotched

$$\sigma_a = A * N^b$$

Cyclic Loading

$R = -1 \quad \sigma_m = 0$

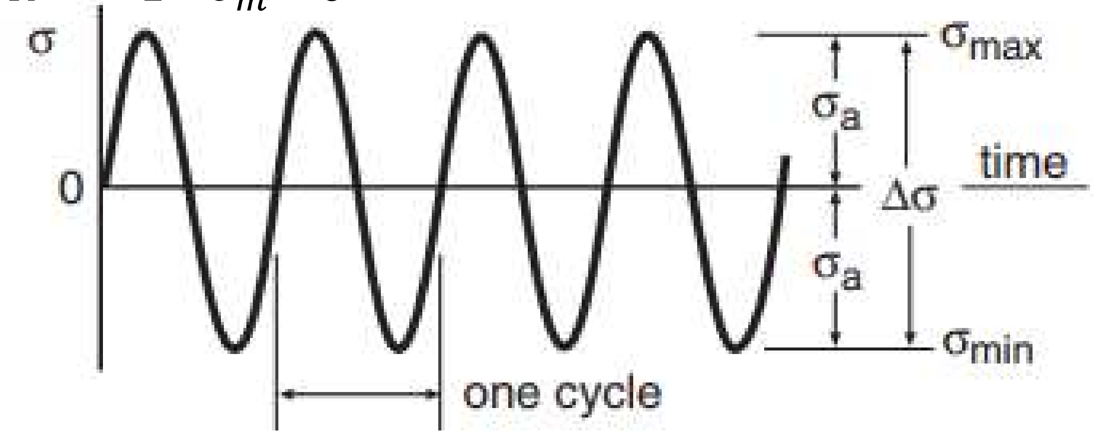

$\Delta\sigma = \sigma_{max} - \sigma_{min}$ …Stress Range

$$\sigma_m = \frac{\sigma_{min} + \sigma_{max}}{2}$$ …Mean Stress

$$R = \frac{\sigma_{min}}{\sigma_{max}}$$ …Stress Ratio

$R = 0 \qquad \sigma_m = \sigma_a$

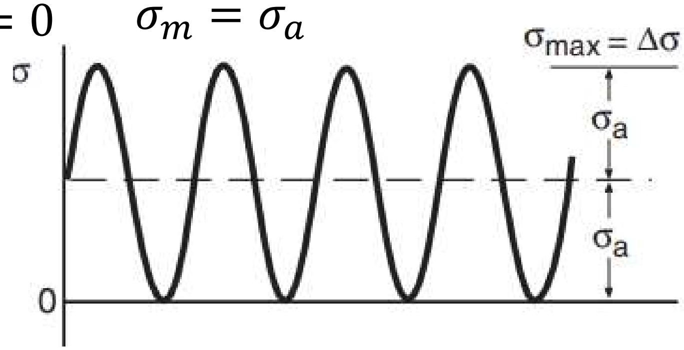

$-1 < R < 0 \qquad 0 < \sigma_m < \sigma_{max}$

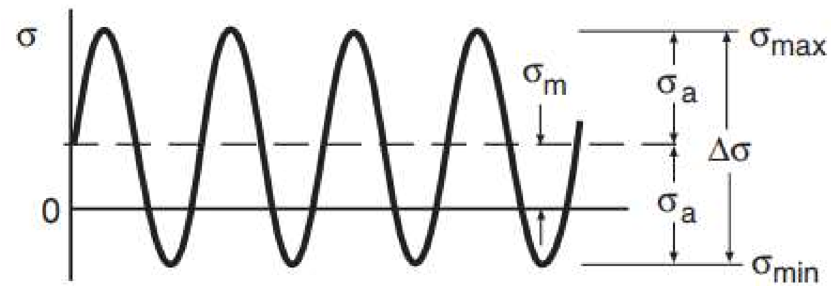

Dowling- Mechanical Behavior of Materials, Fourth Edition, Pearson 2013

Cyclic Loading

$$\sigma_a = \frac{\Delta\sigma}{2} = \frac{\sigma_{max} - \sigma_{min}}{2}$$ …Amplitude

$$A = \frac{\sigma_a}{\sigma_m}$$ …Amplitude Ratio

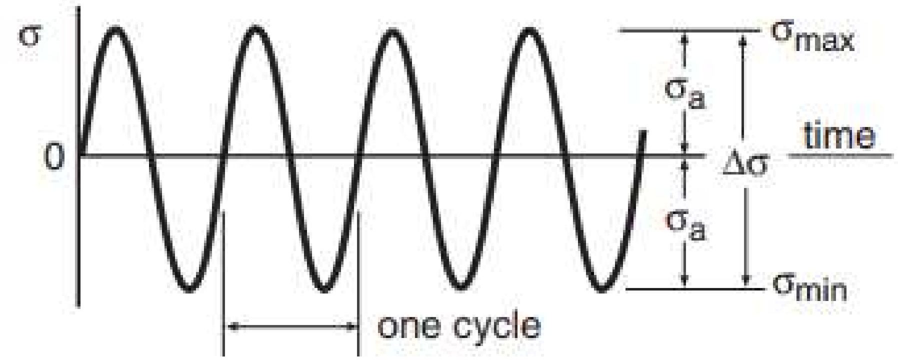

Further Relations

$$\sigma_{max} = \sigma_m + \sigma_a$$

$$\sigma_{min} = \sigma_m - \sigma_a$$

$$\sigma_a = \frac{\sigma_{max}}{2}(1 - R)$$

$$\sigma_m = \frac{\sigma_{max}}{2}(1 + R)$$

$$R = \frac{1 - A}{1 + A}$$

$$A = \frac{1 - R}{1 + R}$$

Woehler Curves- Mean Stress

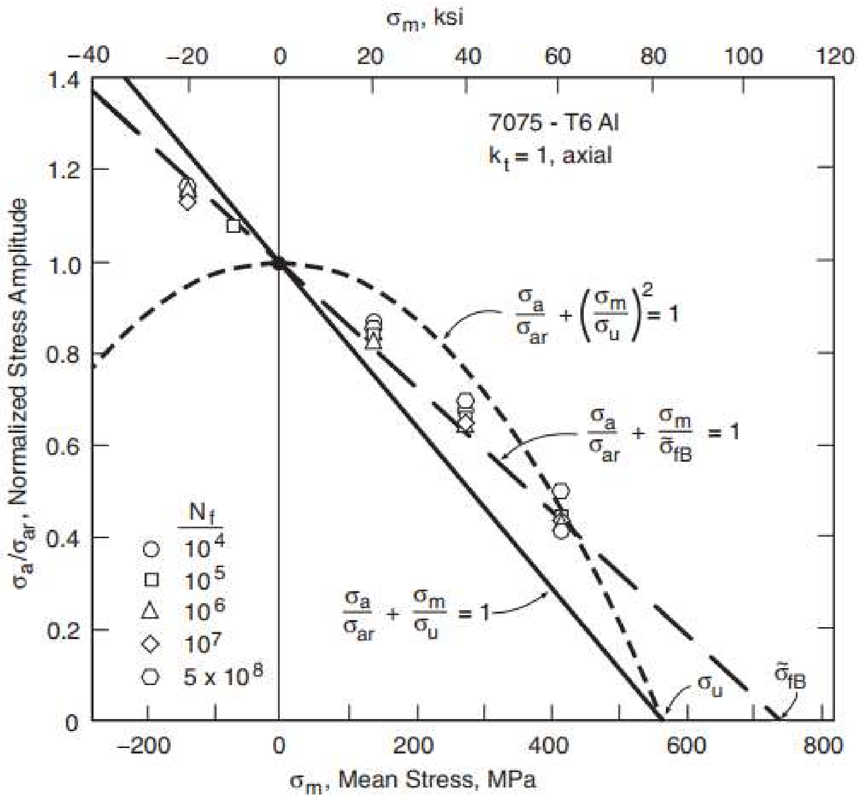

$$\frac{\sigma_a}{\sigma_{ar}} + \frac{\sigma_m}{\sigma_u} = 1$$ Goodman

$$\frac{\sigma_a}{\sigma_{ar}} + \left(\frac{\sigma_m}{\sigma_u}\right)^2 = 1$$ Gerber for sigma_m>=0

$$\frac{\sigma_a}{\sigma_{ar}} + \frac{\sigma_m}{\tilde{\sigma}_{fB}} = 1$$ Goodman correction with true fracture strength

Smith, Watson and Topper

$$\sigma_{ar} = \sqrt{\sigma_{max}\sigma_a} \qquad (\sigma_{max} > 0)$$

$$\sigma_{ar} = \sigma_{max}\sqrt{\frac{1-R}{2}} \qquad (\sigma_{max} > 0)$$

Walker

$$\sigma_{ar} = \sigma_{max}^{1-\gamma}\sigma_a^{\gamma} \qquad (\sigma_{max} > 0)$$

$$\sigma_{ar} = \sigma_{max}\left(\frac{1-R}{2}\right)^{\gamma} \qquad (\sigma_{max} > 0)$$

Woehler Curves- Mean Stress

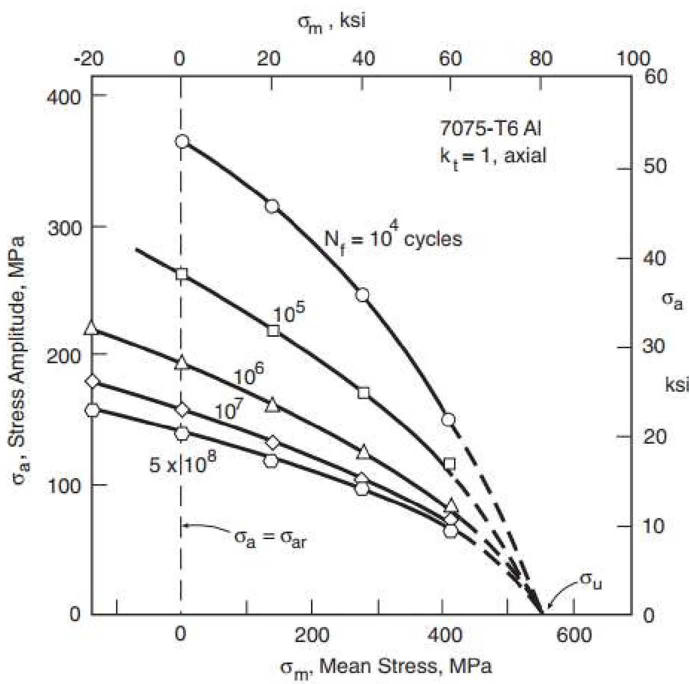

Constant life diagram for 7075-T6 aluminum

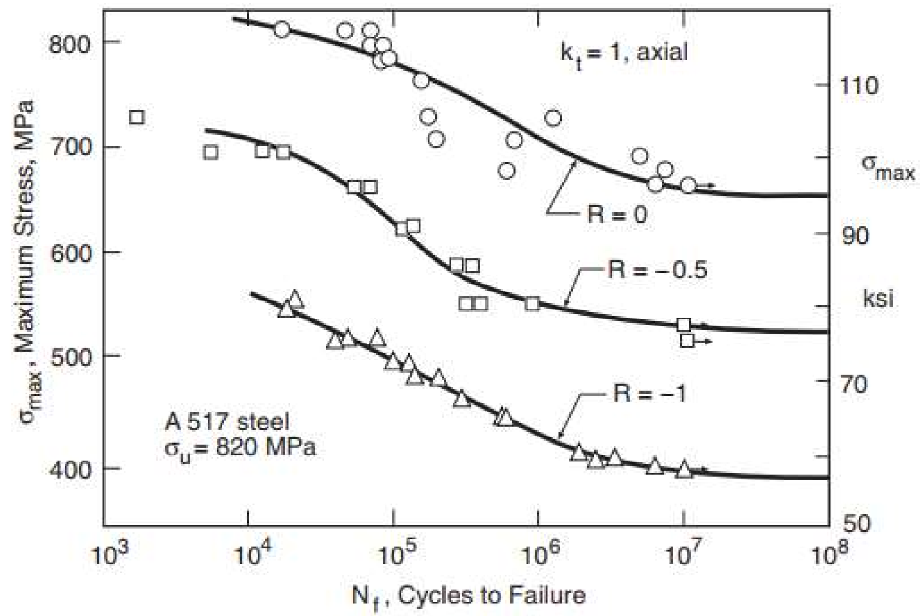

Stress-life curves for axial loading of unnotched A517 steel for constant values of the stress ratio R

Learning Outcome

By the end of this course, you will know

- Material failure under cyclic loading
- The role of plasticity and applicability of LEFM under cyclic loading
- Crack initiation, propagation and final growth until rupture
- Life estimation on a pre-cracked component
- The crack growth rate da/dN and the role of the stress intensity factor K in the crack growth

Pensum book

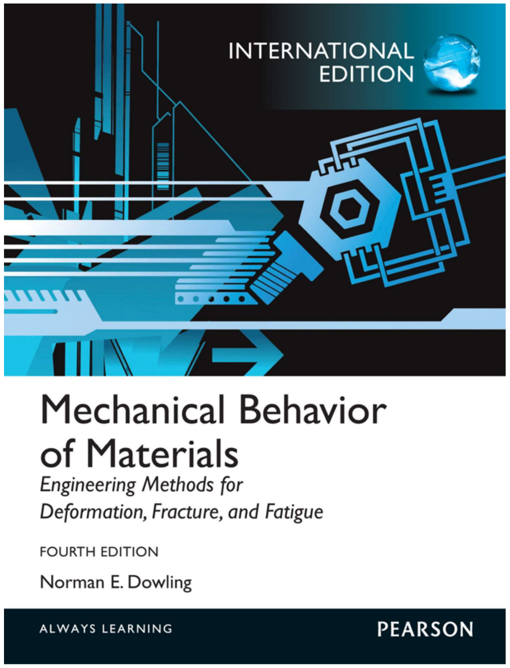

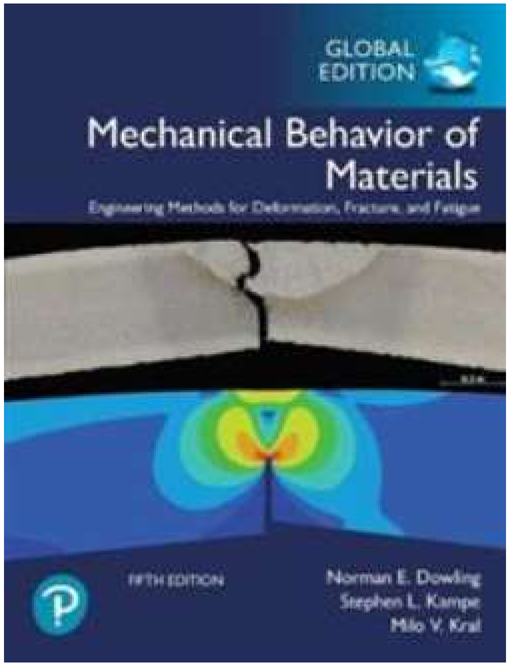

N. E. Dowling, *Mechanical Behavior of Materials*, Pearson, Boston, 4th edition., 2012.

What is a crack?

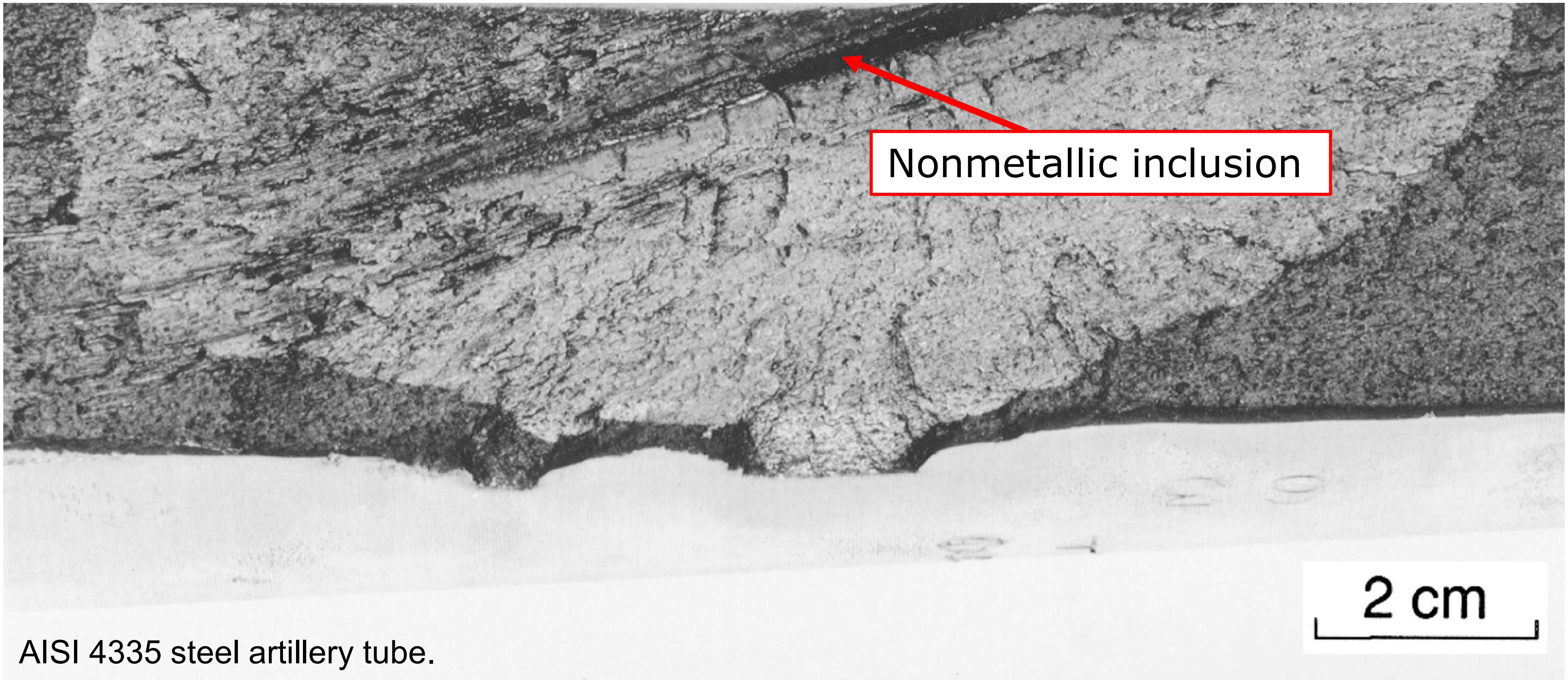

AISI 4335 steel artillery tube.

Photo courtesy of J. H. Underwood, U.S. Army Armament RD&E Center, Watervliet, NY.

Modes of Crack Surface Displacement

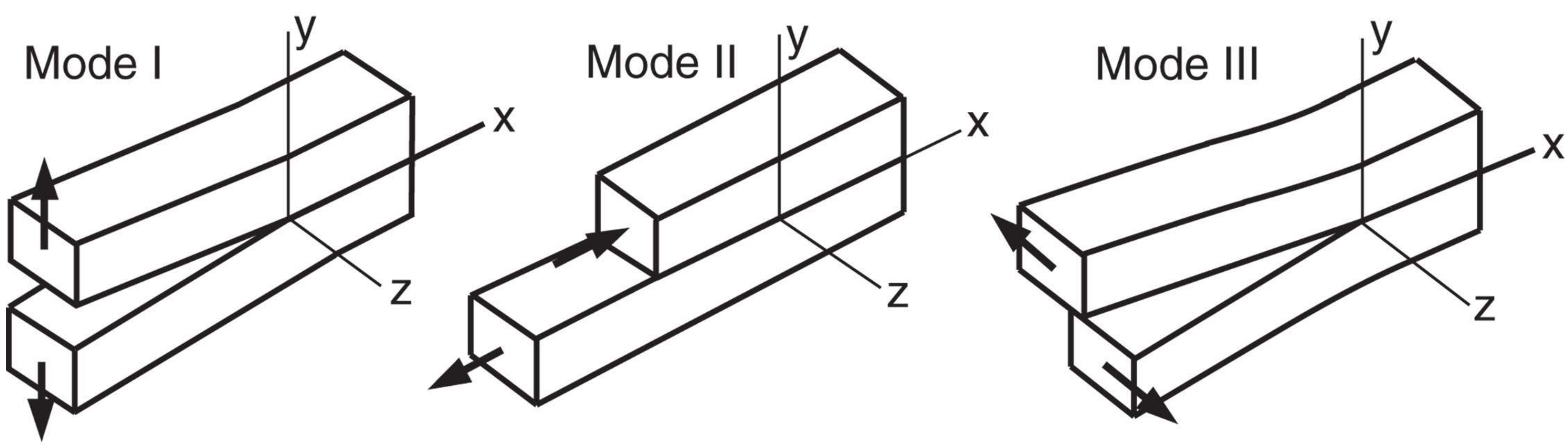

Tension | In plane Shear | Out of plane Shear

Local stresses at the crack tip

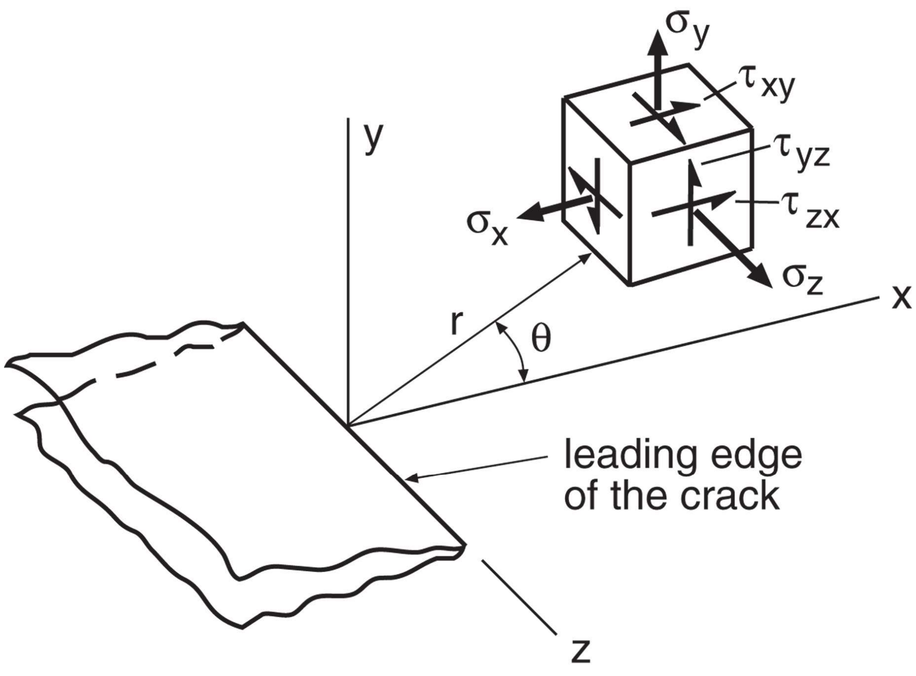

$$\sigma_x = \frac{K_I}{\sqrt{2\pi r}} \cos\frac{\theta}{2}\left[1 - \sin\frac{\theta}{2}\sin\frac{3\theta}{2}\right] + \cdots$$

$$\sigma_y = \frac{K_I}{\sqrt{2\pi r}} \cos\frac{\theta}{2}\left[1 + \sin\frac{\theta}{2}\sin\frac{3\theta}{2}\right] + \cdots$$

$$\tau_{xy} = \frac{K_I}{\sqrt{2\pi r}} \cos\frac{\theta}{2}\sin\frac{\theta}{2}\cos\frac{3\theta}{2} + \ldots$$

$\sigma_z = 0$ (plane stress)

$\sigma_z = \nu(\sigma_x + \sigma_y)$ (plane strain; ε_z=0)

$\tau_{yz} = \tau_{zx} = 0$

$$K_I = FS\sqrt{\pi a}$$

Geometry factor

Crack length

Nominal remote applied stress

K…magnitude (intensity) of the stresses in the vicinity of an ideally sharp crack tip

Plasticity limitation

Plane stress

$$r_{p\sigma} = \frac{1}{\pi}\left(\frac{K}{\sigma_0}\right)^2$$

Yield strength

Plane strain

$$r_{p\varepsilon} = \frac{1}{3\pi}\left(\frac{K}{\sigma_0}\right)^2$$

G.R. Irwin

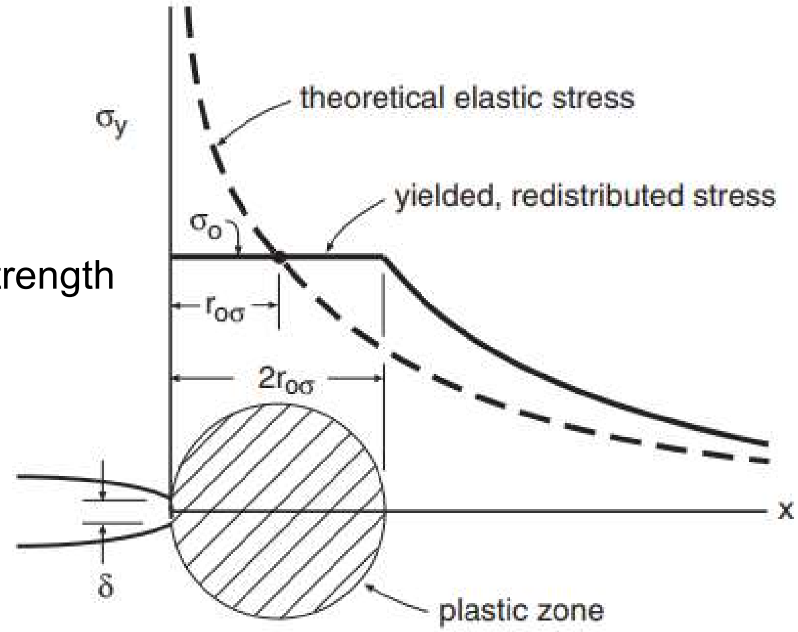

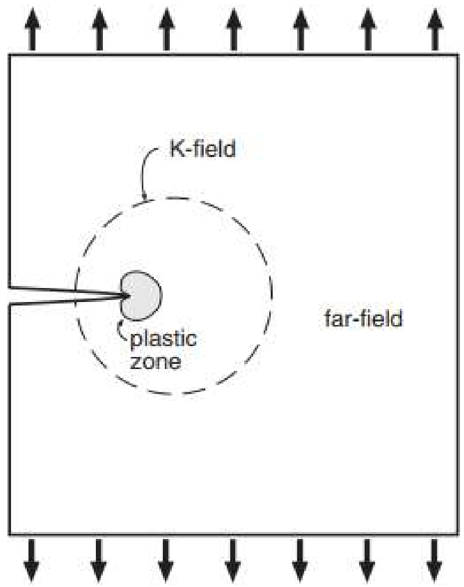

Plasticity limitation

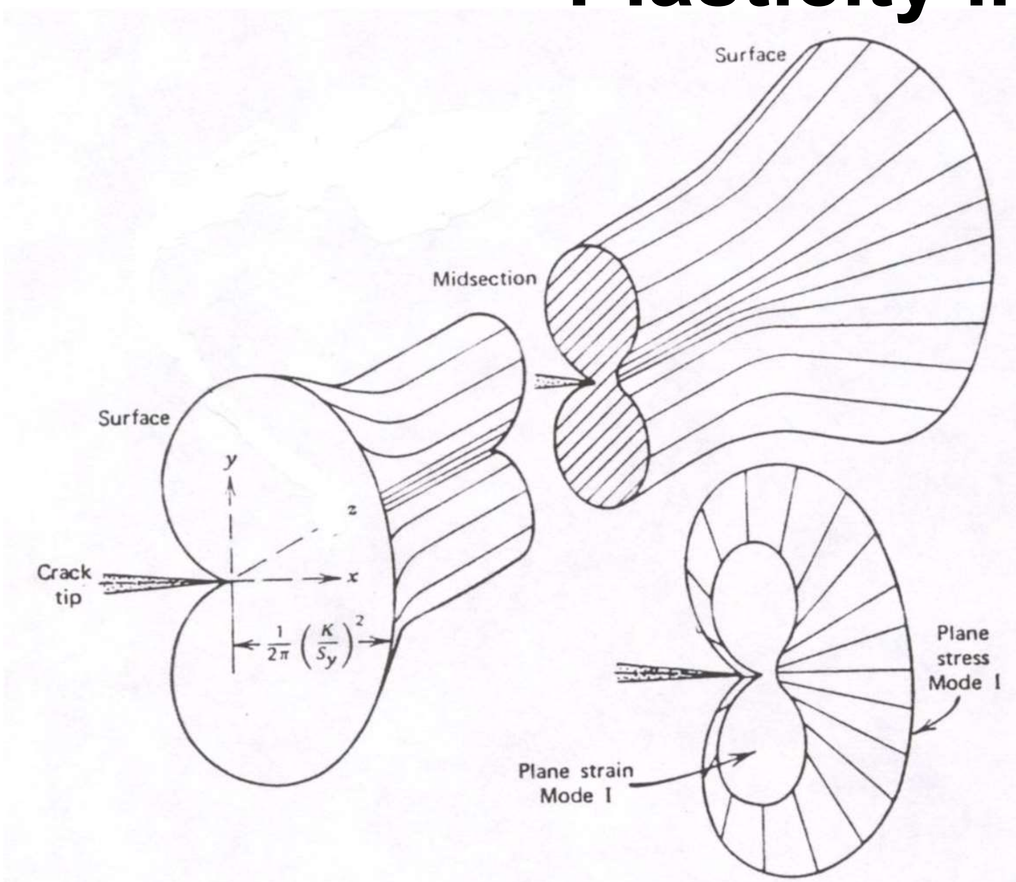

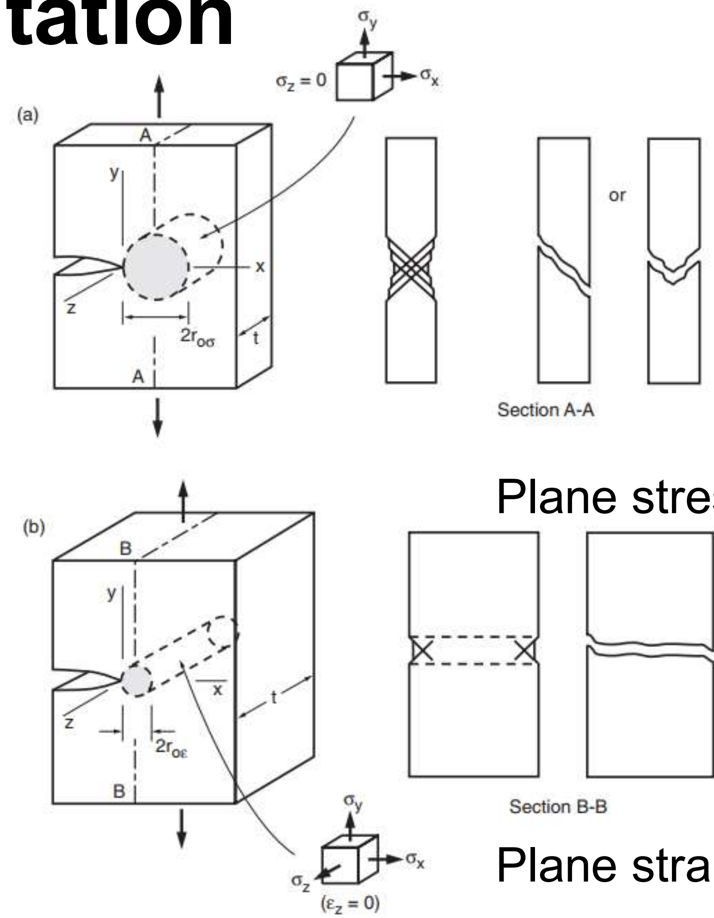

Plane stress

Plane strain

Plasticity limitation- cyclic plastic zone

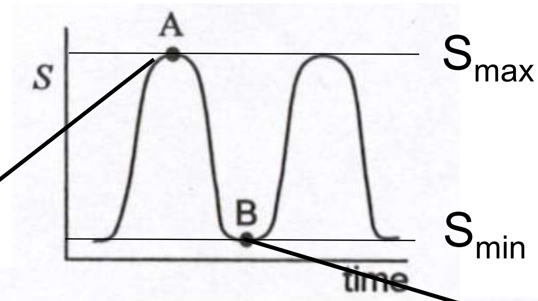

$$R = \frac{K_{min}}{K_{max}}$$

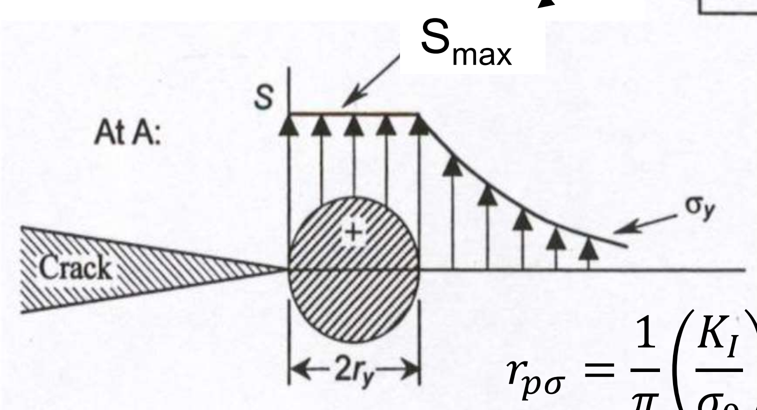

$$r_{p\sigma} = \frac{1}{\pi}\left(\frac{K_I}{\sigma_0}\right)^2$$

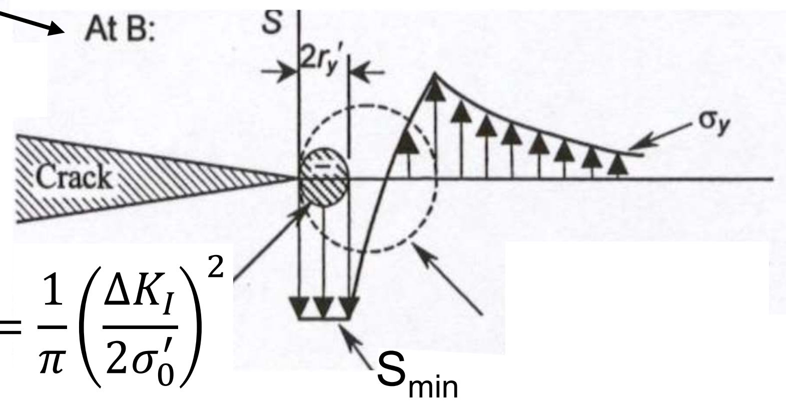

$$r_{c\sigma} = \frac{1}{\pi}\left(\frac{\Delta K_I}{2\sigma_0'}\right)^2$$

- Inelastic stress distribution in plastic zone of opposite sign of the applied stress
- The plastic zone is smaller (for R=0, ¼ of the monotonic zone)
- Fatigue cracks sharp, far filed stresses small => LEFM is applied in fatigue crack growth.

Plasticity limitation

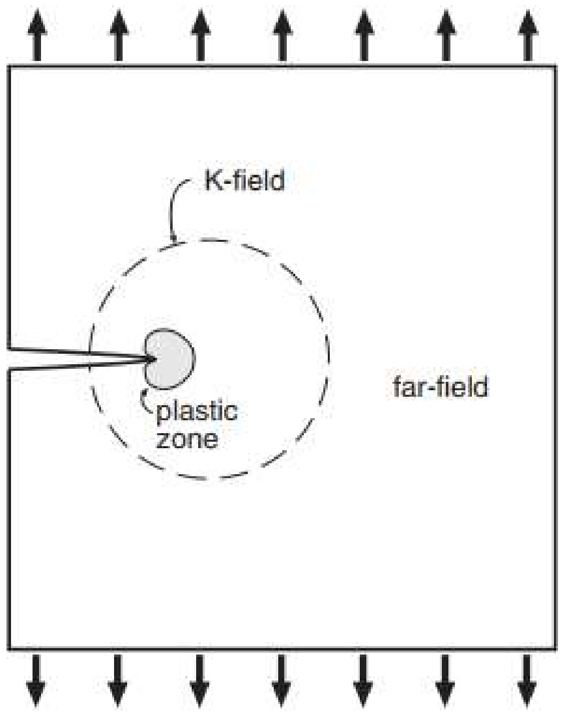

$$a, (b-a), h \geq \frac{4}{\pi}\left(\frac{K}{\sigma_o}\right)^2$$

LEFM applicable

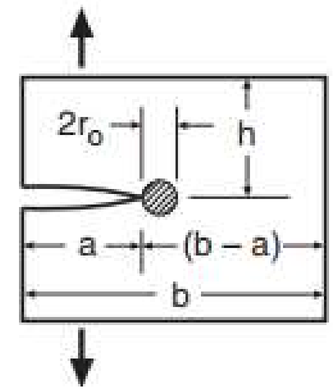

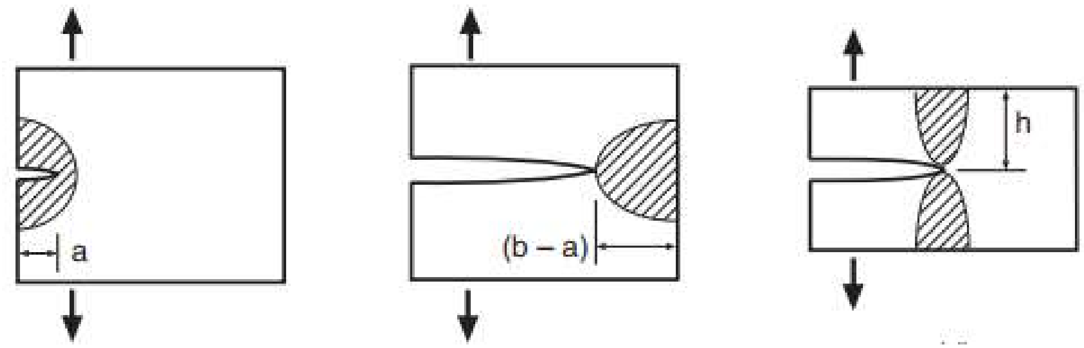

Applicability of LEFM under cyclic loading

Monotonic Loading → **Cyclic Loading**

Stress Intensity Factor

$$K_I = FS\sqrt{\pi a}$$

$$K_{max} = FS_{max}\sqrt{\pi a} \qquad K_{min} = FS_{min}\sqrt{\pi a}$$

$$\Delta K = K_{max} - K_{min} \qquad R = \frac{K_{min}}{K_{max}}$$

Plastic zone size- Plane stress

$$2r_{0\sigma} = \frac{1}{\pi}\left(\frac{K_I}{\sigma_0}\right)^2$$

$$r_c = \frac{1}{\pi}\left(\frac{\Delta K_I}{2\sigma'_{YS}}\right)^2$$

Plastic zone size- Plane strain

$$2r_{0\varepsilon} = \frac{1}{3\pi}\left(\frac{K_I}{\sigma_0}\right)^2$$

$$r_c = \frac{1}{3\pi}\left(\frac{\Delta K_I}{2\sigma'_{YS}}\right)^2$$

Fatigue cracks sharp, far filed stresses are small => LEFM is commonly applied in fatigue crack growth.

N. E. Dowling, *Mechanical Behavior of Materials*, Pearson, Boston, 4th edition., 2012.

Crack Growth under cyclic loading

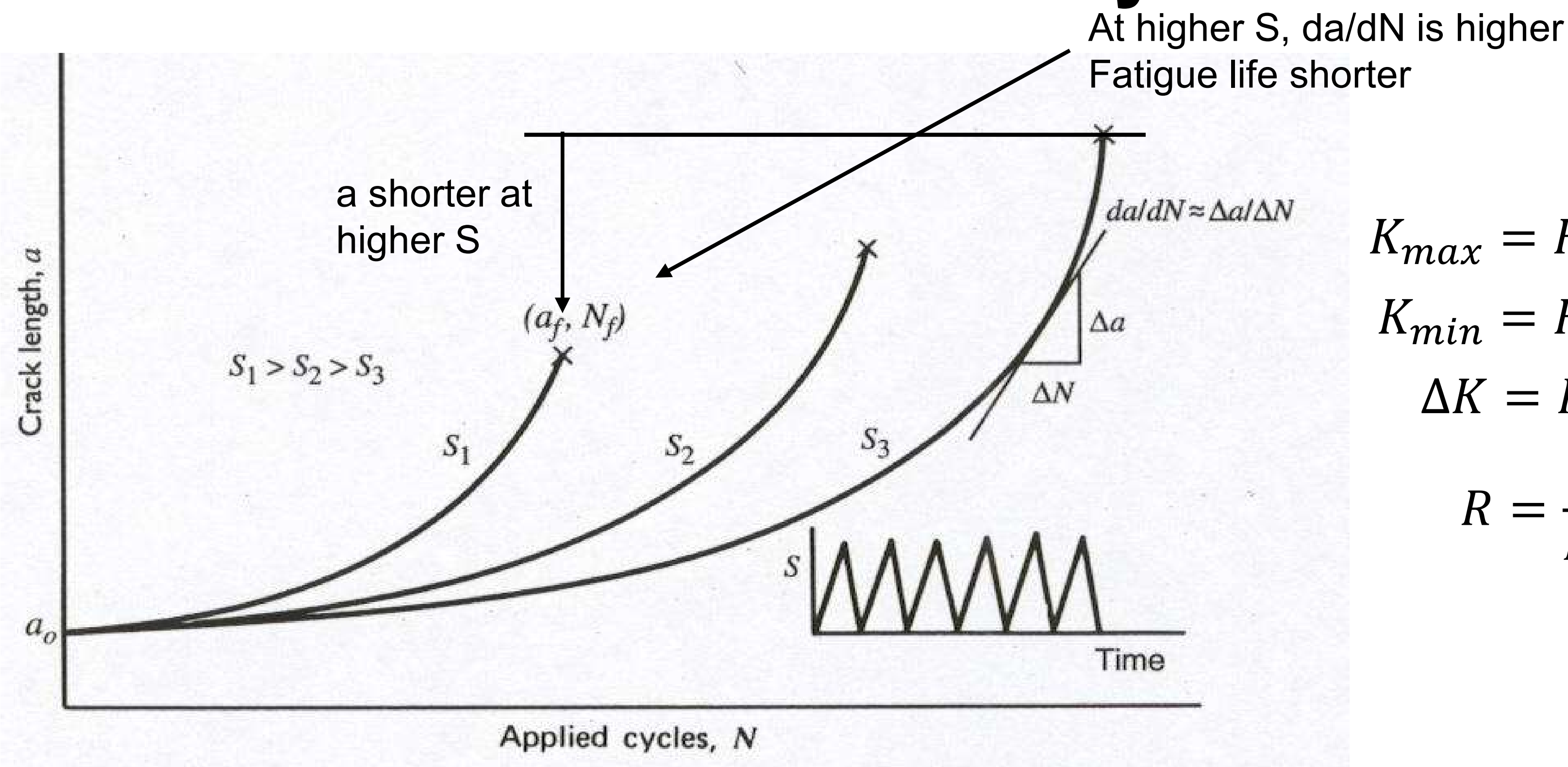

$$K_{max} = FS_{max}\sqrt{\pi a}$$

$$K_{min} = FS_{min}\sqrt{\pi a}$$

$$\Delta K = K_{max} - K_{min}$$

$$R = \frac{K_{min}}{K_{max}}$$

Given and initial a, life to fracture depends on S and the final fracture resistance of the material (which dictates final crack length)

N. E. Dowling, *Mechanical Behavior of Materials*, Pearson, Boston, 4th edition., 2012.

Crack Growth under cyclic loading

Monotonic Loading → **Cyclic Loading**

Stress is constant
Fracture at
- crack length, $a=a_C$,
- Giving $K_I=K_{IC}$

For **$a<a_C$($K_I<K_{IC}$)** the crack will **not propagate**

Stress is dynamic
Fracture at
- $K_I=K_{IC}$ for a certain instant of time
- for $K_I<K_{IC}$, the crack may still propagate

a grows until fracture at $a=a_c$

Growth of fatigue cracks depends on the cyclic value of the Stress Intensity Factor!

Crack Growth under cyclic loading

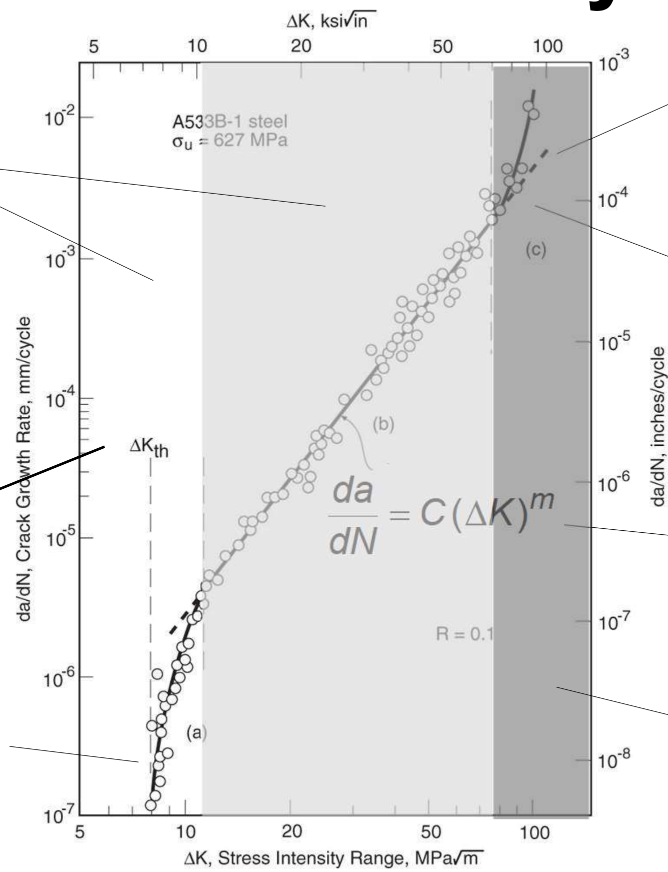

da/dN unstable at high ΔK
Brittle fracture/ gross yielding

K_{max}=K_c governed by fracture toughness of material and thickness

Power relationship between extremes for R~0, $m \approx$ 2-4 for metals

Fatigue crack growth threshold

da/dN slow at low ΔK

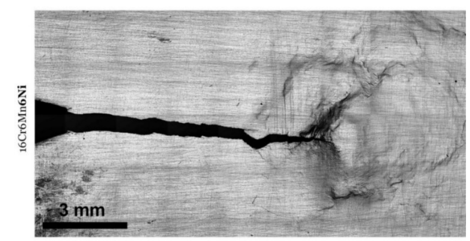

P. Paris and F. Erdogan, Journal of Basic Engineering, 1963, 85, 528–533.

Stages of Crack Evolution

Stage I: Initiation

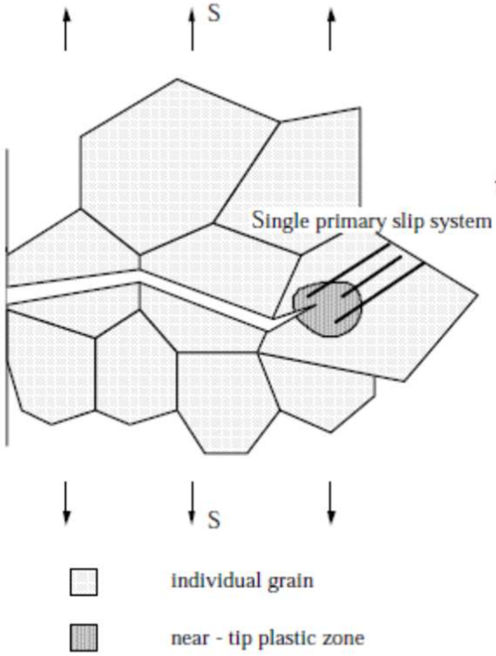

microstructure sensitive ,
difficult to quantify and model

Stage II: Propoagation

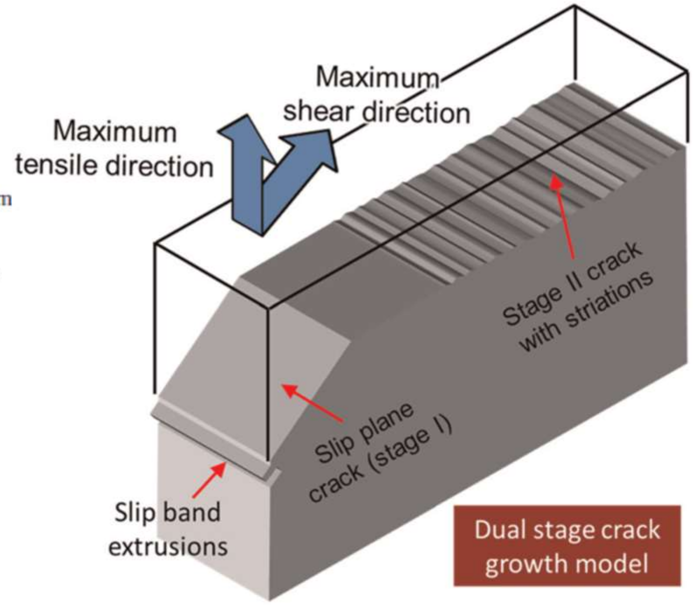

a large part of fatigue life approximated by Paris law

Stage III: Final Growth until rupture

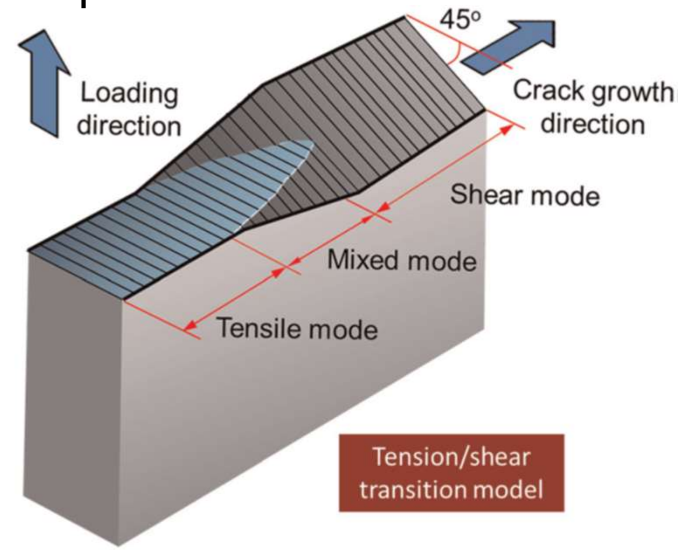

high ΔK with the development of 45deg inclined shear planes

N. E. Dowling, *Mechanical Behavior of Materials*, Pearson, Boston, 4th edition., 2012.

Crack Growth under cyclic loading

- **Small cracks**
  - Shear driven
  - Interact with microstructure
  - Mostly analysed by continuum mechanics + dislocation-based approaches
- **Large cracks**
  - Tension driven
  - Fairly insensitive to the microstructure
  - Mostly analyzed by fracture mechanics models

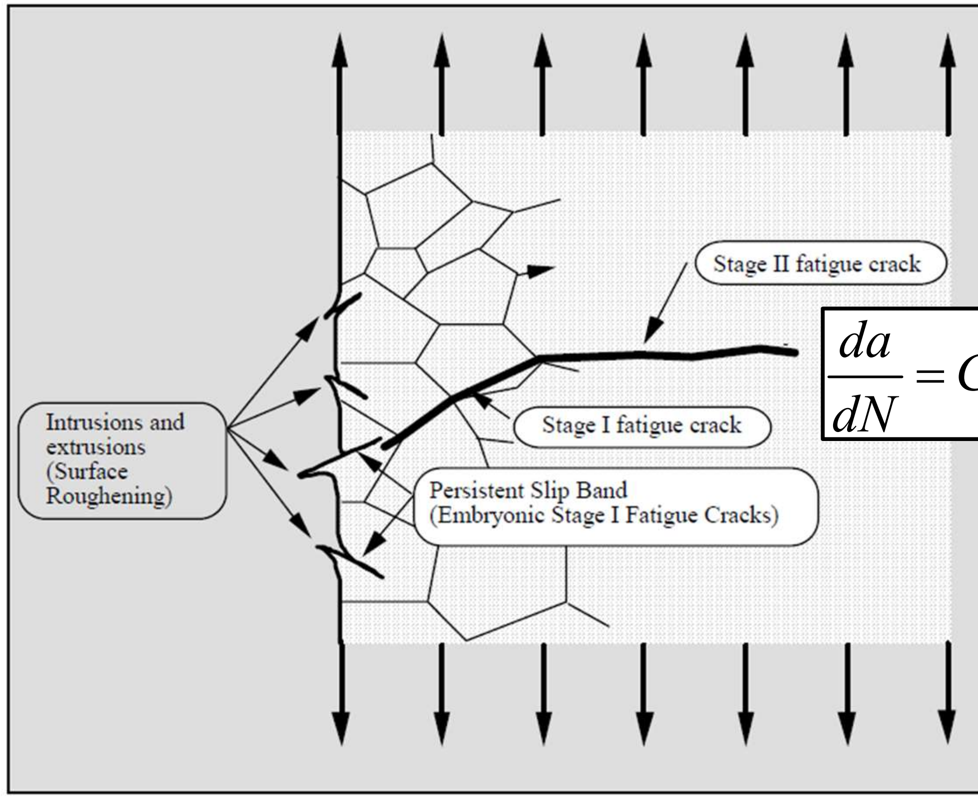

$$\frac{da}{dN} = C(\Delta K)^m$$

N. E. Dowling, *Mechanical Behavior of Materials*, Pearson, Boston, 4th edition., 2012.

Crack Growth under cyclic loading

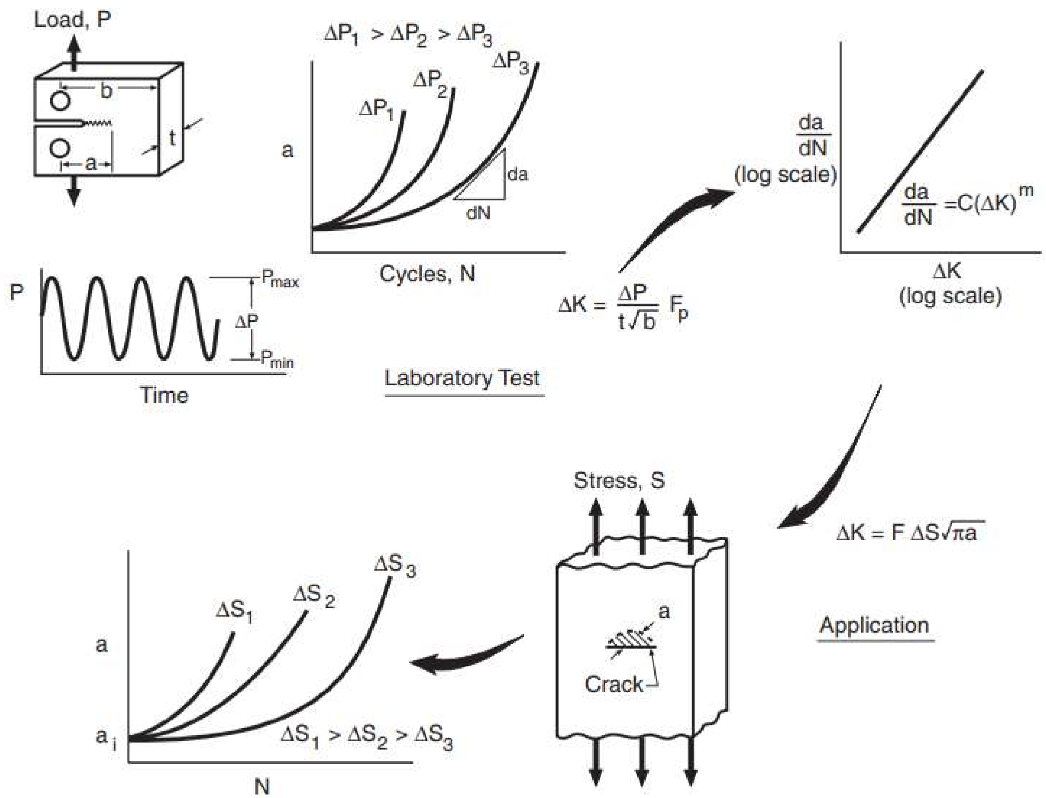

Dowling- Mechanical Behavior of Materials, Fourth Edition, Pearson 2013

Residual life under cyclic loading

- da/dN increases with a

Function including effects of environment, frequency,…

$$\int_{N_i}^{N_f} dN = N_f - N_i = N_{if} = \int_{a_i}^{a_f} \frac{da}{f(\Delta K, R)}$$

Number of cycles from initial a_i at N_i to final a_f at N_f

$$\frac{da}{dN} = f(\Delta K, R) = C(\Delta K)^m \qquad \Delta K = F\Delta S\sqrt{a}$$

$$N_{if} = \int_{a_i}^{a_f} \frac{1}{C(F\Delta S\sqrt{a})^m} \frac{da}{a^{\frac{m}{2}}} = \frac{a_f^{1-\frac{m}{2}} - a_i^{1-\frac{m}{2}}}{C(F\Delta S\sqrt{\pi})^m(1-\frac{m}{2})}$$

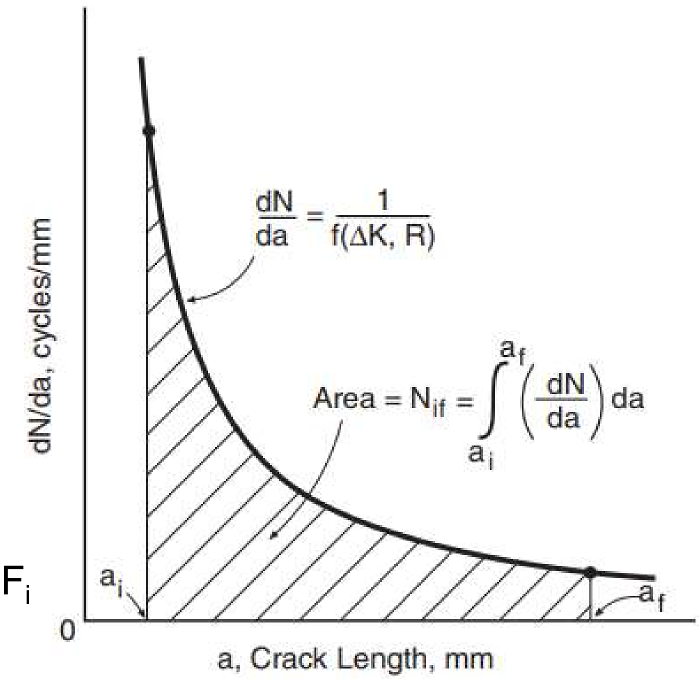

- For m=3, a_i dominates, life insensitive to a_f
- Most of the cycles are accumulated at a_i –> choose F close to F_i
- For m=2 the equation is indeterminate
- Only under constant amplitude!

N. E. Dowling, *Mechanical Behavior of Materials*, Pearson, Boston, 4th edition., 2012.

Effects of Load Ratio R- Walker equation

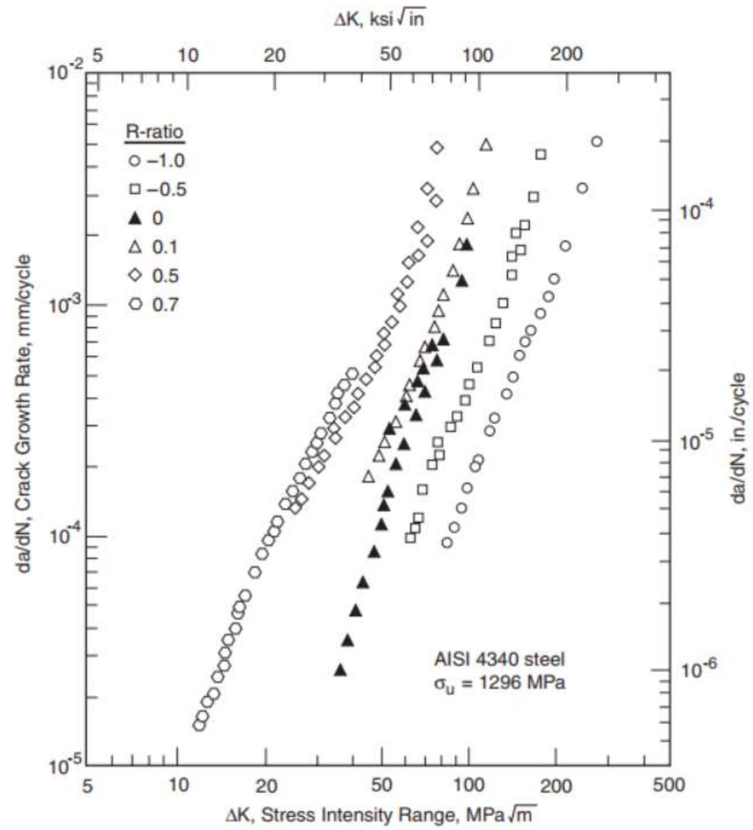

How to compensate for load ratio?

Dowling- Mechanical Behavior of Materials, Fourth Edition, Pearson 2013

Effects of Load Ratio R- Walker equation

$$\Delta K = K_{max} - \cancel{K_{min}},$$

Equivalent zero-to-tension (R=0) stress intensity

$$\overline{\Delta K} = \frac{\Delta K}{(1-R)^{1-\gamma}}$$

Material constant

Constant for R=0

$$\frac{da}{dN} = C_0 \left[\frac{\Delta K}{(1-R)^{1-\gamma}} \right]^m$$

Paris Law for Walker $\overline{\Delta K}$

- γ has to be found from a linear regression of specimen tested at different R
- γ=0 when R=0 such that $\Delta K = K_{max}$

Dowling- Mechanical Behavior of Materials, Fourth Edition, Pearson 2013

Effects of Load Ratio R- Walker equation

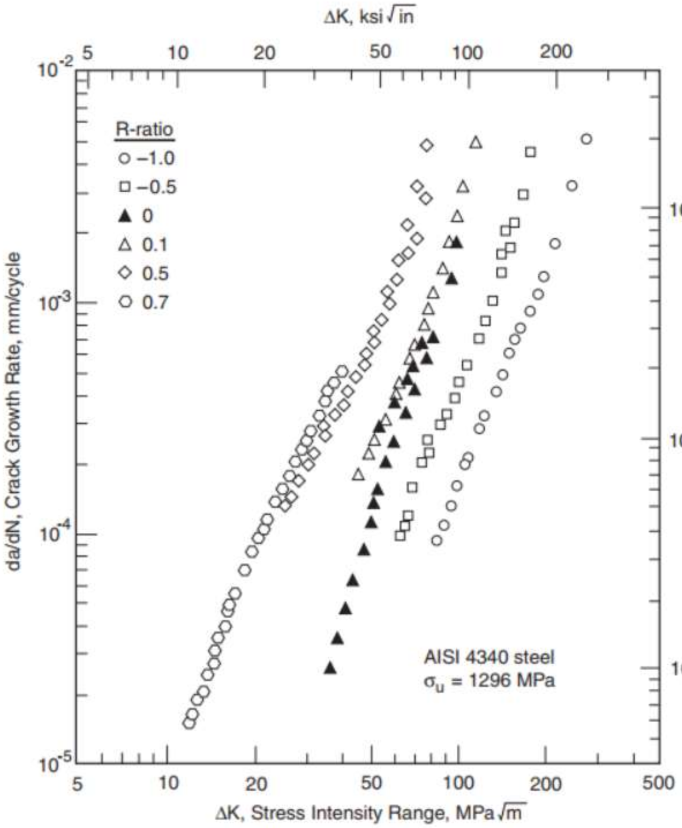

$$\frac{da}{dN} = C_0 \left[\frac{\Delta K}{(1-R)^{1-\gamma}} \right]^m$$

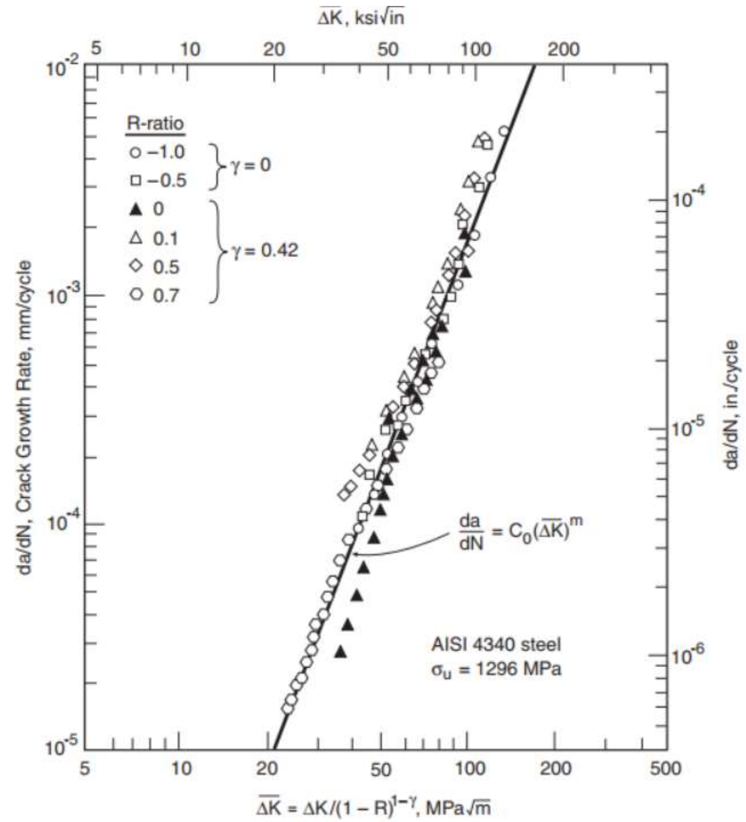

N. E. Dowling, *Mechanical Behavior of Materials*, Pearson, Boston, 4th edition., 2012.

Summary

- Materials fracture brittle under cyclic loading. The load can be under the yield strength of the material
- A crack is a defect from which fatigue failure can be initiated
- As long as the plastic zone remains small, LEFM can be applied, which is generally the case under cyclic loading
- The crack growth behavior can be described by the crack growth rate da/dN and the stress intensity factor ΔK
- Fatigue crack growth can be divided into three regimes, initiation, stable growth and final growth until failure, they are characterized by typical fracture surfaces
- Between ΔK_{th} and K_C, a linear power law describes the crack growth behavior
- The effect of the load ratio R can be compensated via the Walker equation

Local Approaches for fatigue design

Part 2: Fatigue is local

Outlines

- **Introduction**
- Notch and geometrical discontinuities
- Local approaches
- Defects and fatigue design
- Multiaxial loadings
- Additive materials: some examples

Challenges in Design of AM components

- Design in presence of geometrical discontinuity
- Safety in presence of defects due to the process
- Assessment in presence of complex loadings

Fatigue design

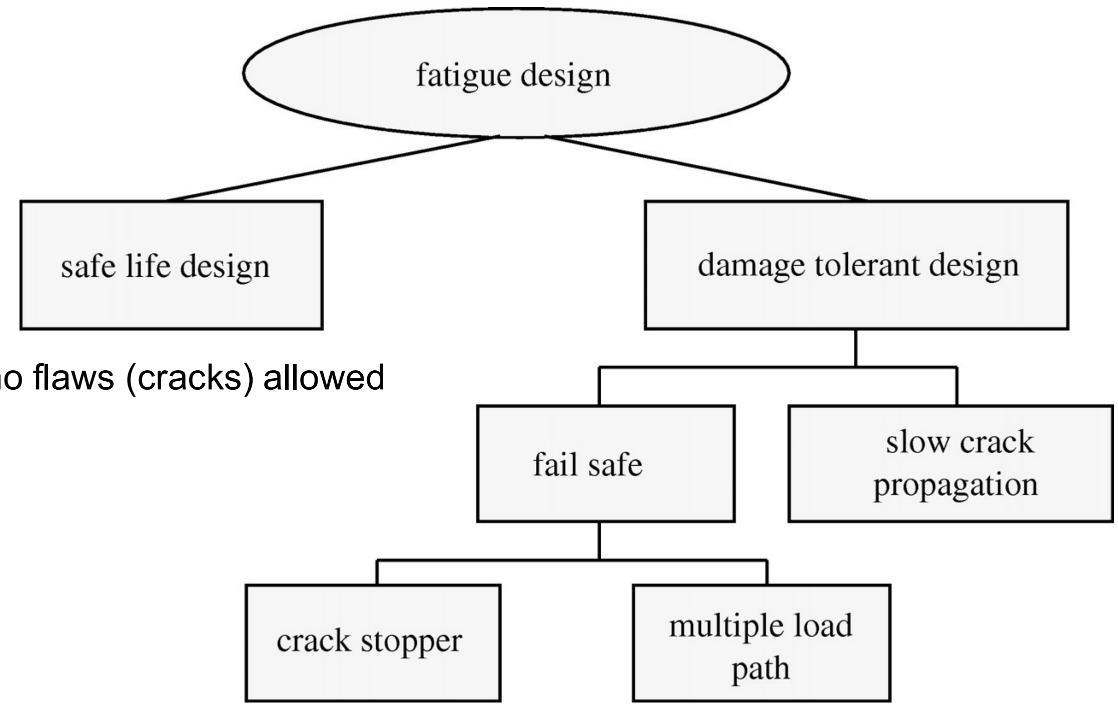

no flaws (cracks) allowed

Stress (strain)-based fatigue design

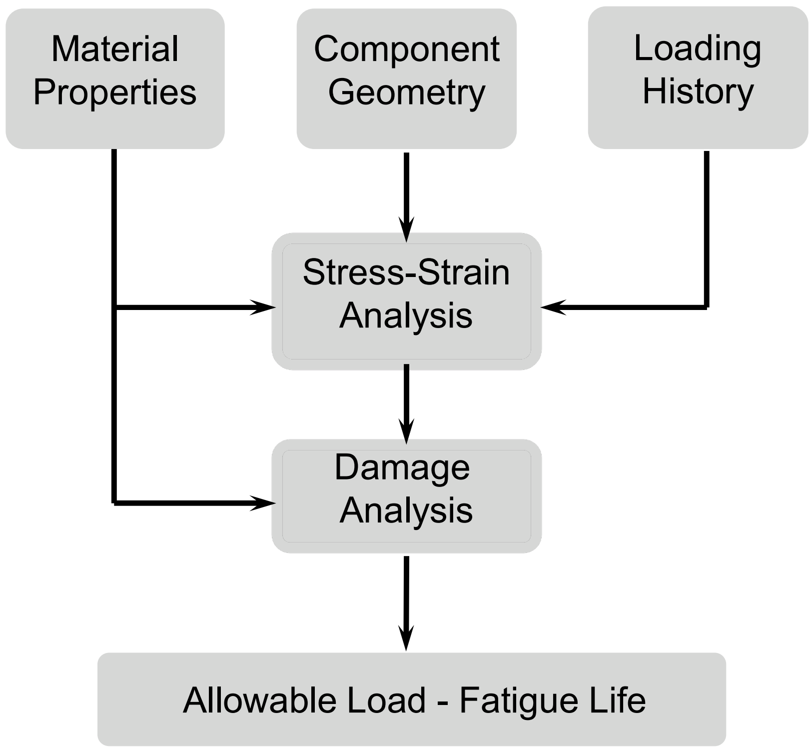

Fracture Mechanics
Pre-requisites

FATIGUE IS LOCAL

Multi-Scale Nature of Fracture

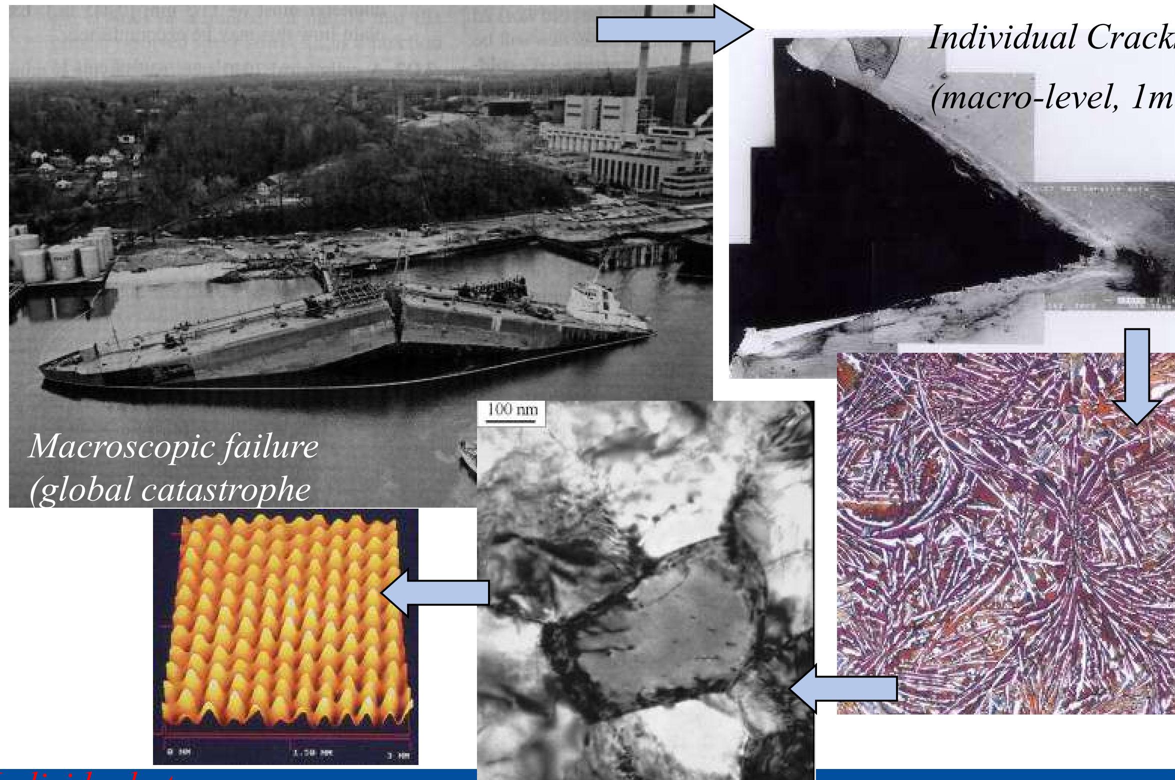

Stages of Fatigue

- Crack initiation I
- Crack growth II
- Final rupture III

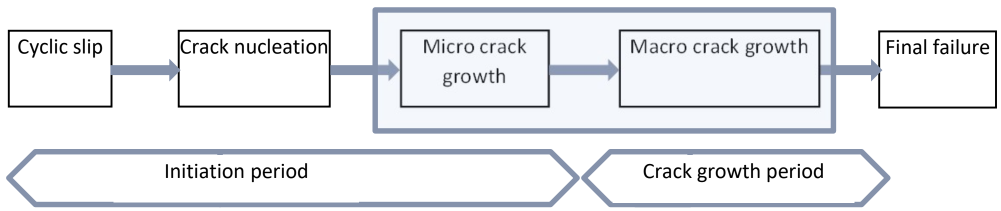

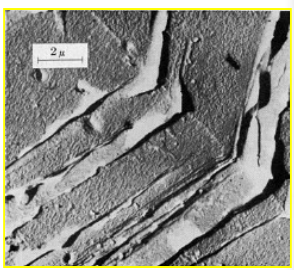

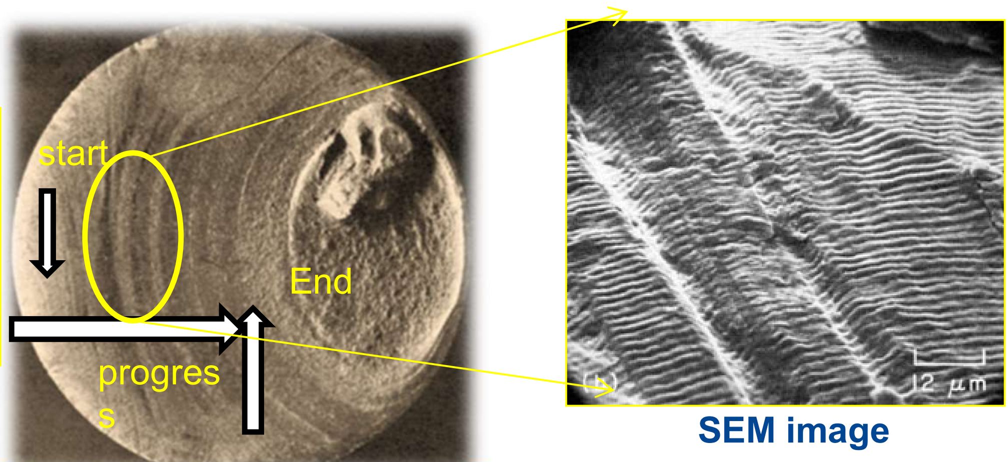

SEM image

Fatigue life diagram in
Ultra High Cycle Fatigue (UHCF) Regime

Predominant crack growth

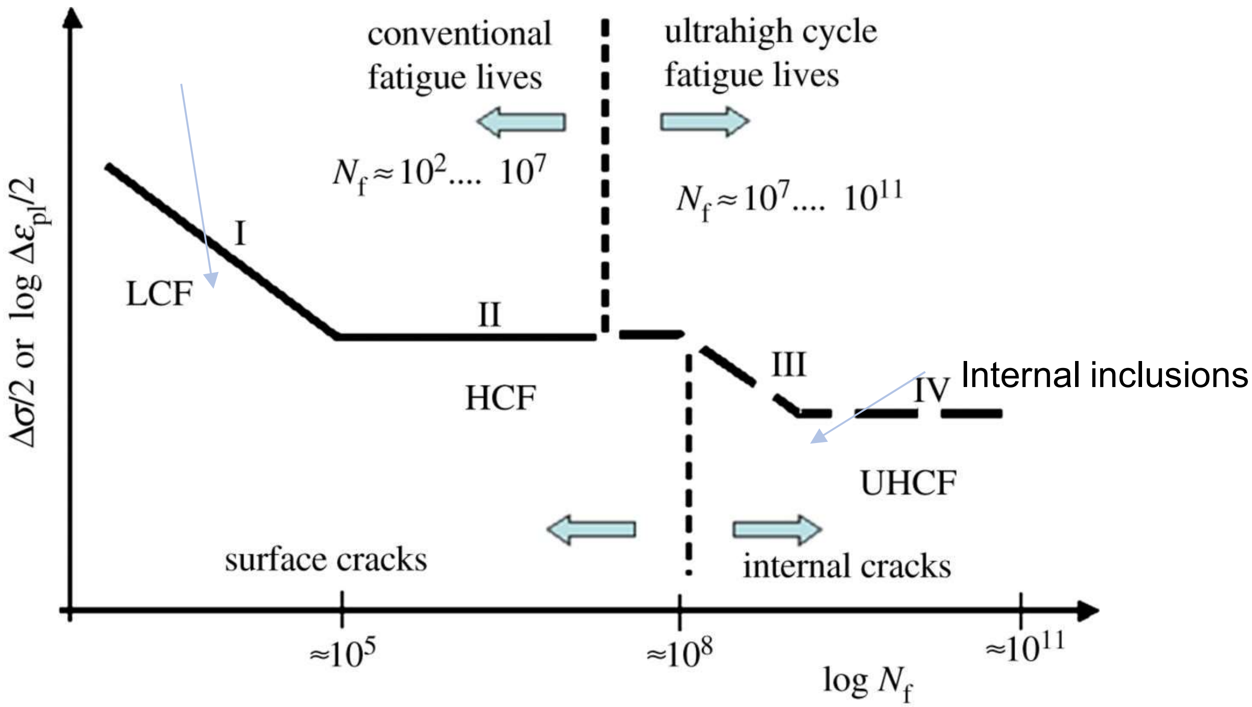

Morphology of Fatigue Initiation

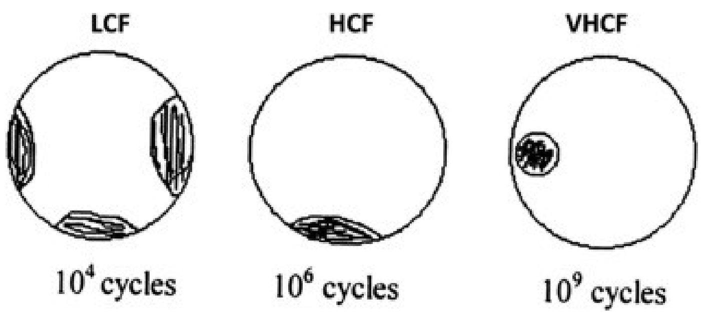

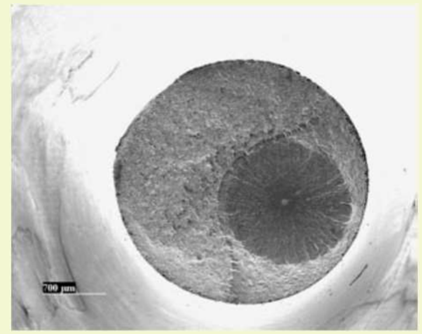

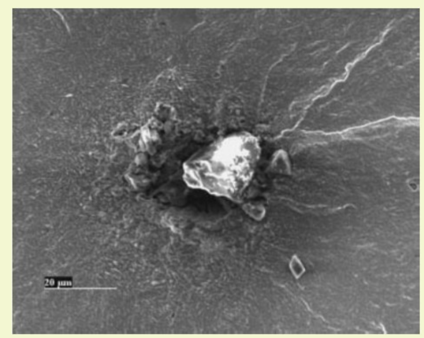

Fatigue crack initiation at inclusion Initiation in high-strength steel 4240

Characteristic Size of Crack Initiation

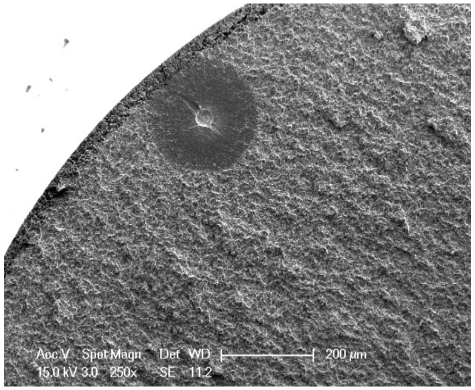

(1% C, 1% Cr)

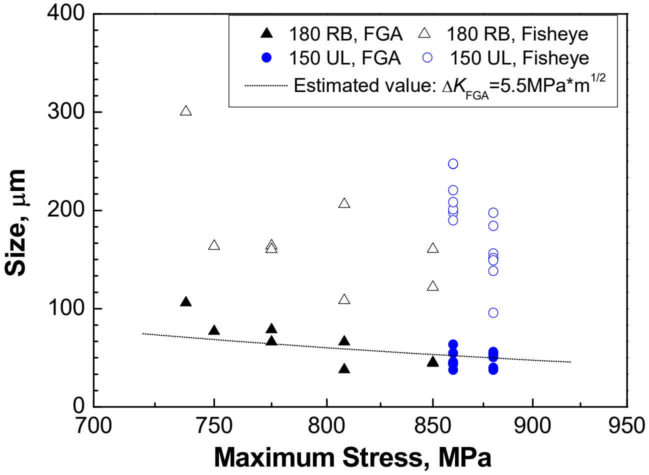

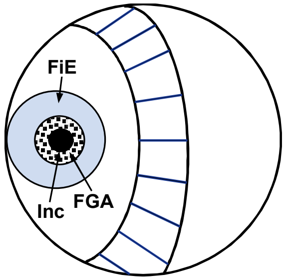

- FGA sizes within a relatively small range: 40 – 100 µm
- Fish-eye sizes distributed in a large range: 100 – 300 µm

• Hong Y, Lei Z, Sun C, Zhao A. *Int J Fatigue*, 2014, 58:144–151

Surface Finish Effects on Fatigue Limit

The scratches, pits and machining marks on the surface of a material add stress concentrations to the ones already present due to component geometry. The correction factor for surface finish is sometimes presented on graphs that use a qualitative description of surface finish such as “polished” or “machined”

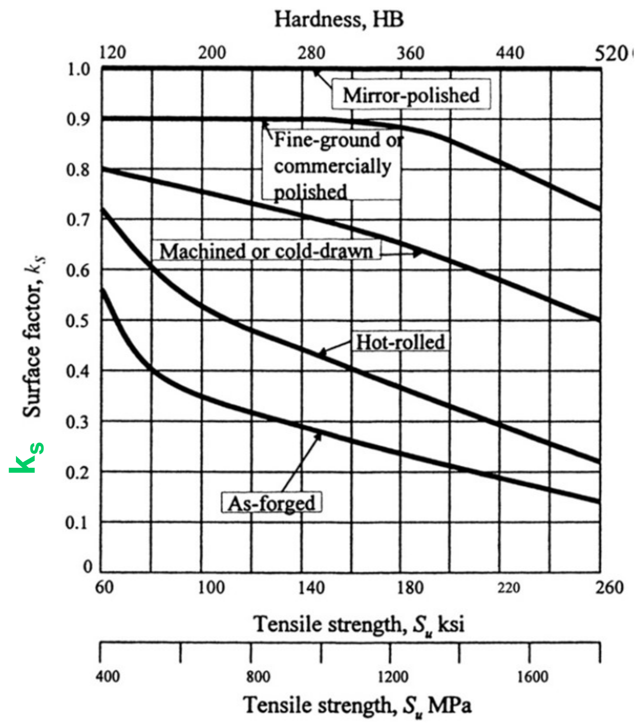

Below a generalized empirical graph is shown which can be used to estimate the effect of surface finish in comparison with mirror-polished specimens [Shigley].

R. Budinas, J.K. Nisbett, Shigley's Mechanical Engineering Design, Mcgraw-Hill series, 2015

Effect of various surface finishes on the fatigue limit of steel. Shown are values of the k_s, the ratio of the fatigue limit to that for polished specimens.

Surface Finish Effects on Fatigue Limit

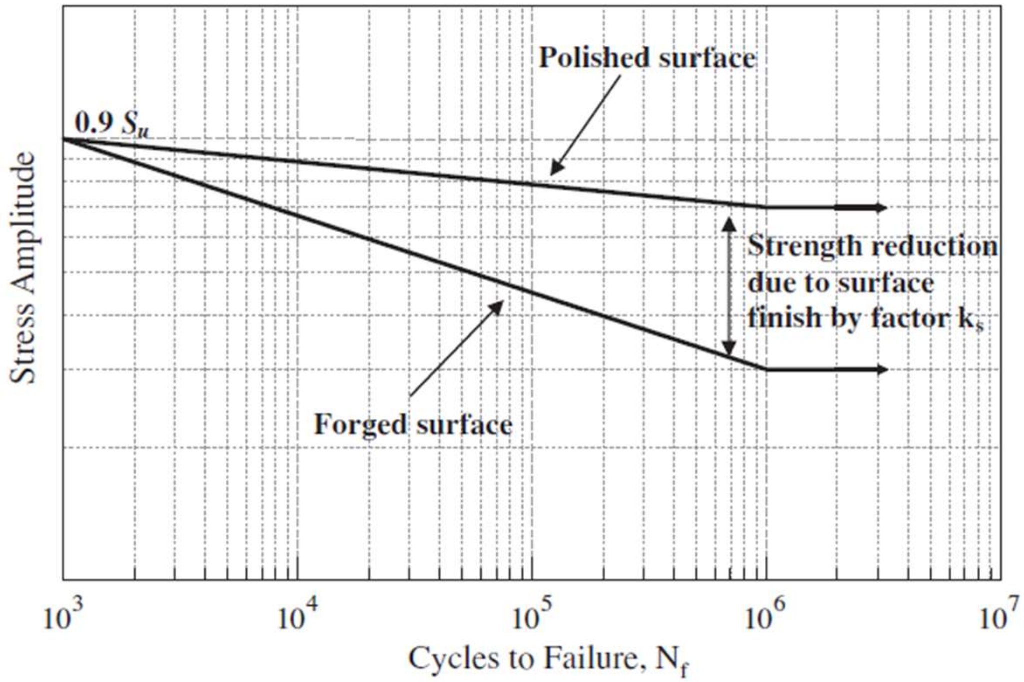

Surface Finish Effects on Fatigue Limit

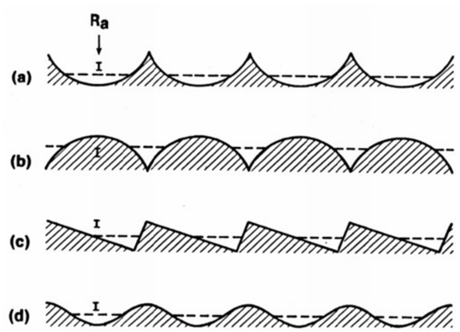

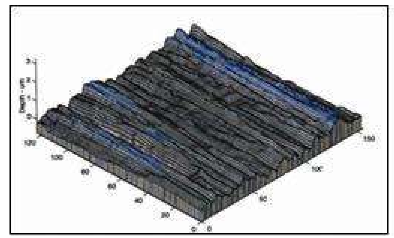

grinded

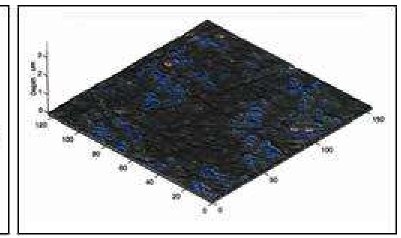

polished

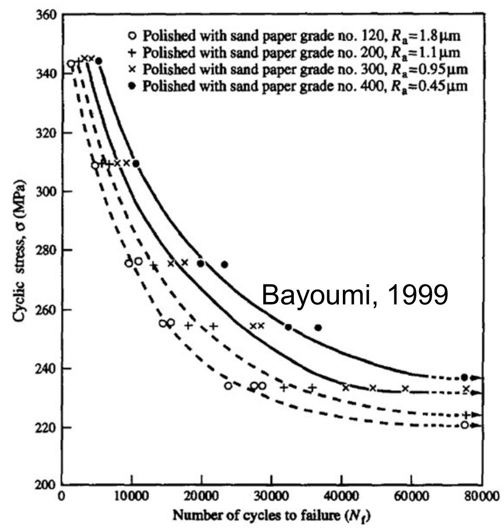

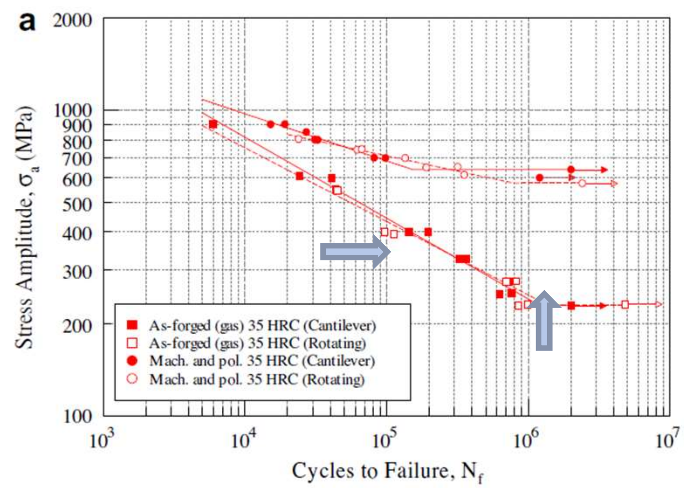

For AM materials

Building direction

Surface finishing

Residual stresses

Post-treatments

Coatings

Outlines

- Introduction
- **Notch and geometrical discontinuities**
- Local approaches
- Defects and fatigue design
- Multiaxial loadings
- Additive materials: some examples

Gustav Ernest Kirsch

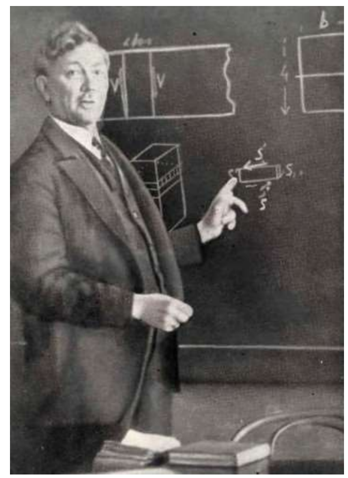

Stephen Timoshenko

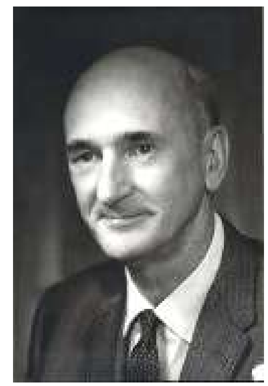

James Goodier

Small circular hole in a plate under uniaxial tension

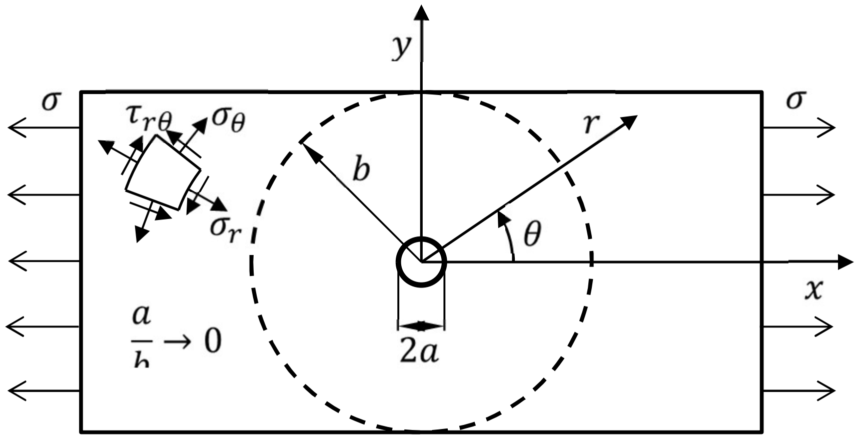

Problem geometry for a small circular hole in a plate

Boundary conditions:

At $r = a$,

$\sigma_r = \tau_{r\theta} = 0.$

At $r = b$,

$\sigma_x = \sigma, \sigma_y = \tau_{xy} = 0.$

$$\text{SCF} = \frac{\text{maximum stress}}{\text{applied stress}} = ?$$

Small circular hole in a plate under uniaxial tension

Assume Airy's stress function of the form $\varphi(r,\theta) = \varphi_1(r,\theta) + \varphi_2(r,\theta)$

where $\varphi_1(r,\theta) = A \ln r + Br^2$

and $\varphi_2(r,\theta) = \{C_1 r^4 + C_2 + C_3 r^2 + C_4 r^{-2}\} \cos 2\theta$

The resulting stress distribution, which satisfies B.Cs is given by:

$$\sigma_r = \frac{\sigma}{2}\left(1 - \frac{a^2}{r^2}\right) + \frac{\sigma}{2}\left(1 + \frac{3a^4}{r^4} - \frac{4a^2}{r^2}\right)\cos 2\theta\,,$$

$$\sigma_\theta = \frac{\sigma}{2}\left(1 + \frac{a^2}{r^2}\right) - \frac{\sigma}{2}\left(1 + \frac{3a^4}{r^4}\right)\cos 2\theta\,,$$

$$\tau_{r\theta} = -\frac{\sigma}{2}\left(1 - \frac{3a^4}{r^4} + \frac{2a^2}{r^2}\right)\sin 2\theta\,.$$

Small circular hole in a plate under uniaxial tension

Visualize the in-plane principal stresses (using MATLAB)

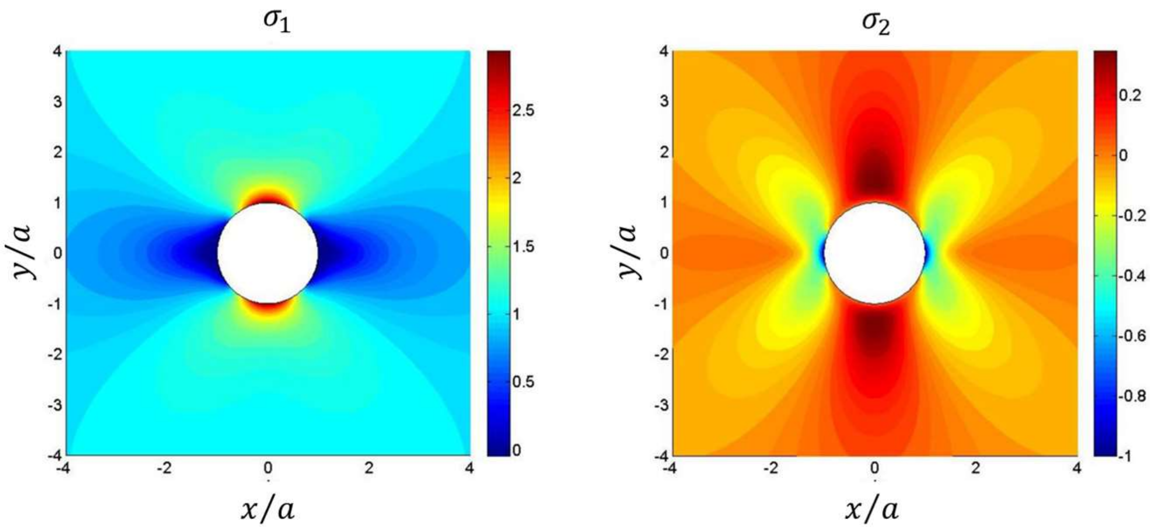

In-plane principal stresses for problem geometry shown before

Small circular hole in a plate under uniaxial tension

The maximum and minimum stresses occur along the hole boundary

$$\sigma_{\max} = \sigma_\theta(r = a, \theta = \pm\pi/2) = 3\sigma \text{ and } \sigma_{\min} = \sigma_\theta(r = a, \theta = 0, \pi) = -\sigma.$$

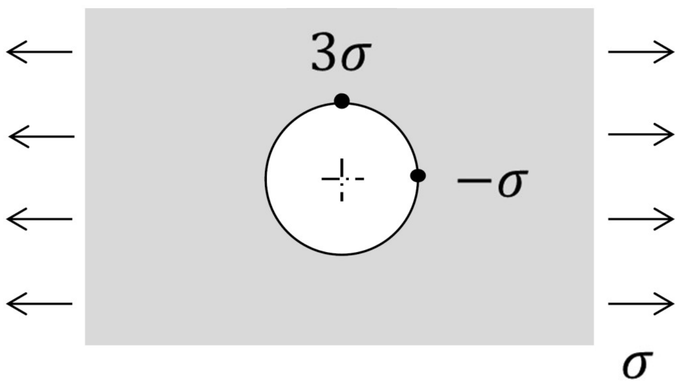

Location of max. and min. stresses

$$\text{SCF} = \frac{\text{maximum stress}}{\text{applied stress}} = 3$$

What about a plate with a small circular hole under:

1. Bi-axial loading?
2. Pure shear loading?

Charles Inglis

Problem of an elliptical hole

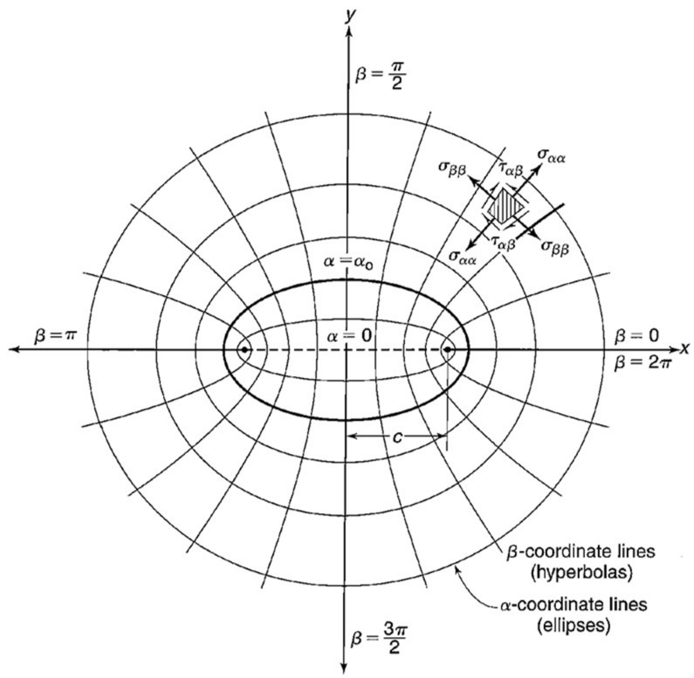

Problem geometry for an elliptical hole in a large plate

First solved by Inglis (1913).

Solution presented in an elliptical coordinate system.

Major axis: a

Minor axis: b

Focal length: $c = \sqrt{a^2 - b^2}$

And $\alpha_o = \text{arctanh}(b/a)$

Boundary conditions at $\alpha = \alpha_o$?

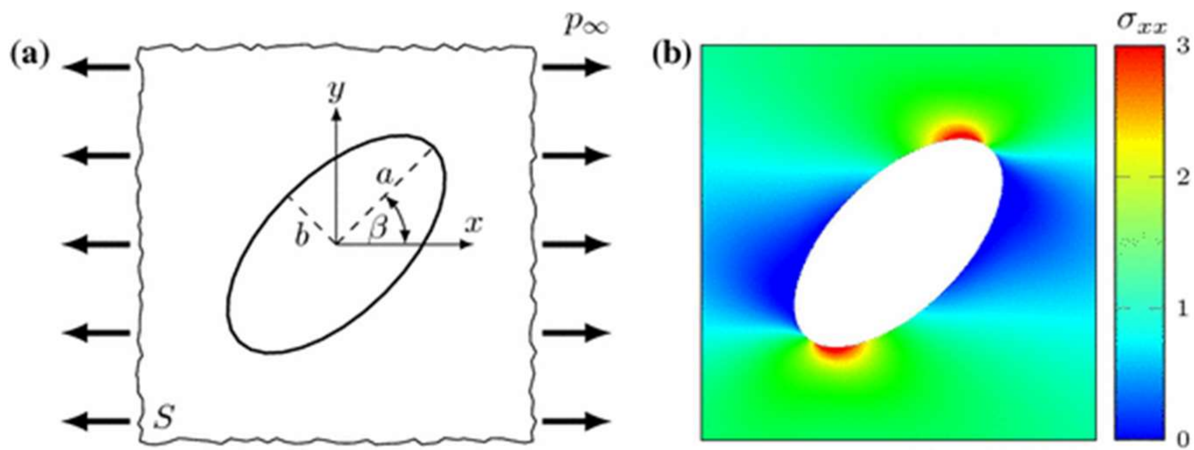
(a)
p_∞
y
a
b
β
x
S
(b)
σ_{xx}
3
2
1
0

Problem of an elliptical hole

$$\text{SCF} = \frac{\text{maximum stress}}{\text{applied stress}} = 1 + 2\left(\frac{\text{a}}{\text{b}}\right)$$

For circular hole, $a = b$ and SCF = 3 as discussed previously.

The above formula can also be expressed as:

$$\boxed{\text{SCF} = 1 + 2\sqrt{\frac{a}{\rho}}}$$

Can be applied to a cavity of *any* shape with total length $2a$ and tip radius ρ

For elliptical hole, ρ is the radius of curvature at the ends of the major axis:

$$\rho = \frac{b^2}{a}$$

Generalized notch solution

Lazzarin-Tovo

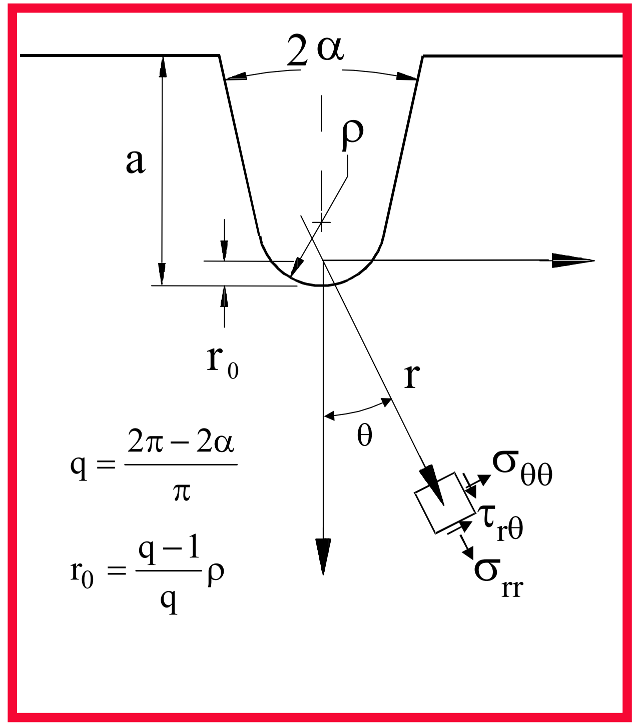

Complex potentials

$$\boxed{\varphi(z) = a z^{\lambda} + d z^{\mu}} \qquad \boxed{\psi(z) = b z^{\lambda} + c z^{\mu}}$$

- coefficients a, b, c and d are complex,
- exponents λ and μ are real, with $\lambda > 0$ and $\lambda > \mu$

When c and d are null, the approach matches Williams' solution (Williams, 1952, Carpenter, 1984).
Then, the general expressions of stress components turn out to be:

$$\boxed{\begin{aligned}\sigma_\theta = {} & \lambda r^{\lambda-1}\left[a_1(1+\lambda)\cos(1-\lambda)\theta + b_1\cos(1+\lambda)\theta + a_2(1+\lambda)\sin(1-\lambda)\theta - b_2\sin(1+\lambda)\theta\right] + \\ & + \mu r^{\mu-1}\left[d_1(1+\mu)\cos(1-\mu)\theta + c_1\cos(1+\mu)\theta + d_2(1+\mu)\sin(1-\mu)\theta - c_2\sin(1+\mu)\theta\right]\end{aligned}}$$

$$\boxed{\begin{aligned}\sigma_r = {} & \lambda r^{\lambda-1}\left[a_1(3-\lambda)\cos(1-\lambda)\theta - b_1\cos(1+\lambda)\theta + a_2(3-\lambda)\sin(1-\lambda)\theta + b_2\sin(1+\lambda)\theta\right] \\ & + \mu r^{\mu-1}\left[d_1(3-\mu)\cos(1-\mu)\theta - c_1\cos(1+\mu)\theta + d_2(3-\mu)\sin(1-\mu)\theta + c_2\sin(1+\mu)\theta\right]\end{aligned}}$$

$$\boxed{\begin{aligned}\tau_{r\theta} = {} & \lambda r^{\lambda-1}\left[a_1(1-\lambda)\sin(1-\lambda)\theta + b_1\sin(1+\lambda)\theta - a_2(1-\lambda)\cos(1-\lambda)\theta + b_2\cos(1+\lambda)\theta\right] + \\ & + \mu r^{\mu-1}\left[d_1(1-\mu)\sin(1-\mu)\theta + c_1\sin(1+\mu)\theta - d_2(1-\mu)\cos(1-\mu)\theta + c_2\cos(1+\mu)\theta\right]\end{aligned}}$$

Boundary conditions

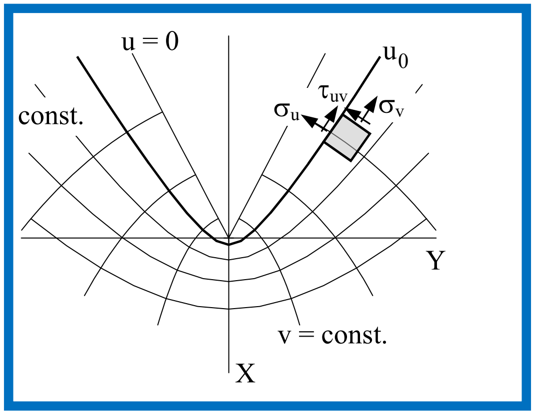

Auxiliary system based on curvilinear coordinates (u, v)

$$\left(\sigma_u\right)_{\substack{u=u_0\\v=0}} = \left(\sigma_r\right)_{\substack{r=r_0\\\theta=0}} = 0$$

$$\left(\tau_{uv}\right)_{\substack{u=u_0\\v=0}} = \left(\tau_{r\theta}\right)_{\substack{r=r_0\\\theta=0}} = 0$$

$$\left(\frac{\partial\sigma_u}{\partial v}\right)_{\substack{u=u_0\\v=0}} = \left(\frac{\partial\sigma_r}{\partial\theta} - \frac{2}{q}\tau_{r\theta}\right)_{\substack{r=r_0\\\theta=0}} = 0$$

$$\left(\frac{\partial\tau_{uv}}{\partial v}\right)_{\substack{u=u_o\\v=0}} = \left(\frac{\partial\tau_{r\theta}}{\partial\theta} - \frac{1}{q}\sigma_\theta\right)_{\substack{r=r_0\\\theta=0}} = 0$$

$$\left(\sigma_u\right)_{\substack{u=u_0\\v>>v_0}} = 0 \Rightarrow \lim_{\substack{r\to\infty\\\theta\to\pm q\frac{\pi}{2}}} \left(r^{1-\lambda}\,\sigma_\theta\right) = 0$$

$$\left(\tau_{uv}\right)_{\substack{u=u_0\\v>>v_0}} = 0 \Rightarrow \lim_{\substack{r\to\infty\\\theta\to\pm q\frac{\pi}{2}}} \left(r^{1-\lambda}\,\tau_{r\theta}\right) = 0$$

Stresses due to Mode I loading

$$\begin{Bmatrix}\sigma_\theta\\ \sigma_r\\ \tau_{r\theta}\end{Bmatrix} = \lambda_1 r^{\lambda_1-1} a_1 \left[\begin{Bmatrix}(1+\lambda_1)\cos(1-\lambda_1)\theta\\ (3-\lambda_1)\cos(1-\lambda_1)\theta\\ (1-\lambda_1)\sin(1-\lambda_1)\theta\end{Bmatrix} + \chi_{b_1}(1-\lambda_1)\begin{Bmatrix}\cos(1+\lambda_1)\theta\\ -\cos(1+\lambda_1)\theta\\ \sin(1+\lambda_1)\theta\end{Bmatrix} + \right.$$

$$\left. + \frac{q}{4(q-1)}\left(\frac{r}{r_0}\right)^{\mu_1-\lambda_1}\left(\chi_{d_1}\begin{Bmatrix}(1+\mu_1)\cos(1-\mu_1)\theta\\ (3-\mu_1)\cos(1-\mu_1)\theta\\ (1-\mu_1)\sin(1-\mu_1)\theta\end{Bmatrix} + \chi_{c_1}\begin{Bmatrix}\cos(1+\mu_1)\theta\\ -\cos(1+\mu_1)\theta\\ \sin(1+\mu_1)\theta\end{Bmatrix}\right)\right]$$

Stresses due to Mode II loading

$$\begin{Bmatrix}\sigma_\theta\\ \sigma_r\\ \tau_{r\theta}\end{Bmatrix} = \lambda_2 r^{\lambda_2-1} a_2 \left[\begin{Bmatrix}(1+\lambda_2)\sin(1-\lambda_2)\theta\\ (3-\lambda_2)\sin(1-\lambda_2)\theta\\ (1-\lambda_2)\cos(1-\lambda_2)\theta\end{Bmatrix} + \chi_{b_2}(1+\lambda_2)\begin{Bmatrix}\sin(1+\lambda_2)\theta\\ -\sin(1+\lambda_2)\theta\\ \cos(1+\lambda_2)\theta\end{Bmatrix} + \right.$$

$$\left. + \frac{1}{4(\mu_2-1)}\left(\frac{r}{r_0}\right)^{\mu_2-\lambda_2}\left(\chi_{d_2}\begin{Bmatrix}(1+\mu_2)\sin(1-\mu_2)\theta\\ (3-\mu_2)\sin(1-\mu_2)\theta\\ (1-\mu_2)\cos(1-\mu_2)\theta\end{Bmatrix} + \chi_{c_2}\begin{Bmatrix}-\sin(1+\mu_2)\theta\\ \sin(1+\mu_2)\theta\\ -\cos(1+\mu_2)\theta\end{Bmatrix}\right)\right]$$

2α	λ_1	μ_1	χ_{b1}	χ_{c1}	χ_{d1}
0	0.5	-0.5	1	4	0
$\pi/4$	0.5050	-0.4319	1.1656	3.5721	0.0828
$\pi/3$	0.5122	-0.4057	1.3123	3.2832	0.0960
$\pi/2$	0.5448	-0.3449	1.8414	2.5057	0.1046
$2\pi/3$	0.6157	-0.2678	3.0027	1.5150	0.0871
$3\pi/4$	0.6736	-0.2198	4.1530	0.9933	0.0673
$5\pi/6$	0.7520	-0.1624	6.3617	0.5137	0.0413

Characteristic parameters for mode I loading.

2α	λ_2	μ_2	χ_{b2}	χ_{c2}	χ_{d2}
0	0.5	-0.5	1	-12	0
$\pi/4$	0.6597	-0.4118	0.8140	-10.1876	-0.4510
$\pi/3$	0.7309	-0.3731	0.6584	-8.3946	-0.4788
$\pi/2$	0.9085	-0.2882	0.2189	-2.9382	-0.2436
$2\pi/3$	1.1489	-0.1980	-0.3139	4.5604	0.5133
$3\pi/4$	1.3021	-0.1514	-0.5695	8.7371	1.1362
$5\pi/6$	1.4858	-0.1034	-0.7869	12.9161	1.9376

Characteristic parameters for mode II loading.

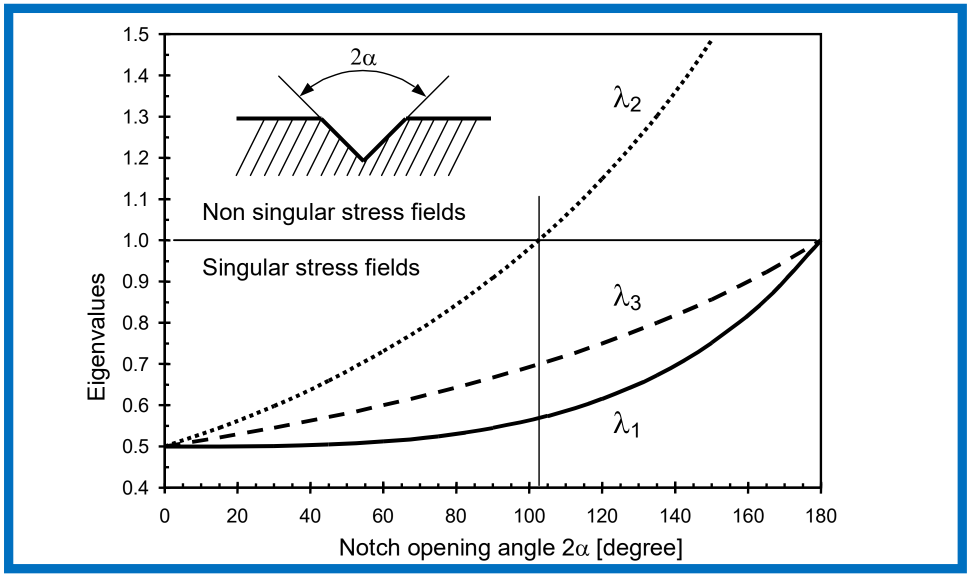

Eigenvalues λ_1, λ_2 and λ_3 against the notch opening angle 2α.

Notch stress intensity factor

The stress field in the neighbourhood of the notch tip can be expressed as a function of a stress field parameter, mode I N-SIF. Its definition is consistent with the usual Stress Intensity Factor definition if the notch radius and opening angle are both null. **Gross and Mendelsson** (1972) definition:

$$\boxed{K_I = \sqrt{2\pi} \lim_{r \to 0} (\sigma_\theta)_{\theta=0} \, r^{1-\lambda_1}}$$

$$\boxed{K_I = \lambda_1 \sqrt{2\pi} \left[1 + \lambda_1 + \chi_{b1} (1 - \lambda_1)\right] a_1}$$

where the constant a_1 has to be determined at a convenient distance from the notch tip, where the stress fields of the rounded and sharp notch practically coincide

Special sharp notch case

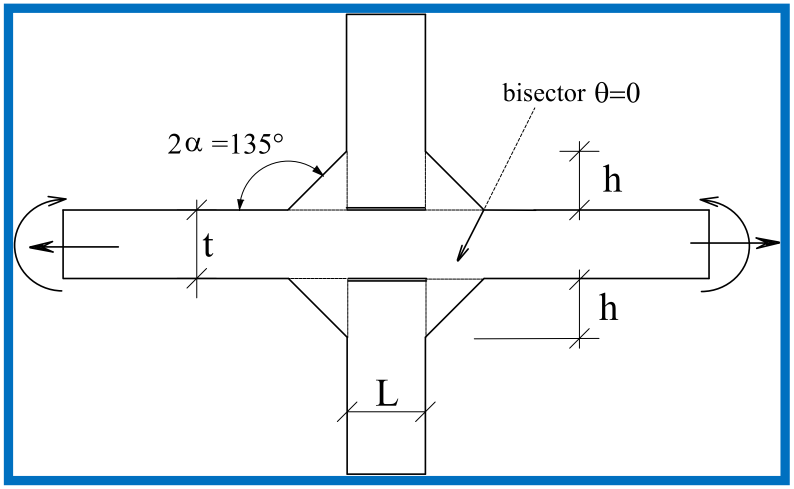

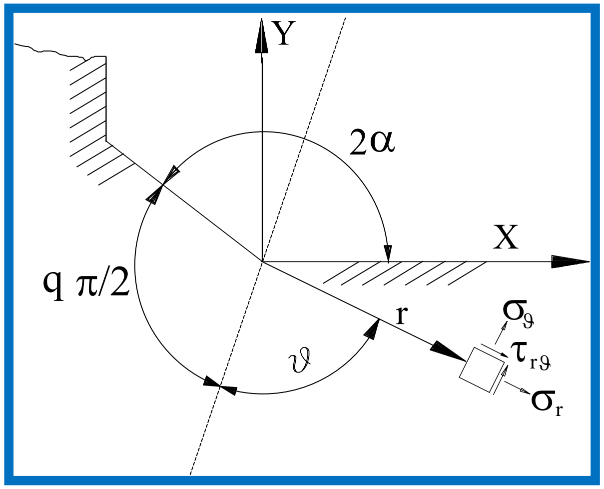

Stress field at the weld toe

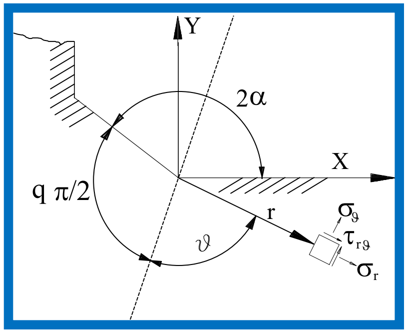

In the direction normal to the main plate ($\theta = 22.5°$)

$$\boxed{\sigma_\theta = 0.361 \cdot r^{-0.326} \cdot K_1^N + 0.322 \cdot r^{0.302} \cdot K_2^N}$$

Along the free edge (ϑ=112.5°)

$$\boxed{\sigma_r = K_1 \cdot 0.423 \cdot r^{-0.326} + K_2 \cdot 0.553 \cdot r^{0.302}}$$

For Mode I fracture

$$\left\{\begin{matrix} \sigma_\vartheta \\ \sigma_r \\ \tau_{r\vartheta} \end{matrix}\right\}_{\rho=0} = \frac{1}{\sqrt{2\pi}} \frac{r^{\lambda_1-1} K_1}{(1+\lambda_1)+\chi_1(1-\lambda_1)} \left[\left\{\begin{matrix} (1+\lambda_1)\cos(1-\lambda_1)\vartheta \\ (3-\lambda_1)\cos(1-\lambda_1)\vartheta \\ (1-\lambda_1)\sin(1-\lambda_1)\vartheta \end{matrix}\right\} + \chi_1(1-\lambda_1) \left\{\begin{matrix} \cos(1+\lambda_1)\vartheta \\ -\cos(1+\lambda_1)\vartheta \\ \sin(1+\lambda_1)\vartheta \end{matrix}\right\} \right]$$

For Mode II fracture,

$$\left\{\begin{matrix} \sigma_\vartheta \\ \sigma_r \\ \tau_{r\vartheta} \end{matrix}\right\}_{\rho=0} = \frac{1}{\sqrt{2\pi}} \frac{r^{\lambda_2-1} K_2}{(1-\lambda_2)+\chi_2(1+\lambda_2)} \left[\left\{\begin{matrix} -(1+\lambda_2)\sin(1-\lambda_2)\vartheta \\ -(3-\lambda_2)\sin(1-\lambda_2)\vartheta \\ (1-\lambda_2)\cos(1-\lambda_2)\vartheta \end{matrix}\right\} + \chi_2(1+\lambda_2) \left\{\begin{matrix} -\sin(1+\lambda_2)\vartheta \\ \sin(1+\lambda_2)\vartheta \\ \cos(1+\lambda_2)\vartheta \end{matrix}\right\} \right]$$

Validity of the equations

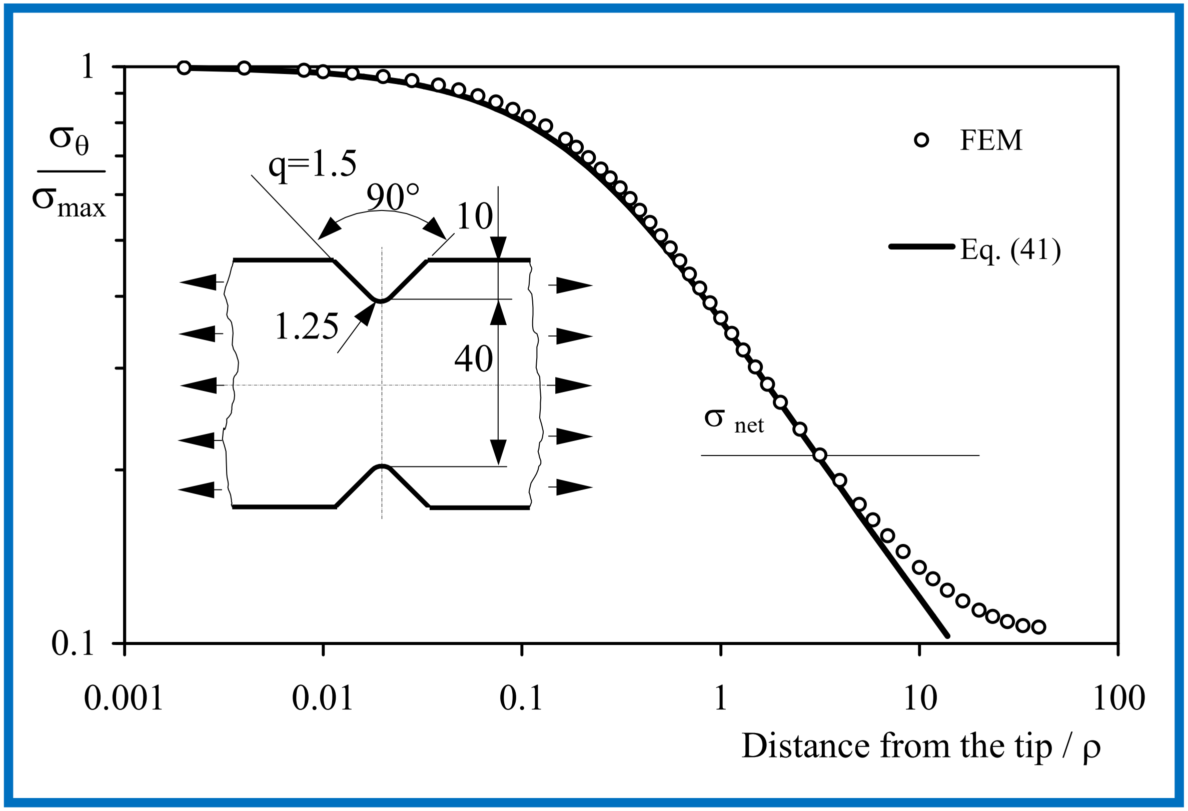

Neuber's modified solution

$$\Phi = C_1\left\{u^{t+q} - \binom{t+q}{2}u^{t+q-2}v^2 + \binom{t+q}{4}u^{t+q-4}v^4 - \binom{t+q}{6}u^{t+q-6}v^6 + \binom{t+q}{8}u^{t+q-8}v^8 - \binom{t+q}{10}u^{t+q-10}v^{10} + \right.$$
$$+ C_2\left[u^{2q} + \binom{q}{1}u^{2q-2}v^2 + \binom{q}{2}u^{2q-4}v^4 + \binom{q}{3}u^{2q-6}v^6 + \binom{q}{4}u^{2q-8}v^8 + \binom{q}{5}u^{2q-10}v^{10}\right]\left[u^{t-q} - \binom{t-q}{2}u^{t-q-2}v^2 + \right.$$
$$\left.\left. + \binom{t-q}{4}u^{t-q-4}v^4 - \binom{t-q}{6}u^{t-q-6}v^6 + \binom{t-q}{8}u^{t-q-8}v^8 - \binom{t-q}{10}u^{t-q-10}v^{10}\right] + C_3 u + C_4\right\}$$

Airy stress function

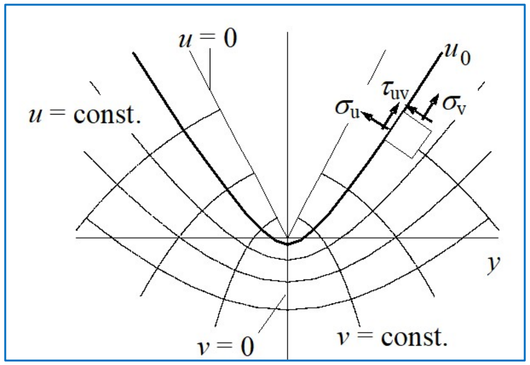

$$\boxed{t = \frac{1}{2} + q - \sqrt{2q - \frac{7}{4}}}$$

Stress field exponent

Stress field along the notch bisector line

$$\boxed{(\sigma_\theta)_{\theta=0} = \frac{\partial^2 \Phi}{\partial x^2} = C_1(1+C_2)\frac{t+q}{q}\left[\frac{t}{q}x^{\frac{t}{q}-1} - \frac{1-q}{q}x_0^{\frac{t+q-1}{q}}x^{\frac{1-2q}{q}}\right]}$$

Neuber's modified solution

2α	q	t	t/q	λ	λq	μ–1	(1-2q)/q
0°	2.000	1.000	0.500	0.500	1.000	-1.500	-1.500
60°	1.667	0.908	0.545	0.512	0.854	-1.406	-1.400
90°	1.500	0.882	0.588	0.545	0.817	-1.345	-1.333
120°	1.333	0.876	0.657	0.616	0.821	-1.268	-1.250
135°	1.250	0.884	0.707	0.674	0.842	-1.220	-1.200
150°	1.167	0.903	0.774	0.752	0.878	-1.162	-1.143
180°	1.000	1.000	1.000	1.000	1.000	-1.000	-1.000

Neuber's exponents q, t and Williams' mode I eigenvalue λ for tension-loaded V-notches; Neuber's exponent (1-2q)/q compared with Lazzarin's exponent μ–1.

F. Berto, P. Lazzarin, D. Radaj
Eng Fract Mech 2009

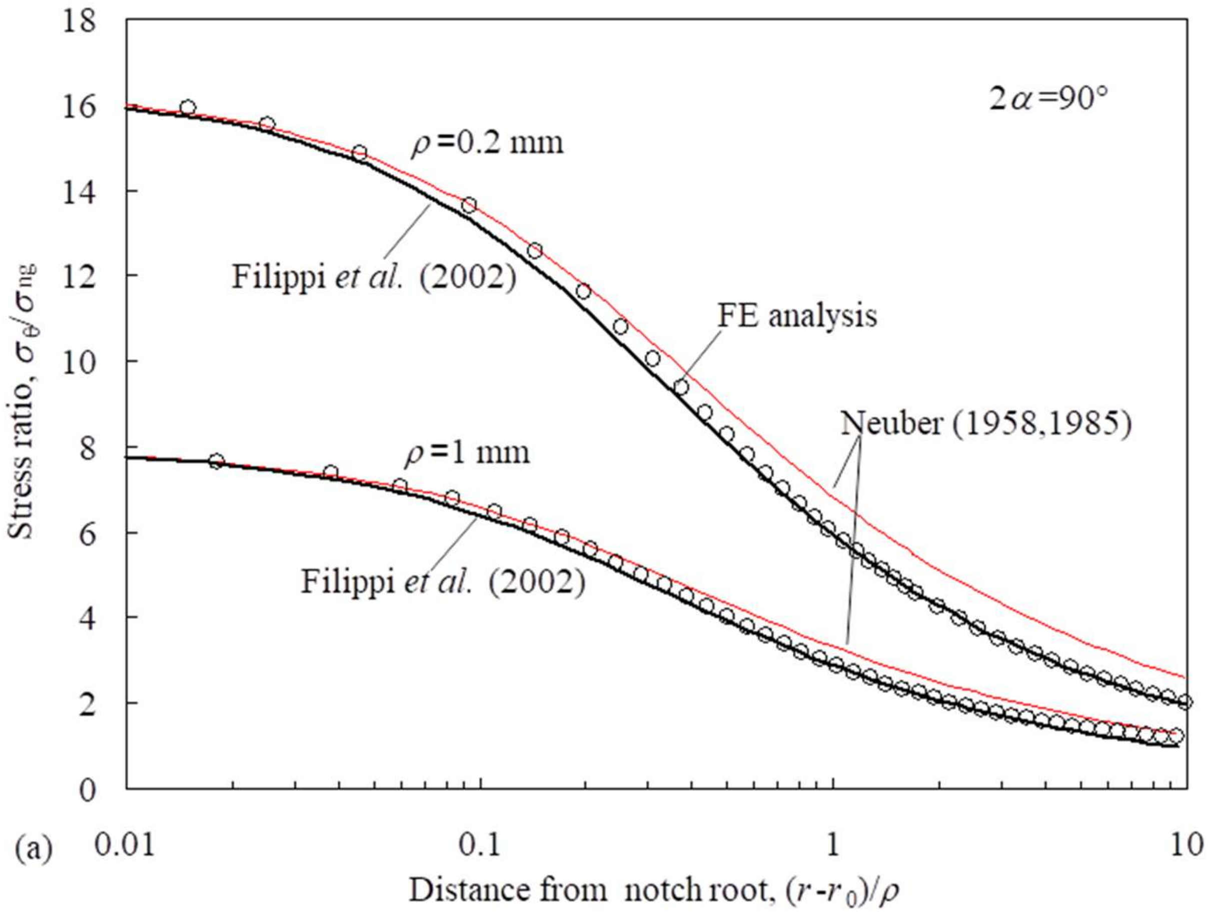

Stress ratio, $\sigma_\theta/\sigma_{ng}$
2α=90°
ρ=0.2 mm
Filippi et al. (2002)
FE analysis
Neuber (1958,1985)
ρ=1 mm
Filippi et al. (2002)
(a)
Distance from notch root, $(r-r_0)/\rho$

Outlines

- Introduction
- Notch and geometrical discontinuities
- **Local approaches**
- Defects and fatigue design
- Multiaxial loadings
- Additive materials: some examples

Neuber's procedure of fictitious notch rounding

The averaged notch stresses σ at the real notch with radius ρ can directly be determined without an averaging procedure by analysing a substitute notch with fictitiously enlarged notch radius ρ_f :

$$\rho_f = \rho + s\rho^*$$

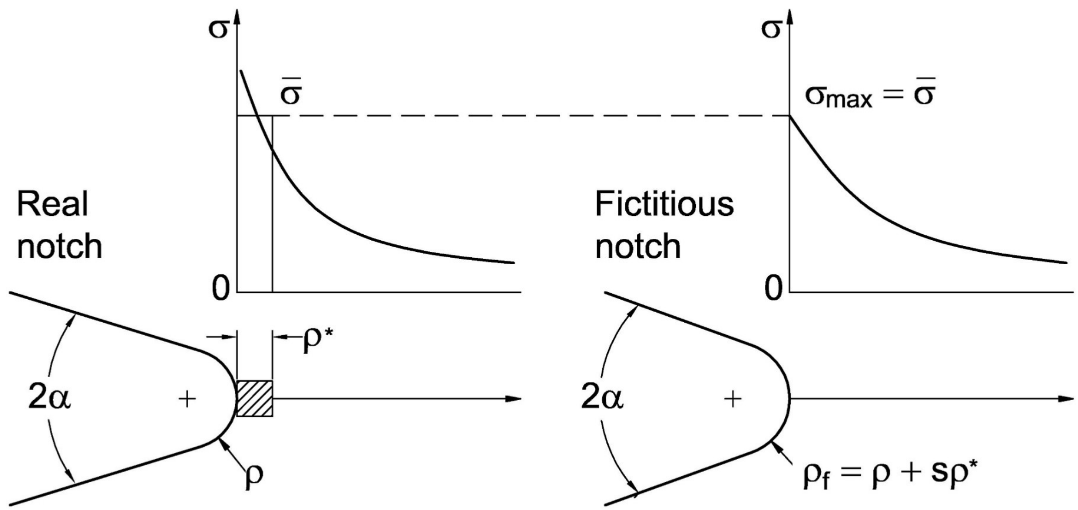

Neuber’s concept of microsupport

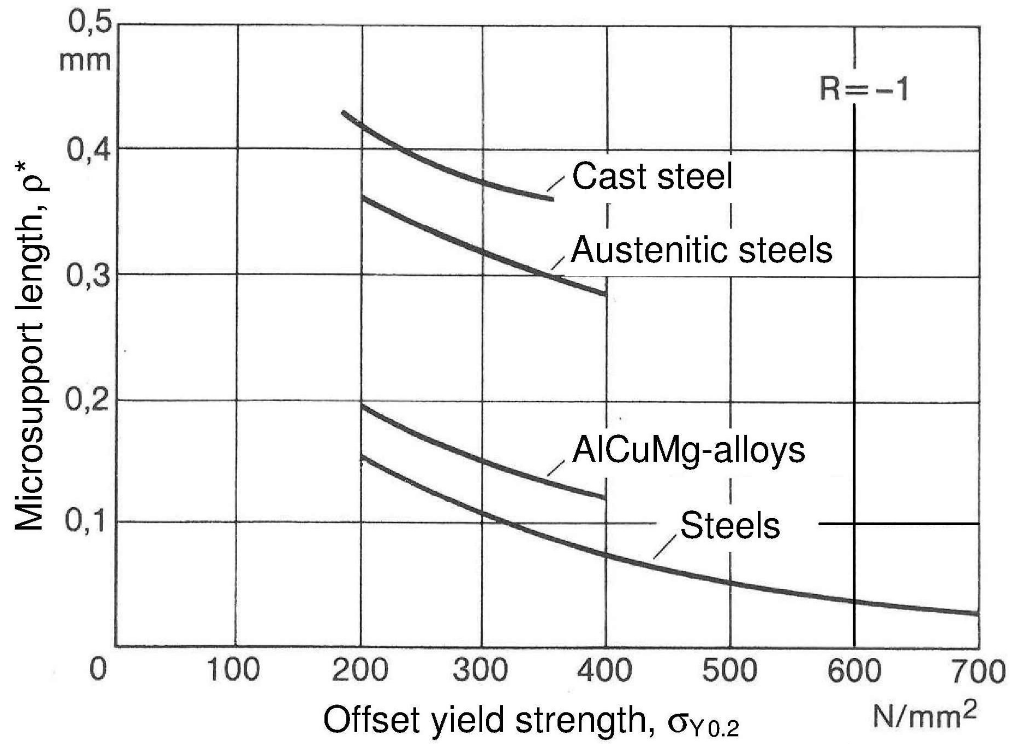

Neuber's procedure of fictitious notch rounding

$$\rho_f = \rho + s\rho^*$$

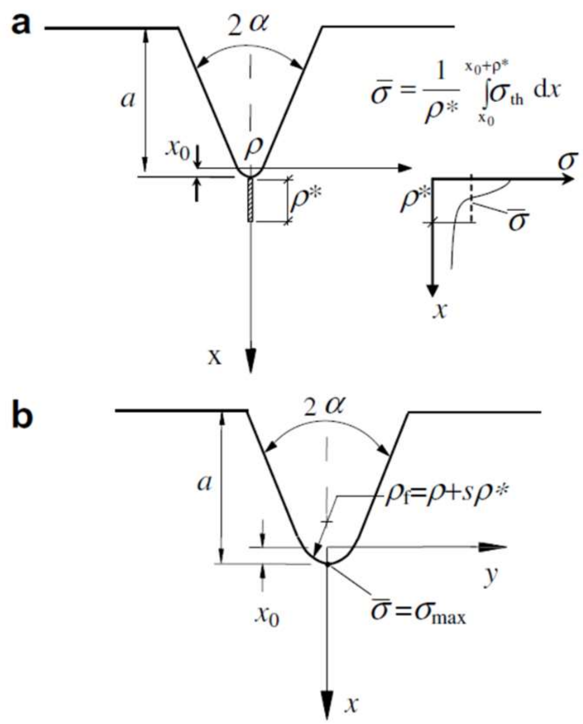

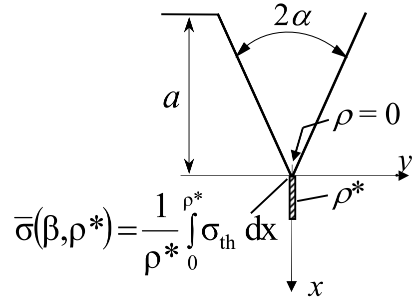

Worst case

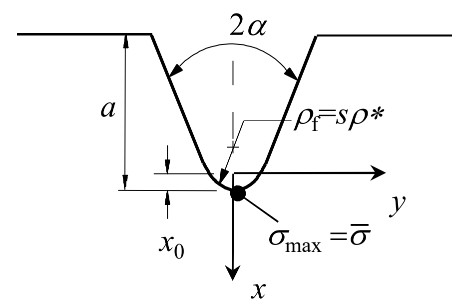

Fictitious notch rounding concept for welded joints

Fictitious notch rounding simulating stress averaging over ρ^* in the direction of crack propagation has successfully been applied to the fatigue assessment of welded joints (Radaj 1969, 1975, 1990).

Within a worst case consideration, the parameter values:

- $\rho = 0$ (worst case), $\rho^* \approx 0.4$ mm (welded steel), $s \approx 2.5$

result in the fictitious notch radius:

- $\rho_f = \rho + s\rho^* = 1$ mm

This very rough estimate is applied to the cross-sectional model of welded joints in the form of a blunt circular notch at the weld toe and a keyhole at the weld root.

The SCFs at these notches are considered as theoretical fatigue notch factors characterising the endurance limit of the joints.

IIW recommendations for fatigue design of welded joints and components

2.2.4.3 Measurement of Effective Notch Stress

Because the effective notch radius is an idealization, the effective notch stress cannot be measured directly in the welded component. In contrast, the simple definition of the effective notch can be used for photo-elastic stress measurements in resin models.

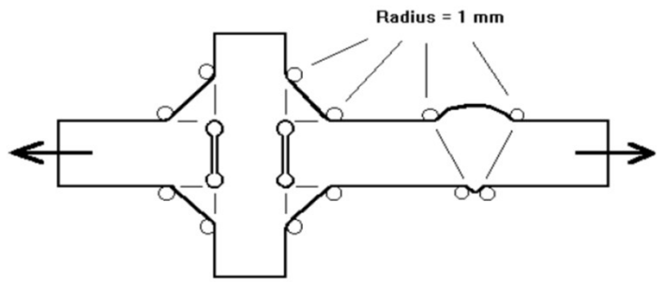

Fig. (2.2)-14 Fictitious rounding of weld toes and roots

ρ_f=1 mm indipendent of the notch opening angle

"s" is referred to the case of normal stress (under plane stress)

$\rho_f = \rho + s\,\rho^* = 1.0$ mm **s=2.5, $\rho = 0$, $\rho^* = 0.4$ mm**

Notch rounding approach

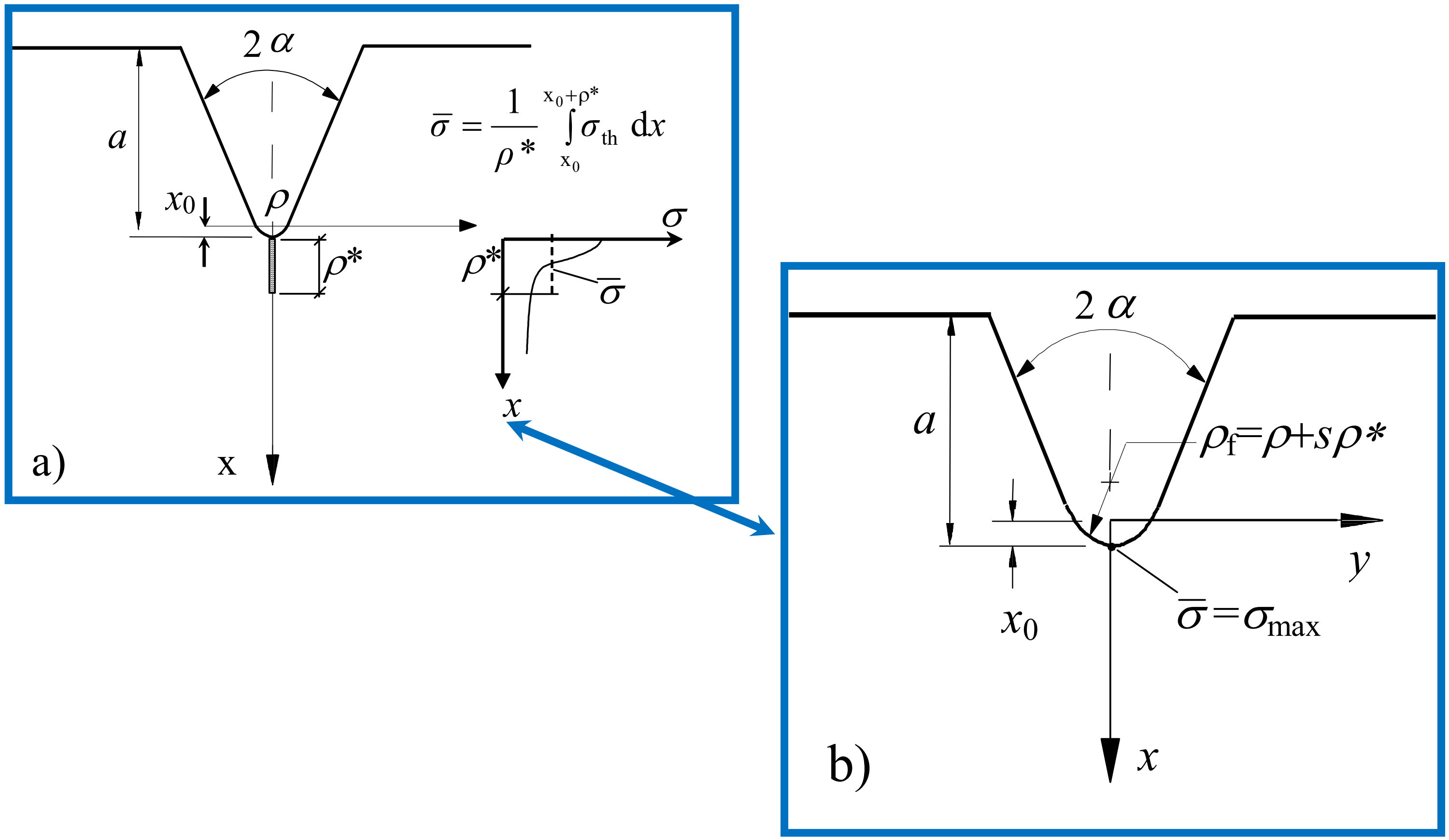

STEPS FOR THE APPLICATION OF THE FNR APPROACH

STEP 1

Choice of the fracture criterion (normal stress, von Mises, Beltrami) and Write the equivalent stress accordingly to the selected criterion σ (or τ) along the bisector line by means of the expressions valid for V-notches

STEP 2

Determine the effective stress as a function of ρ and $\rho*$

$$\boxed{\overline{\sigma}(\rho, \rho*) = \frac{1}{\rho*}\int_{x_0}^{x_0+\rho*} \sigma_{th}\, dx}$$

STEP 3

Solve the limit $\boxed{\overline{\sigma}\max(\rho_f) = \lim_{\rho* \to 0} \overline{\sigma}}$

Solve the equation: **STEP 4**

$$\boxed{\bar{\sigma}\max(\rho_f) = \bar{\sigma}(\rho^*, \rho)}$$

STEP 5

Determine $\rho_f(\rho,\rho^*)$:

$$\boxed{\rho_f = f(\rho^*, \rho)}$$

STEP 6

Evaluation of s:

$$\boxed{s=(\rho_f-\rho)/\rho^*}$$

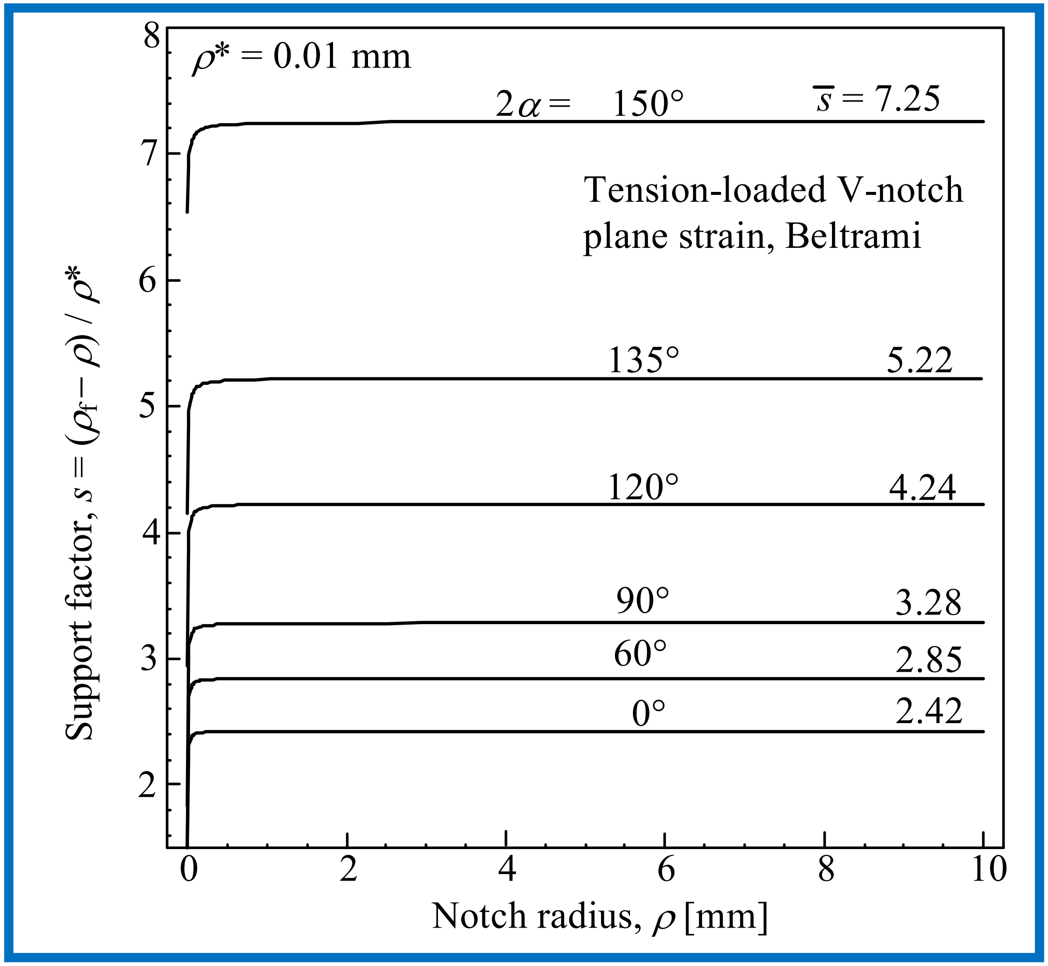

$\rho^* = 0.01$ mm
$2\alpha =$ 150°
$\overline{s} = 7.25$
Tension-loaded V-notch
plane strain, Beltrami
135°
5.22
120°
4.24
90°
3.28
60°
2.85
0°
2.42
Support factor, $s = (\rho_f - \rho) / \rho^*$
Notch radius, ρ [mm]
8
7
6
5
4
3
2
0
2
4
6
8
10

Values of "s" for different notch angles

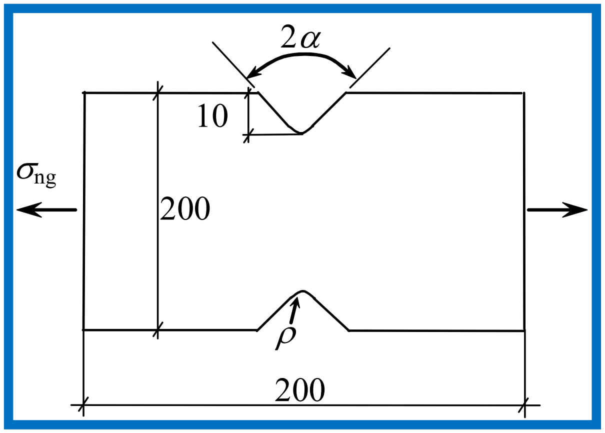

2α	Neuber	Filippi, Lazzarin and Tovo				
	Normal stress	Normal stress	von Mises plane stress	von Mises plane strain	Beltrami plane stress	Beltrami plane strain
0°	2.00	2.00	2.50	2.90	2.30	2.42
60°	2.36	2.41	2.90	3.33	2.72	2.85
90°	2.72	2.81	3.37	3.80	3.14	3.28
120°	3.47	3.67	4.32	4.84	4.06	4.24
135°	4.21	4.56	5.33	5.94	5.02	5.22
150°	5.73	6.38	7.41	8.20	6.99	7.25

Reference notch concept Pedersen's diagram

(Pedersen 2011)

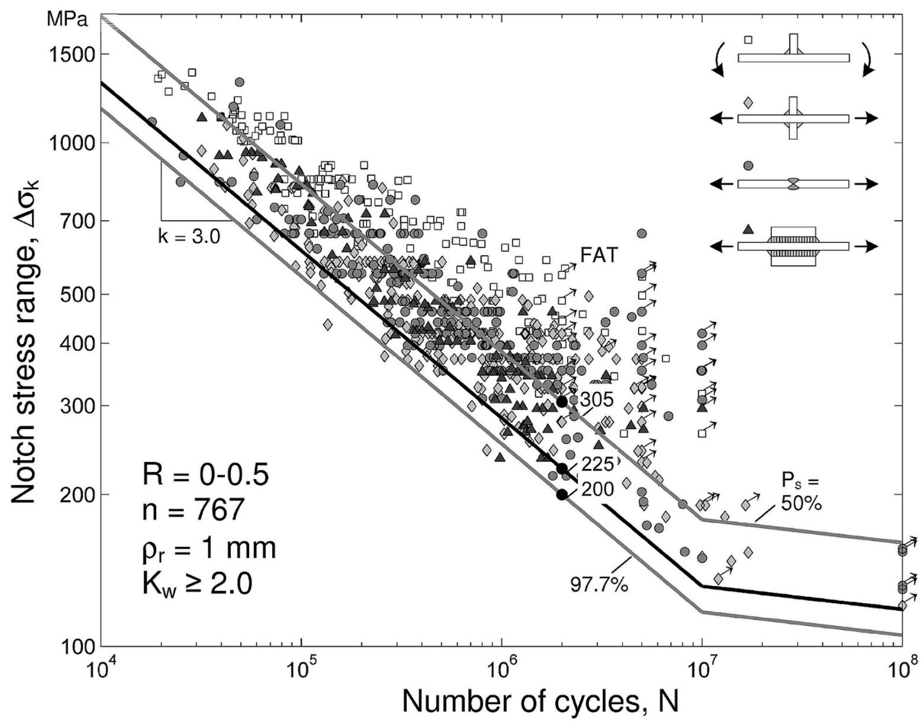

Microhole at weld root of thin-sheet lap joint

Thin-sheet lap joints (t = 0.7-5 mm), resistance spot-welded or laser beam seam-welded, require a special procedure because of increasing problems with cross-sectional weakening and slit-parallel loading.

These peculiarities are overcome by application of a microhole at the weld root (ρ = 0.05 mm) followed by notch stress averaging over ρ*.

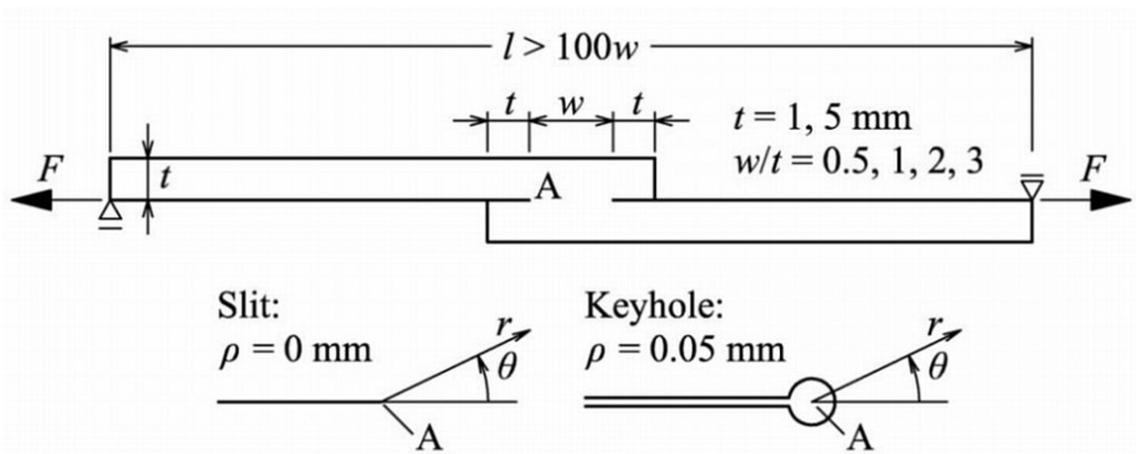

Theory of Critical Distance

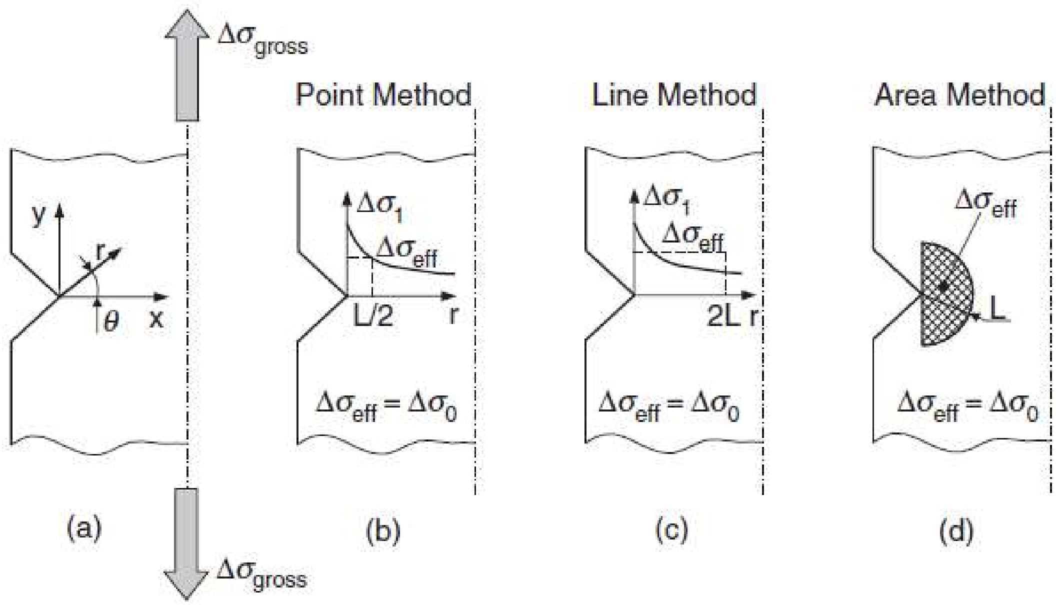

D. Taylor, The Theory of Critical Distances 2007
L. Susmel, Multiaxial Notch Fatigue 2009

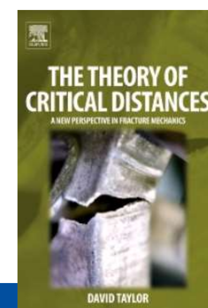

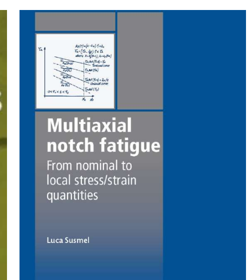

Peterson RE. Notch sensitivity. In: Sines G, Waisman JL, editors. Metal fatigue. New York, USA: McGraw Hill; 1959. p. 293–306.

Tanaka K. Engineering formulae for fatigue strength reduction due to cracklike notches. Int J Fract 1983;22:R39–46.

Taylor D. Geometrical effects in fatigue: a unifying theoretical model. Int J Fatigue 1999;21:413–20.

Seweryn A. Brittle fracture criterion for structures with sharp notches. Eng Fract Mech 1994;47:673–81.

A. Seweryn

K. Tanaka

ENGINEERING FORMULAE FOR FATIGUE STRENGTH REDUCTION DUE TO CRACK-LIKE NOTCHES

K. Tanaka
Department of Mechanical Engineering and Mechanics, Lehigh University
Bethlehem, Pennsylvania 18015 USA
tel: (215) 861-4547

Among fatigue engineers, it is well known that the fatigue strength reduction factor K_f is lower than the elastic stress concentration factor K_t. This discrepancy means that the highest stress alone is no longer appropriate for characterizing the microprocess of fatigue occurring in the microstructure at the notch tip. To rectify this microstructural size effect, Neuber [1-3] has hypothesized that the controlling fracture parameter is the mean stress over the structural size ahead of the notch tip. On the other hand, Ishibashi [4] and Peterson [5] postulated that the controlling factor is the stress at the distance of the structural size ahead of the notch tip. Both Neuber [1] and Peterson [5] started with the stress distribution for deep notches and derived the following approximate formulae of the K_f-K_t relationship which were claimed to be applicable to various notches:

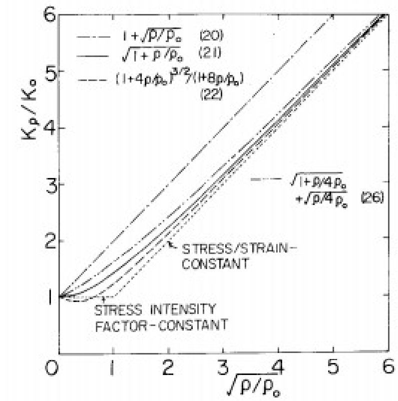

Figure 4. Effect of notch-tip radius on critical stress intensity.

$$\bar{\sigma}_o = \frac{1}{\ell_o}\int_a^{a+\ell_o} \sigma_y \, dx = \frac{1}{\ell_o}\int_o^{\ell_o} \sigma_y \, dx'$$

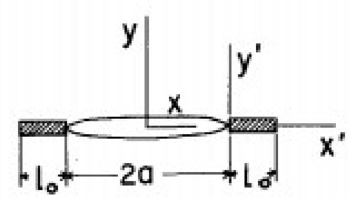

NTNU

Volume method

Sheppard, S. D. (1991) Field effects in fatigue crack initiation:long life fatigue strength.Trans. ASME. J. Mech. Des.113,188–194

S. Sheppard

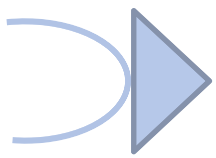

A semi-circular sector of radius M (then restricted to the inscribed triangle) was used, for example, by Sheppard who quantified the stress state near a notch by means of a single parameter, the average value of the principal stress

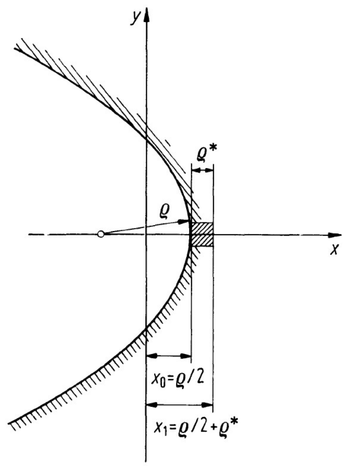

Bild 4.8. Zur Definition der Mikrostützwirkung

Die gemäß dem Konzept der Mikrostützwirkung gewonnenen Spannungen seien „fiktive Spannungen" genannt und mit σ_F bezeichnet. Es gilt

$$\sigma_F = \frac{1}{\varrho^*} \int_{x_0}^{x_1} \sigma_e dx = 4C_1 / \sqrt{\varrho_F/2} . \tag{16}$$

Die fiktiven Spannungen können direkt auf (9) bezogen werden, wenn der Krümmungsradius ϱ formal durch den „fiktiven" Krümmungsradius ϱ_F ersetzt wird, wie die rechte Seite von (16) zeigt. Damit ist das Verfahren der Mikrostützwirkung auf die Ermittlung von ϱ_F zurückgeführt.

Bei Anwendung auf *die 0°-Spitzkerbe bzw. den Riß* ($\varrho = 0$) ergibt sich für die erste, zweite und dritte Hypothese der gemeinsame Wert

$$\varrho_F = 2\varrho^* . \tag{17}$$

BRITTLE FRACTURE CRITERION FOR STRUCTURES WITH SHARP NOTCHES

ANDRZEJ SEWERYN

Białystok Technical University, Faculty of Mechanics, ul. Wiejska 45C, 15-351 Białystok, Poland

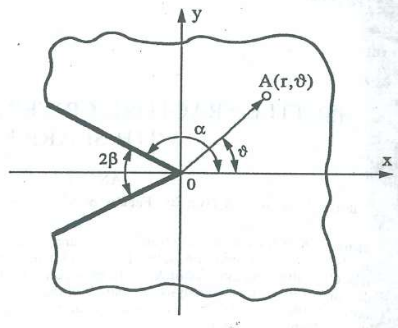

Fig. 1. Notch geometry in polar coordinate system.

The Mode I stress intensity factor K_{I}, the Mode II stress intensity factor K_{II} and
III stress intensity factor K_{III} for V-shaped notches may be defined in a manner similar to
for cracks [5, 6]

$$K_{\mathrm{I}} = \lim_{\vartheta = 0\, r \to 0+} [(2\pi r)^{\lambda_{\mathrm{I}}} \sigma_{\vartheta}],$$

$$K_{\mathrm{II}} = \lim_{\vartheta = 0\, r \to 0+} [(2\pi r)^{\lambda_{\mathrm{II}}} \tau_{r\vartheta}],$$

$$K_{\mathrm{III}} = \lim_{\vartheta = 0\, r \to 0+} [(2\pi r)^{\lambda_{\mathrm{III}}} \tau_{z\vartheta}],$$

$$\max\left(\int_0^{d_0} \sigma_{\vartheta}\, \mathrm{d}r\right) \geqslant d_o \sigma_c,$$

NTNU

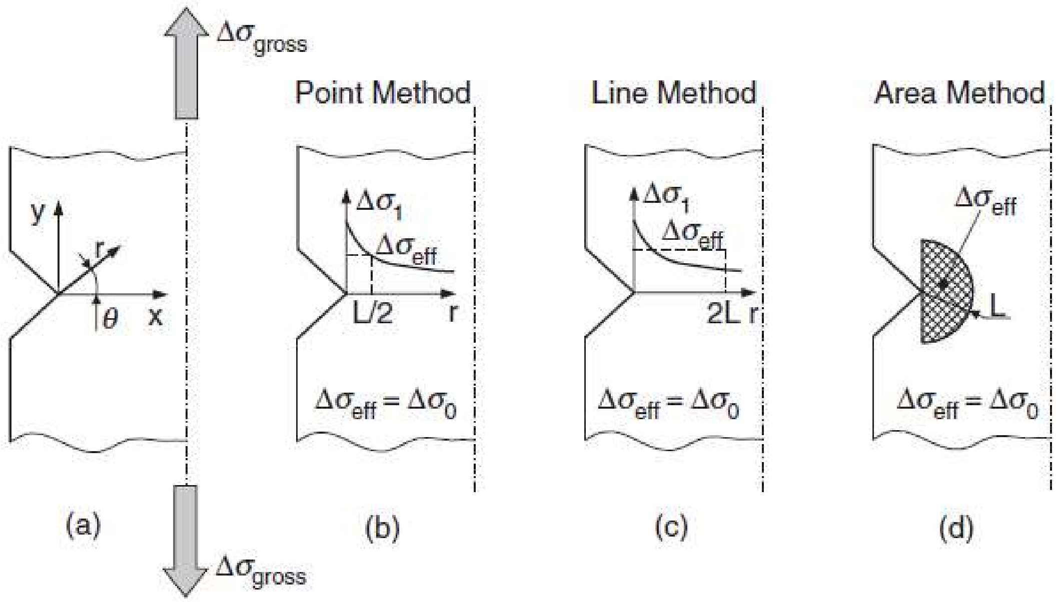

$$\Delta\sigma_{\mathrm{eff}} = \Delta\sigma_1\left(\theta = 0, r = \frac{L}{2}\right) = \Delta\sigma_0$$

Point Method

$$\Delta\sigma_{\mathrm{eff}} = \frac{1}{2L}\int_0^{2L} \Delta\sigma_1(\theta = 0, r)\,\mathrm{d}r = \Delta\sigma_0$$

Line Method

$$\Delta\sigma_{\mathrm{eff}} = \frac{4}{\pi L^2}\int_0^{\pi/2}\int_0^{L} \Delta\sigma_1(\theta, r)\cdot r\cdot \mathrm{d}r\cdot \mathrm{d}\theta \cong \Delta\sigma_0$$

Area Method

Brittle Failure by TCD

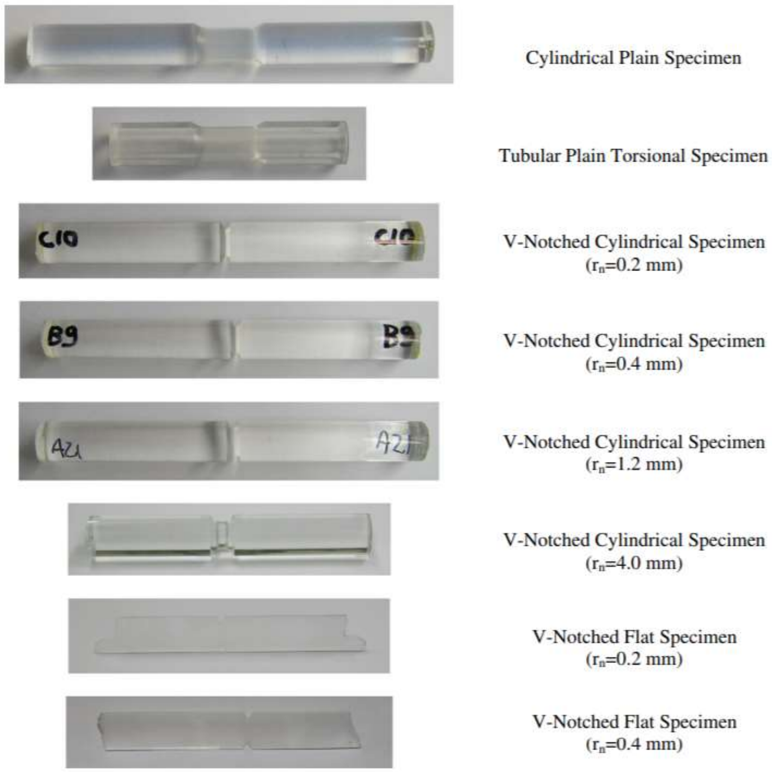

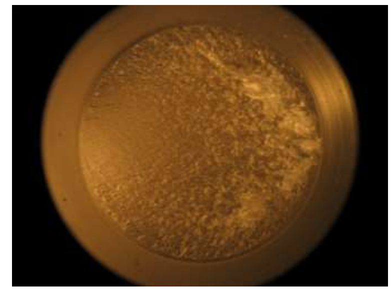

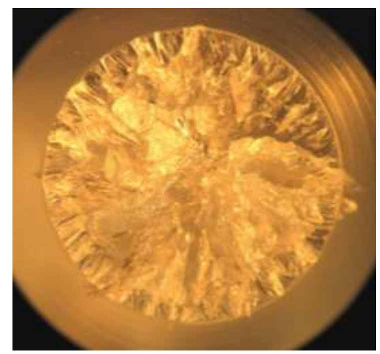

L. Susmel, D. Taylor, Engineering Fracture Mechanics 75 (2008) 534–550

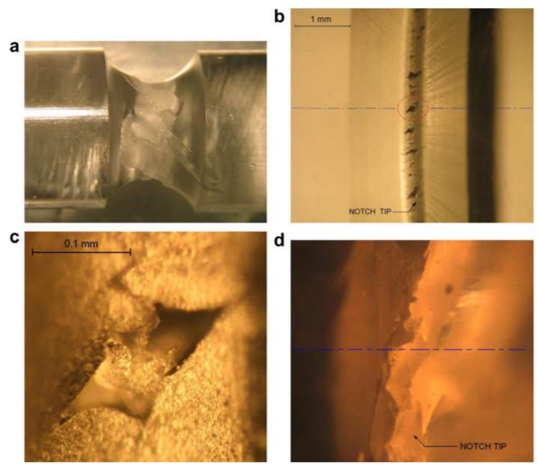

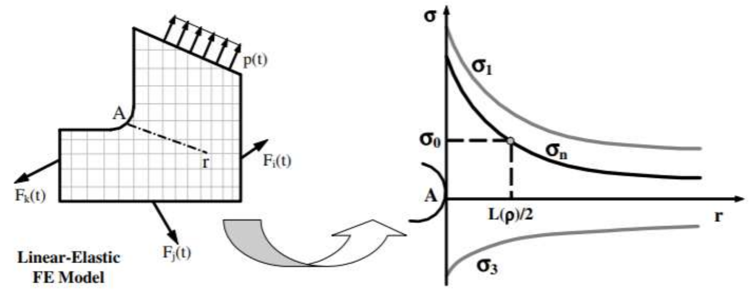

Multiaxial PM accuracy in predicting failures in the tested notched specimens

σ_{nom}/τ_{nom}	σ_{eff} [MPa]				Error [%]		
	$r_n = 0.2$ mm	$r_n = 0.4$ mm	$r_n = 1.2$ mm	$r_n = 4.0$ mm	$r_n = 0.2$ mm	$r_n = 0.4$ mm	$r_n = 1.2$ mm
∞	119.4	120.6	100.1	71.3	4.9	5.9	−12.1
1	127.8	128.2	125.3	109.9	12.2	12.6	10.0
0.55	134.5	126.1	105.7	91.3	18.1	10.7	−7.2
0.23	110.4	103.1	99.1	81.9	−3.1	−9.5	−13.0
0	113.7	117.5	115.1	65.2	−0.2	3.2	1.1

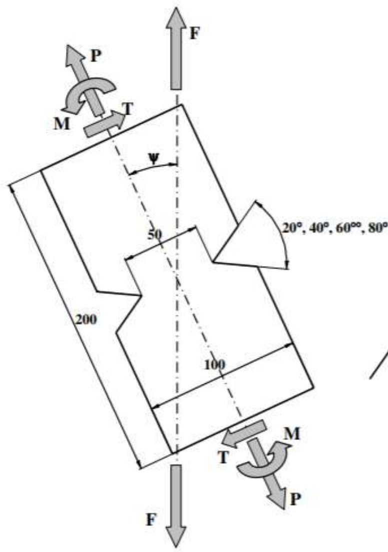

F
P
M
T
ψ
50
20°, 40°, 60°°, 80°
200
100
T
M
P
F

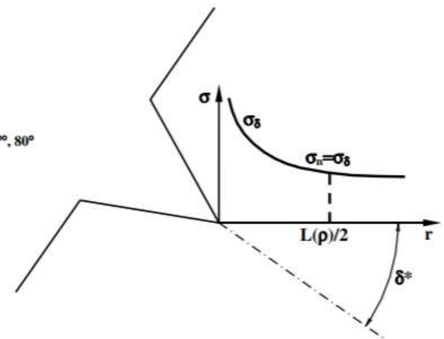

σ
σδ
σn=σδ
L(ρ)/2
r
δ*

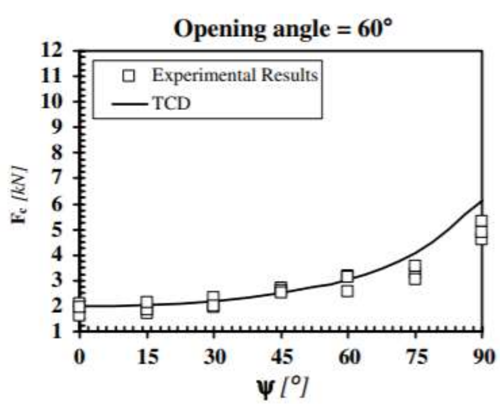

Opening angle = 60°
Experimental Results
TCD
Fc [kN]
ψ [°]

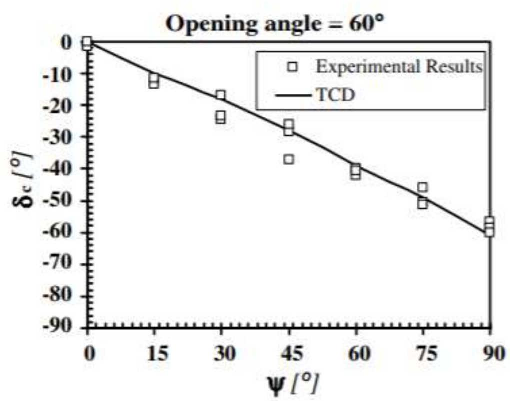

Opening angle = 60°
Experimental Results
TCD
δc [°]
ψ [°]

Notch Stress Intensity Factor

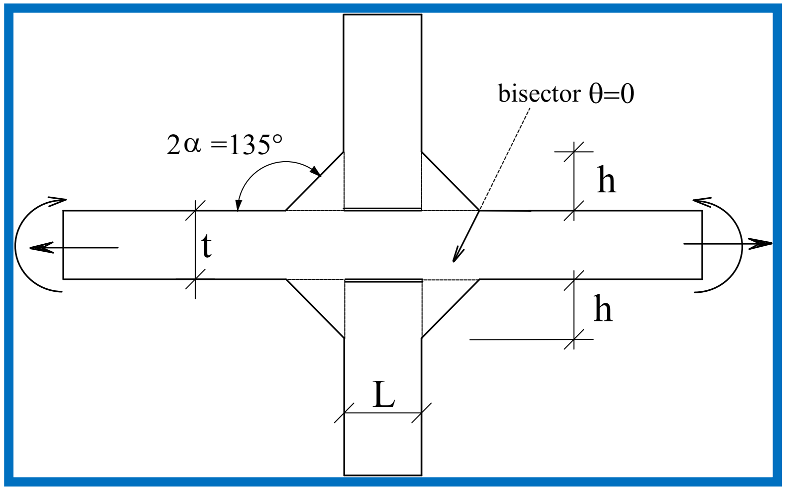

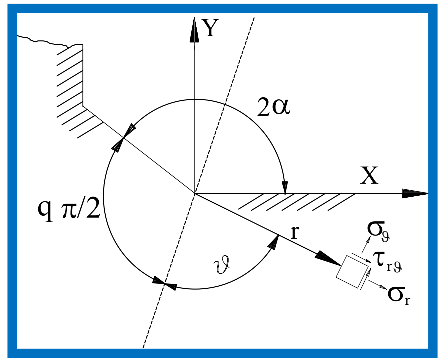

According to Gross and Mendelson's definition (1972), the N-SIFs related to the mode I stress distribution are:

$$K_1^N = \sqrt{2\pi} \lim_{r \to 0^+} r^{1-\lambda_1} \sigma_{\theta\theta}(r)$$

$$K_2^N = \sqrt{2\pi} \lim_{r \to 0^+} r^{1-\lambda_2} \sigma_{r\theta}(r)$$

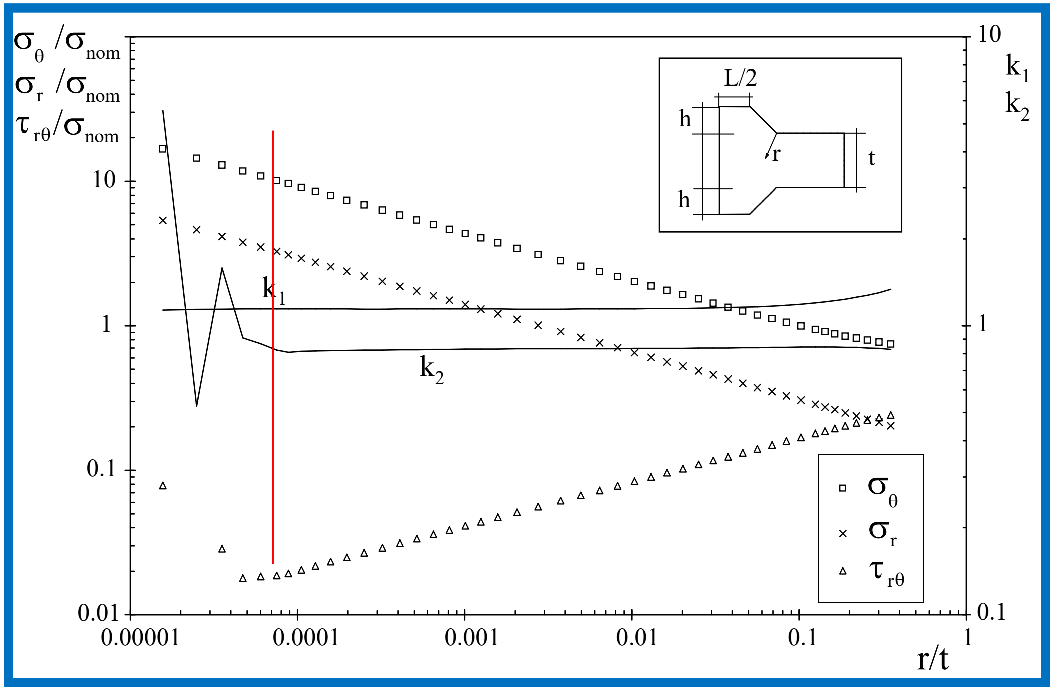

Stress components along the bisector and k1 and k2 evaluation

Local NSIFs can be linked to nominal stress according to the expression

$$\Delta K_1^N = k_1 \cdot t^{1-\lambda_1} \cdot \Delta\sigma_{nom}$$

Original data from Gurney (1991) and Maddox (1987)

Main Plate thickness ranging from 6 to 100 mm;

Transverse plate thickness ranging from 3.0 to 200 mm.

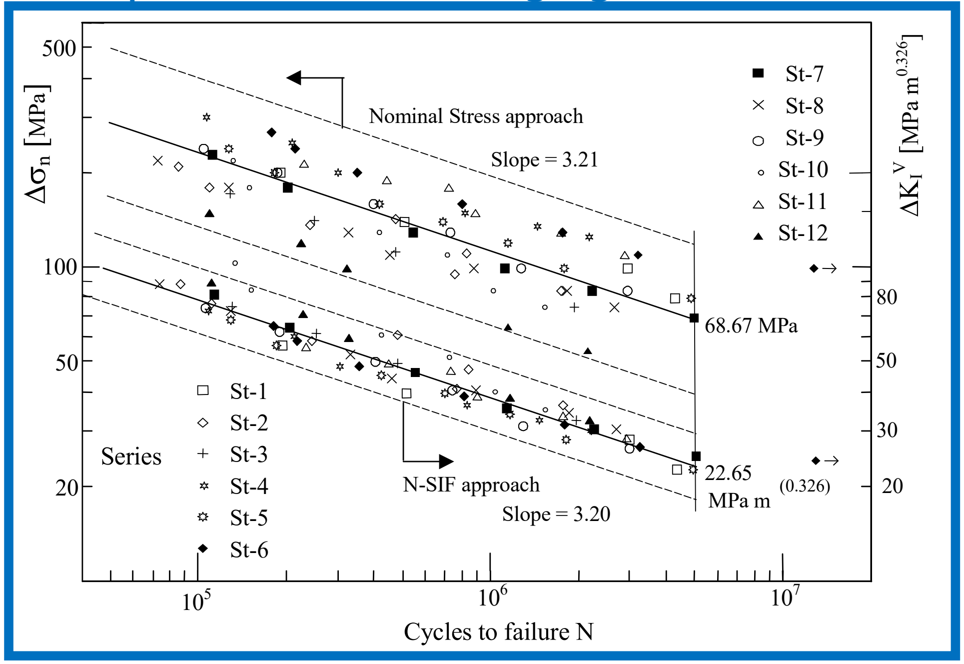

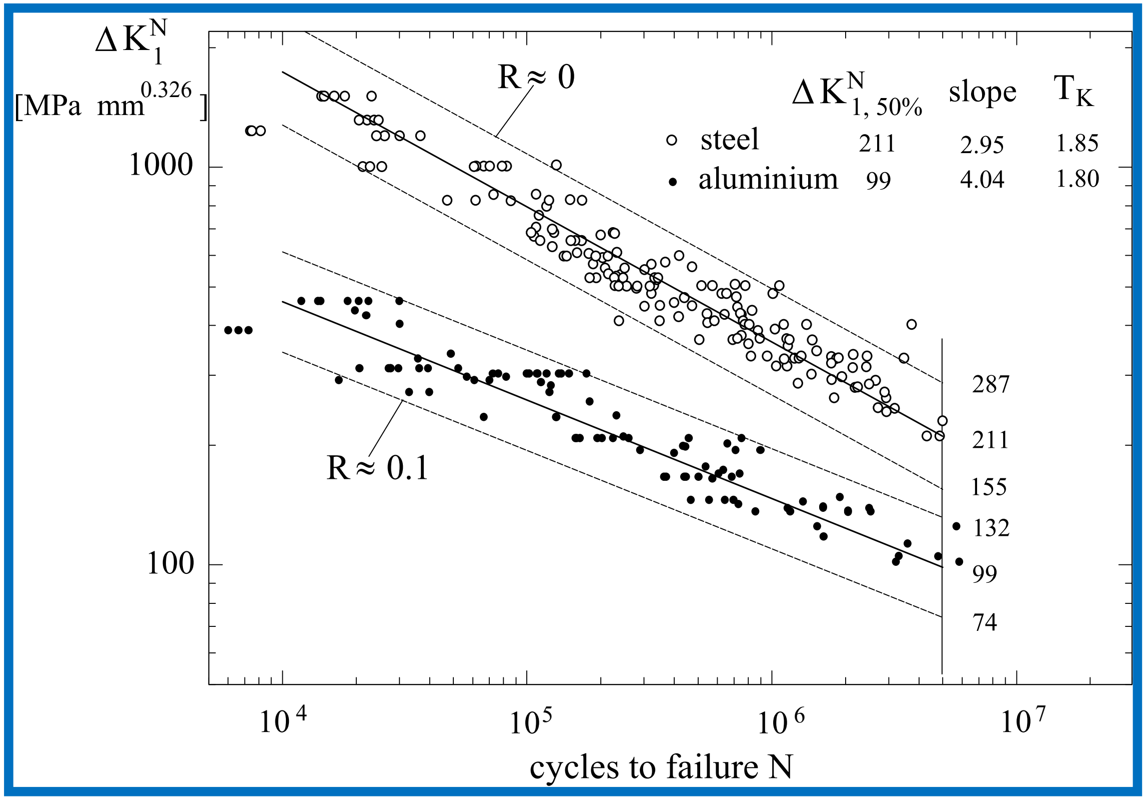

Fatigue strength of aluminium and steel welded joints as a function of Mode I Notch Stress Intensity Factor. Scatter band related to mean values plus/minus 2 standard deviations

STRAIN ENERGY DENSITY

- **Beltrami E** (1885) Sulle condizioni di resistenza dei corpi elastici, Rend. R. Ist. Lombardo di Scienze, Lettere e Arti, **18**, 704 (in Italian)
- **Gillemot L** (1965) Brittle fracture of welded materials. Commonwealth Welding Conference C.7.353-358.
- **Gillemot L** (1976) Criterion of crack initiation and spreading, Engng Fract Mech **8** 239-253.
- **Gillemot L, Czoboly E and Havas I** (1985) Fracture mechanics applications of absorbed specific fracture energy: Notch and unnotched specimens Theor Appl Fract Mech **4** 39-45
- **Sih GC** (1974) Strain-energy-density factor applied to mixed mode crack problems.Int J Fract **10** 305-321.
- **Sih GC** (1991) Mechanics of Fracture Initiation and Propagation: Surface and volume energy density applied as failure criterion, Kluwer Academic Publisher, Dordrecht
- **Sih GC, Tang XS** (2005) Scaling of volume energy density function reflecting damage by singularities at macro-, meso- and microscopic level. Theor Appl Fract Mech **43** 211–231.
- **Sih GC** (2007) *Multiscaling in molecular and continuum mechanics: interaction of time and size from macro to nano*. Dordrecht: Springer.
- **Sih G.C.** (2011) *Pseudo global energy released locally by crack extension involving multiscale reliability*

  Theoretical and Applied Fracture Mechanics 55 (2011) 52–59
- **Ellyin F., Kujawski D** (1989) Generalization of notch analysis and its extension to cyclic loading. Engineering Fracture Mechanics **32** 819-826
- **Ellyin F** (1997) *Fatigue Damage, Crack Growth and Life Prediction*, Chapman & Hall, London
- **Glinka G** (1985) Energy density approach to calculation of inelastic strain-stress near notches and cracks Engng Fract Mech **22** 485-508.
- **Gdoutos EE** (1990) *Fracture Mechanics Criteria and Applications*, Dodrecht: Kluwer Academic Publishers; 1990.
- **Park J, Nelson D** (2000) Evaluation of an energy-based approach and a critical plane approach for predicting constant amplitude multiaxial fatigue life. Int J Fatigue **22** 23-39.

Eugenio Beltrami

(16 November 1835 – 18 February 1900) was an Italian mathematician notable for his work concerning differential geometry and mathematical physics. His work was noted especially for clarity of exposition. He was the first to prove consistency of non-Euclidean geometry by modeling it on a surface of constant curvature, the pseudosphere, and in the interior of an n-dimensional unit sphere, the so-called Beltrami–Klein model. He also developed singular value decomposition for matrices, which has been subsequently rediscovered several times. Beltrami's use of differential calculus for problems of mathematical physics indirectly influenced development of tensor calculus by Gregorio Ricci-Curbastro and Tullio Levi-Civita.

Advantages of a local-energy approach based on NSIFS

- Permits consideration of the scale effect.
- Permits consideration of the contribution of different Modes.
- Permits consideration of the cycle nominal load ratio.
- Overcomes the complex problem tied to the different NSIF units of measure in the case of crack initiation at the toe ($2a=135°$) or root ($2a=0°$).
- Overcomes the problem of multiple crack initiation and their interaction.
- SED can be evaluated with coarse meshes
- It directly takes into account the T-stress
- It directly includes three-dimensional effects

Sharp notches and the SED approach

$$\boxed{W(r,\theta) = W_1(r,\theta) + W_2(r,\theta) + W_{12}(r,\theta)}$$

$$\boxed{W_1(r,\theta) = \frac{1}{2E} r^{2(\lambda_1 - 1)} \cdot \left(K_1^N\right)^2 \left[\tilde{\sigma}_{\theta\theta}^{(1)^2} + \tilde{\sigma}_{rr}^{(1)^2} + \tilde{\sigma}_{zz}^{(1)^2} - 2\nu\left(\tilde{\sigma}_{\theta\theta}^{(1)}\tilde{\sigma}_{rr}^{(1)} + \tilde{\sigma}_{\theta\theta}^{(1)}\tilde{\sigma}_{zz}^{(1)} + \tilde{\sigma}_{rr}^{(1)}\tilde{\sigma}_{zz}^{(1)}\right) + 2(1+\nu)\tilde{\sigma}_{r\theta}^{(1)^2} \right]}$$

$$\boxed{W_2(r,\theta) = \frac{1}{2E} r^{2(\lambda_2 - 1)} \cdot \left(K_2^N\right)^2 \left[\tilde{\sigma}_{\theta\theta}^{(2)^2} + \tilde{\sigma}_{rr}^{(2)^2} + \tilde{\sigma}_{zz}^{(2)^2} - 2\nu\left(\tilde{\sigma}_{\theta\theta}^{(2)}\tilde{\sigma}_{rr}^{(2)} + \tilde{\sigma}_{\theta\theta}^{(2)}\tilde{\sigma}_{zz}^{(2)} + \tilde{\sigma}_{rr}^{(2)}\tilde{\sigma}_{zz}^{(2)}\right) + 2(1+\nu)\tilde{\sigma}_{r\theta}^{(2)^2} \right]}$$

Since the integration field is symmetric with respect to the notch bisector the contribution of $W_{12}=0$

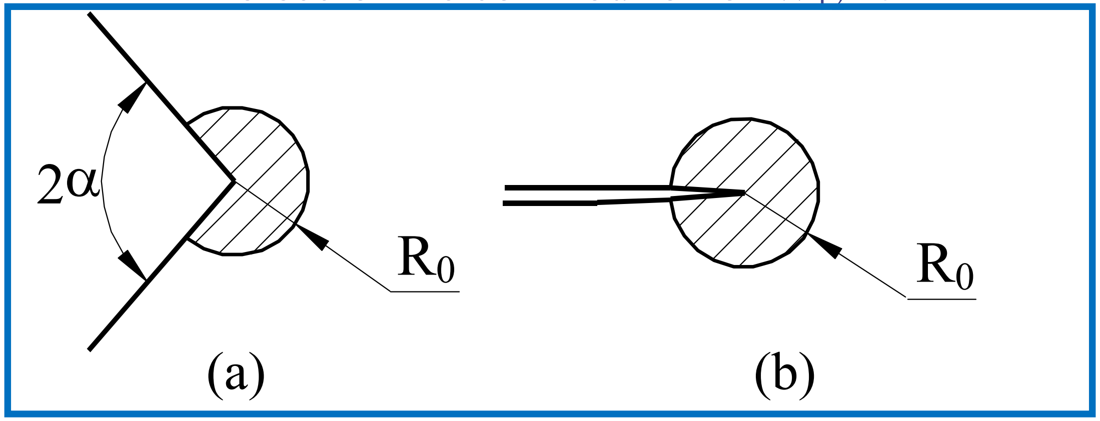

Sharp notches and the SED approach

$$\boxed{E(R) = \int_A W \cdot dA = \int_0^R \int_{-\gamma}^{+\gamma} \left[W_1(r,\theta) + W_2(r,\theta)\right] \cdot r dr d\theta}$$

$$\boxed{E(R) = E_1(R) + E_2(R)}$$

$$\boxed{= \frac{1}{E} \frac{I_1(\gamma)}{4\lambda_1} \cdot \left(K_1^N\right)^2 \cdot R^{2\lambda_1} + \frac{1}{E} \frac{I_2(\gamma)}{4\lambda_2} \cdot \left(K_2^N\right)^2 \cdot R^{2\lambda_2}}$$

$$\boxed{A(R) = \int_0^R \int_{-\gamma}^{+\gamma} r dr d\theta = R^2 \gamma}$$

$$\boxed{\overline{W} = \frac{E(R)}{A(R)} = \frac{1}{E} \cdot e_1 \cdot \left(K_1^N\right)^2 \cdot R^{2(\lambda_1 - 1)} + \frac{1}{E} \cdot e_2 \cdot \left(K_2^N\right)^2 \cdot R^{2(\lambda_2 - 1)}}$$

Mean value of the Strain Energy Density
V-sharp notches (mode I+ II)

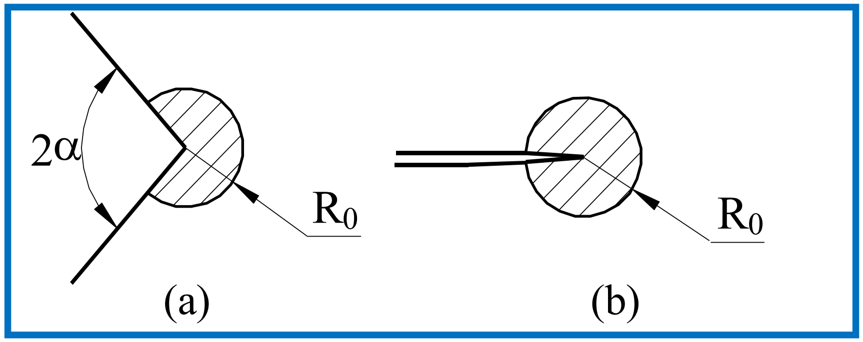

$$\Delta\overline{W} = \frac{e_1}{E}\left[\frac{\Delta K_1^N}{R_0^{1-\lambda_1}}\right]^2 + \frac{e_2}{E}\left[\frac{\Delta K_2^N}{R_0^{1-\lambda_2}}\right]^2$$

$$e_1 = -5.373 \cdot 10^{-6}\,(2\alpha)^2 + 6.151 \cdot 10^{-4}\,(2\alpha) + 0.1330$$

R_0: control volume radius

$$e_2 = 4.809 \cdot 10^{-6}\,(2\alpha)^2 - 2.346 \cdot 10^{-3}\,(2\alpha) + 0.3400$$

$e_{1,2}$: shape functions, which depend on the notch angle and Poisson's ratio

Blunt notches and the Sed approach under mode I loading

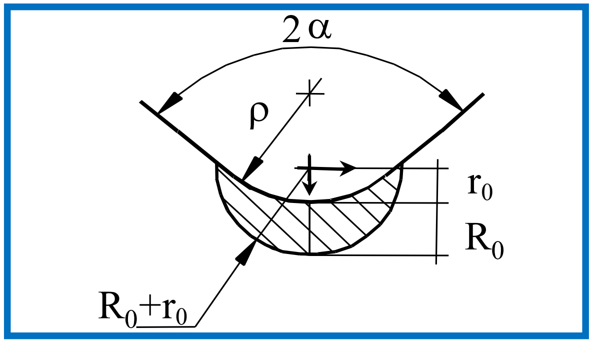

The criterion based on the local energy and valid for brittle or quasi-brittle material considers that the strain energy averaged over a control volume is critical for notched components

$$\overline{W}_1^{(e)} = H(2\alpha, R_0/\rho) \left(\frac{q-1}{q}\right)^{2(1-\lambda_1)} \left[\frac{\sqrt{2\pi}}{1+\tilde{\omega}_1}\right]^2 \frac{\sigma^2{}_{\max}}{E}$$

$$\overline{W}_1^{(e)} = H(2\alpha, R_0/\rho) \frac{(K_{1\rho}^V)^2}{E} \frac{1}{\rho^{2(1-\lambda_1)}}$$

Control volume definition under static loadig

$$\overline{W} = \frac{E(R)}{A(R)} = \frac{1}{E}\cdot e_1 \cdot \left(K_1^N\right)^2 \cdot R^{2(\lambda_1-1)} + \frac{1}{E}\cdot e_2 \cdot \left(K_2^N\right)^2 \cdot R^{2(\lambda_2-1)}$$

The critical energy

$$W_C = \sigma_t^2 / 2E$$

Unnotched material

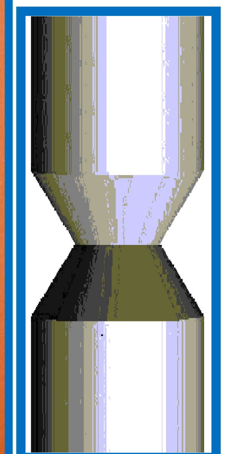

$$\overline{W}_1^{(e)} = \frac{E_1^{(e)}}{A} = \frac{I_1}{4\,E\,\lambda_1\,\pi}\left(\frac{K_{IC}}{R_0^{0.5}}\right)^2$$

cracked material

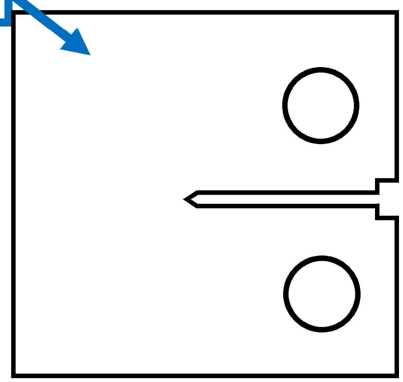

$$\overline{W} = W_C$$

$$R_0 = \frac{(1+\nu)(5-8\nu)}{4\pi}\left(\frac{K_{IC}}{\sigma_t}\right)^2$$

Notched samples under static loading

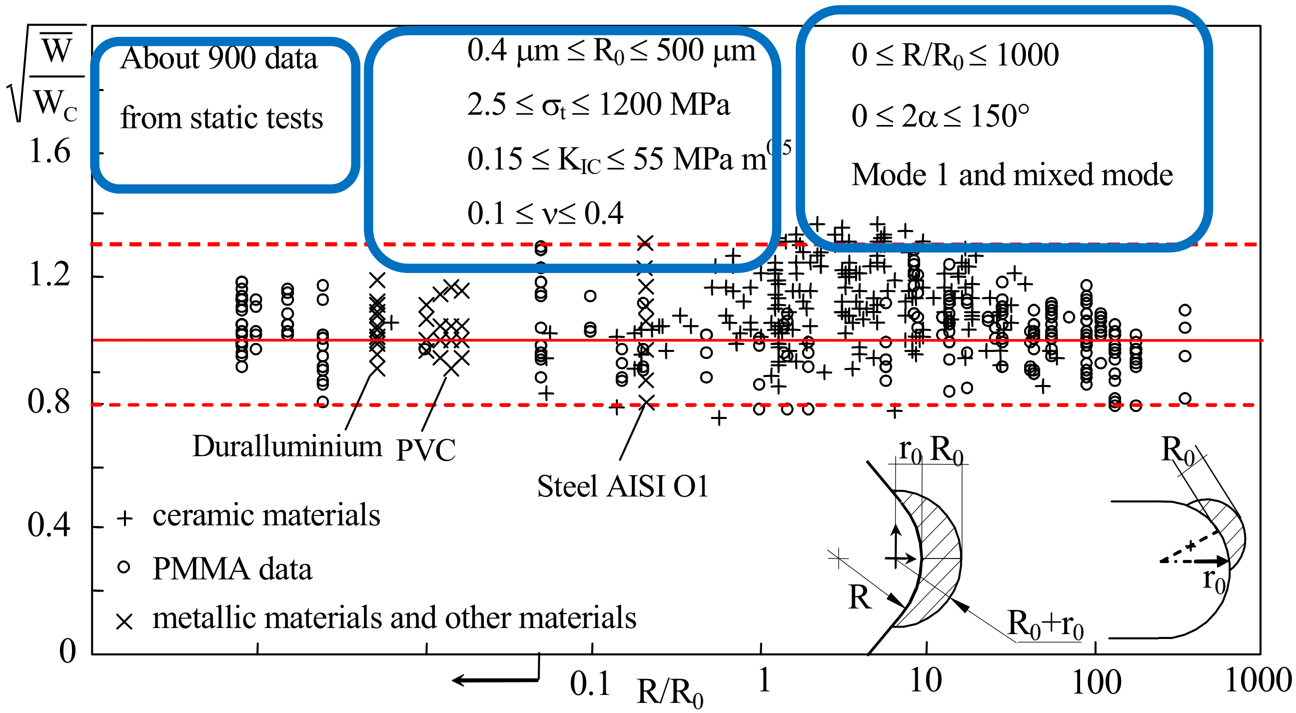

Synthesis of data taken from the literature. Different materials are summarised, among the others AISI O1 and duralluminium

Toe failures: NSIF approach

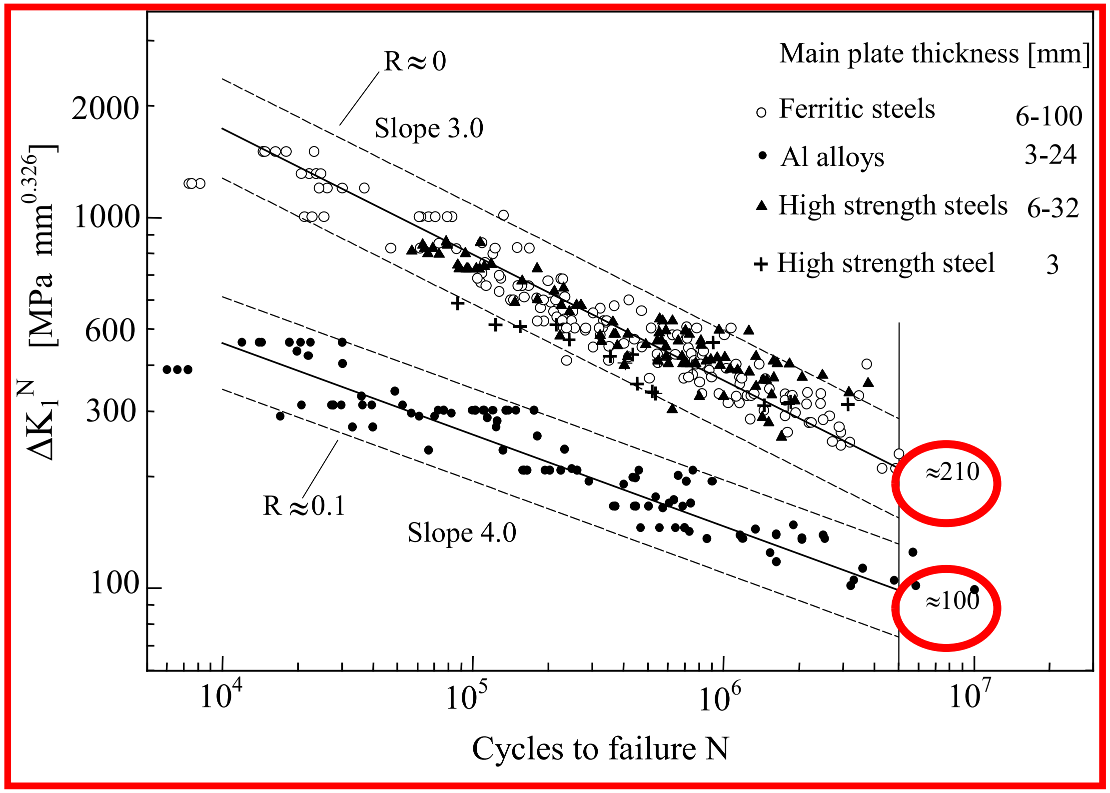

Fatigue strength of steel and aluminum fillet welded joints in terms of the Mode I NSIF (Lazzarin and Tovo 1998, Lazzarin and Livieri 2001). Scatter bands defined by mean values of ± 2 standard deviations.

CRITICAL RADIUS EVALUATION

$2\alpha = 180°$
ground butt welded joints

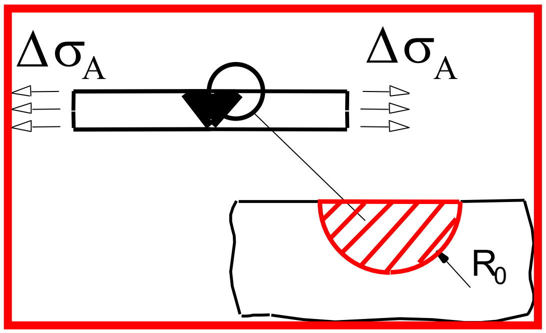

$2\alpha = 135°$

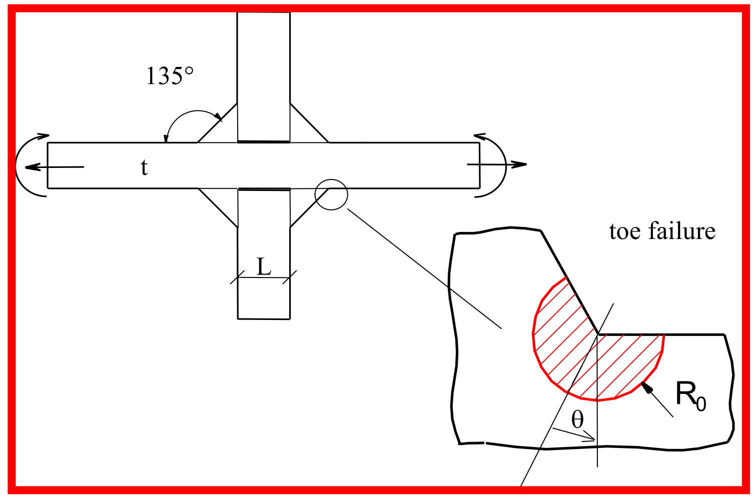

$$R_0 = \left(\frac{\sqrt{2e_1}\,\Delta K_{1A}^{N}}{\Delta\sigma_A}\right)^{\frac{1}{1-\lambda_1}}$$

211 MPamm$^{0.326}$

155 MPa

Averaged Sed as a fatigue parameter

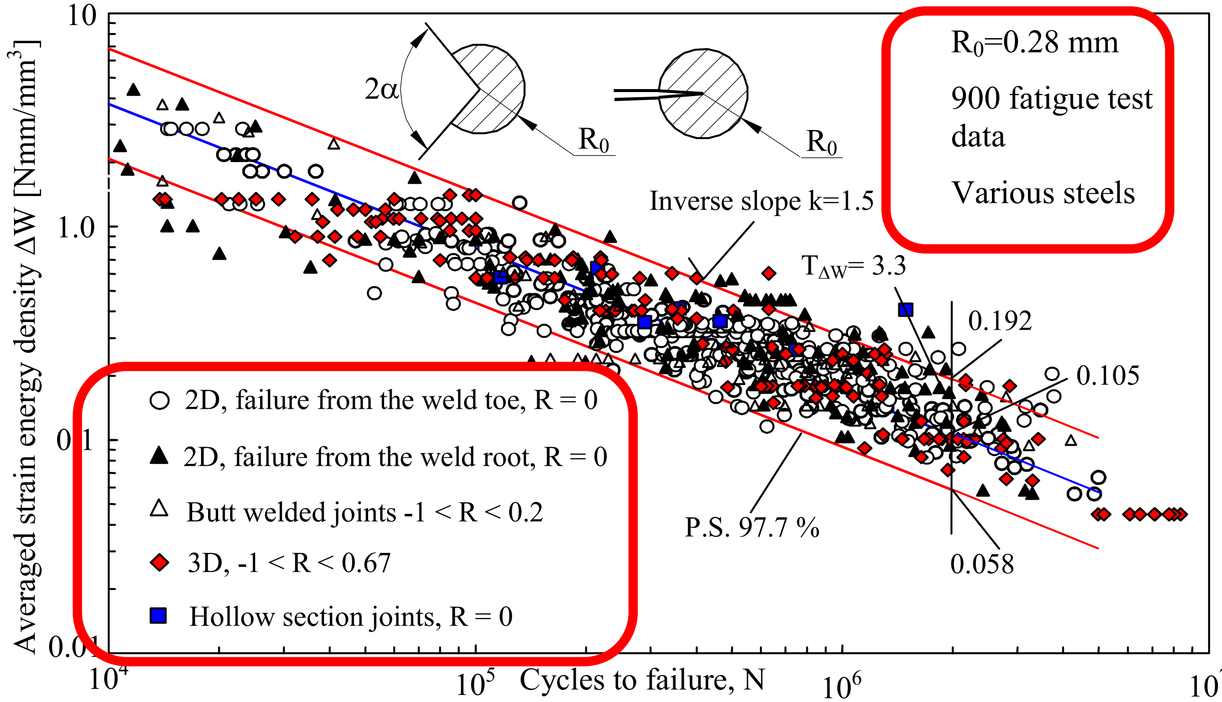

Fatigue strength of welded joints as a function of the averaged local strain energy density; *R* is the nominal load ratio

Coarse mesh: example

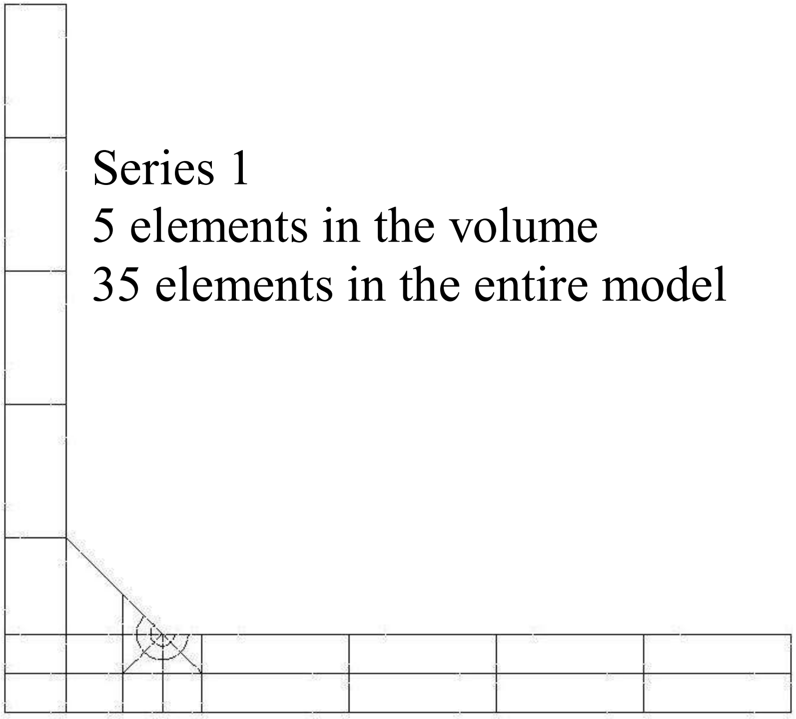

Series 1
5 elements in the volume
35 elements in the entire model

The SED can be accurately evaluated by using coarse meshes.

The NSIFs evaluation requires fine mesh with concentration keypoint.

Fine meshes usually used for Nsifs evaluation

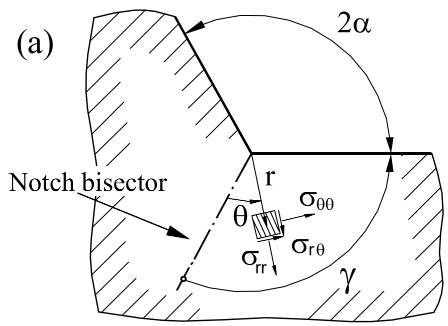

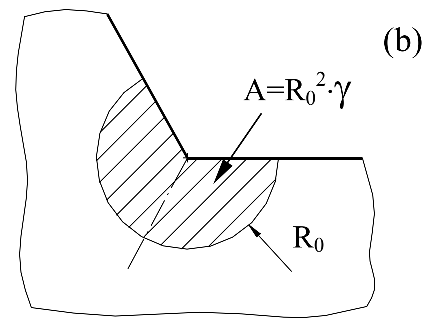

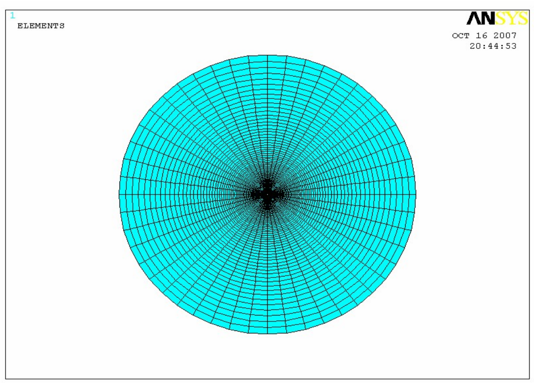

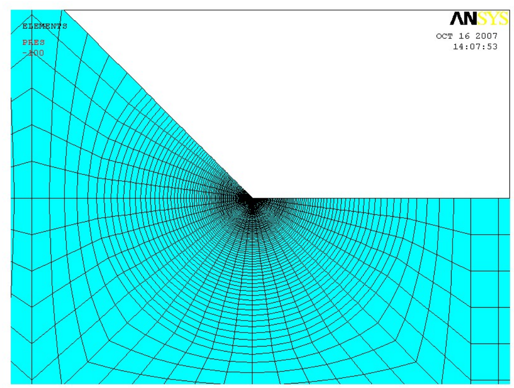

COARSE MESHES

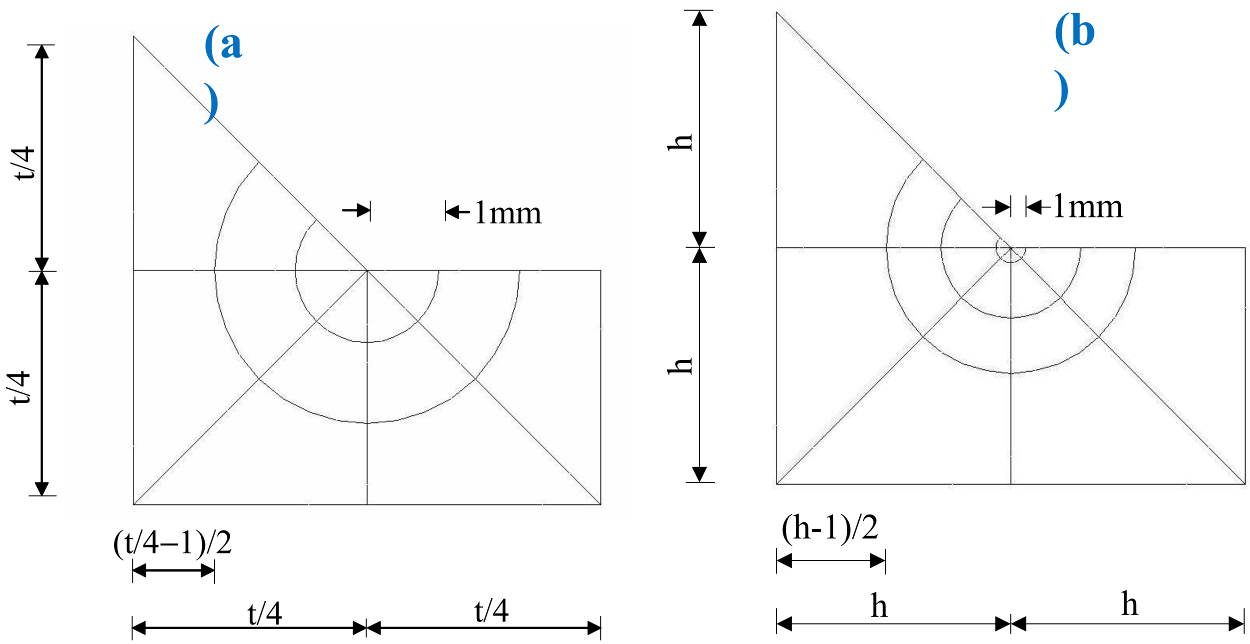

Modulus used for the geometries with *h>t*/2 (a); modulus used when *h<t*/2 (b)

Comparison of K_1 obtained with fine and coarse meshes

Series	t [mm]	h [mm]	L [mm]	Fine mesh K_1 [MPa mm$^{0.326}$]	Parabolic FE (Coarse mesh) $\overline{W}$ [N mm/mm^3]	K_1 [MPa mm$^{0.326}$]	Δ %
1	13	8	10	265.0	4.28×10^{-2}	274.3	3.5
2	50	16	50	396.	9.07×10^{-2}	399.3	0.7
3	100	16	50	413.0	9.94×10^{-2}	417.9	1.2
4	13	5	3	228.8	3.25×10^{-2}	238.9	4.4
5	13	10	8	267.5	4.23×10^{-2}	272.8	2.0
6	25	5	3	231.0	3.32×10^{-2}	241.6	4.6
7	25	9	32	329.5	6.11×10^{-2}	327.7	-0.5
8	25	15	220	405.0	9.08×10^{-2}	399.4	-1.4
9	38	8	13	296.7	5.21×10^{-2}	302.5	2.0
10	38	15	220	476.0	1.25×10^{-1}	469.0	-1.5
11	100	5	3	228.1	3.28×10^{-2}	240.2	5.3
12	100	15	220	589.5	1.87×10^{-1}	573.0	-2.8

Three dimensional models

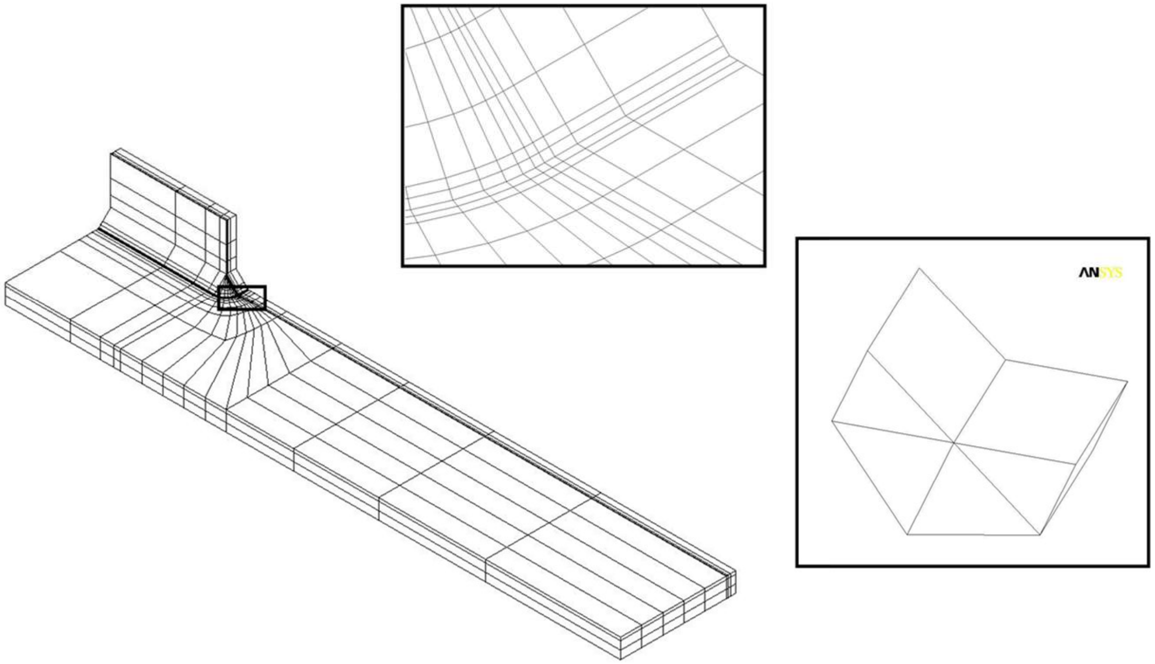

Geometry of the welded joints with a longitudinal stiffener tested by Maddox

Different meshes for three dimensional models

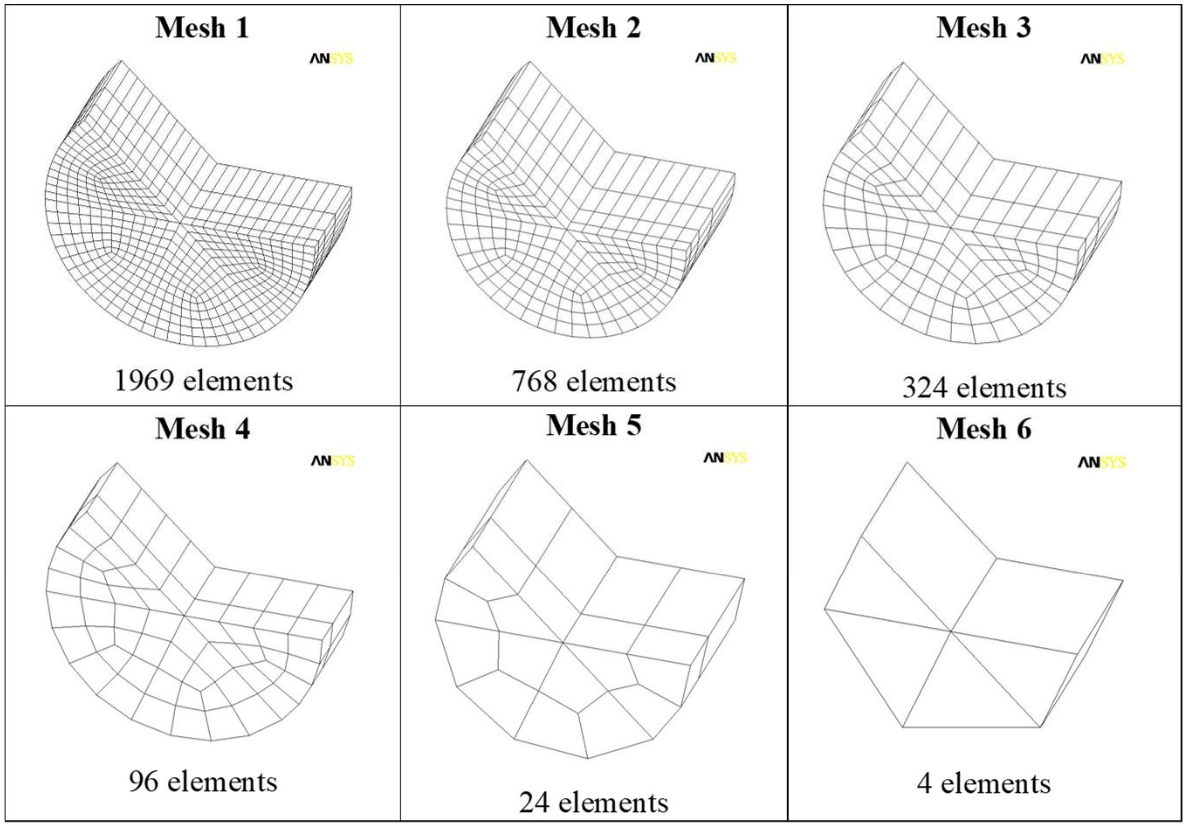

Different meshes for three dimensional models

3D models	Number of FE in the volume	Degrees of freedom (complete model)	$\overline{W}$ Nmm/mm^3	K_1 [MPa mm$^{0.326}$]	Δ%
1	1696	$8.6 \cdot 10^5$	0.07937	373.5	0
2	768	$4.6 \cdot 10^5$	0.07903	372.7	0.21
3	324	$2.5 \cdot 10^5$	0.07896	372.5	0.26
4	96	$1.7 \cdot 10^5$	0.07895	372.5	0.26
5	24	$4.5 \cdot 10^4$	0.07790	370.0	0.93
6	4	$1.1 \cdot 10^4$	0.07594	365.3	2.18

recent paper (2014)

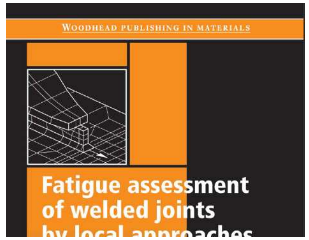

Engineering Fracture Mechanics 76 (2009) 1109–1130

Contents lists available at ScienceDirect

Engineering Fracture Mechanics

journal homepage: www.elsevier.com/locate/engfracmech

ELSEVIER

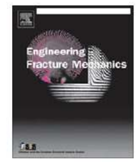

Local fatigue strength parameters for welded joints based on strain energy density with inclusion of small-size notches

D. Radaj [1], F. Berto, P. Lazzarin *

Department of Management and Engineering, University of Padova, Stradella San Nicola 3, 36100 Vicenza, Italy